UNIWERSYTET
WARMIŃSKO-MAZURSKI
W OLSZTYNIE

WYDZIAŁ BIOLOGII I BIOTECHNOLOGII

Dziedzina nauk ścisłych i przyrodniczych

Dyscyplina: Nauki biologiczne

mgr Jan Kamiński

Rozprawa doktorska

Reakcje fizjologiczno-biochemiczne roślin na zanieczyszczenia środowiska naturalnego związkami fluoru

Physiological and biochemical reactions of plants to environmental contamination with fluorine compounds

Praca wykonana w Katedrze Fizjologii, Genetyki i Biotechnologii Roślin

prof. dr hab. Agnieszka I. Piotrowicz-Cieślak

Katedra Fizjologii, Genetyki i Biotechnologii Roślin,
Wydział Biologii i Biotechnologii, Uniwersytet Warmińsko-Mazurski w Olsztynie

dr Alicja Stachelska-Wierzchowska

Katedra Fizyki i Biofizyki,
Wydział Nauki o Żywności, Uniwersytet Warmińsko-Mazurski w Olsztynie

Olsztyn, 2026

Składam najserdeczniejsze podziękowania
Pani prof. dr hab. Agnieszce I. Piotrowicz-Cieślak oraz
Pani dr Alicji Stachelskiej-Wierzchowskiej
za wyrozumiałość, poświęcony czas, motywację do pracy i merytoryczną pomoc w przygotowaniu niniejszej rozprawy doktorskiej.

Kolegom i Koleżankom z Katedry Fizjologii, Genetyki i Biotechnologii Roślin za wsparcie emocjonalne i gotowość do pomocy przy pracy.

SPIS TREŚCI

Wykaz oryginalnych prac będących przedmiotem rozprawy doktorskiej....4
Wykaz oryginalnych prac niebędących przedmiotem rozprawy doktorskiej....5
Streszczenie....6
Abstract....8
Stan wiedzy i uzasadnienie badań....10
Cel pracy....14
Materiał i metodyka badań....15
Wyniki i dyskusja....17
Wnioski....23
Bibliografia....24
Publikacje....32

WYKAZ ORYGINALNYCH PRAC BĘDĄCYCH PRZEDMIOTEM ROZPRAWY DOKTORSKIEJ:

Publikacja 1.

Kamiński, **J**., Stachelska-Wierzchowska, A., Michalczyk, D. J., Klimkowicz-Pawlas, A., Olkowska, E., Wolska, L., & Piotrowicz-Cieślak, A. I. 2024. Changes in metabolism and content of chlorophyll in common duckweed (*Lemna minor* L.) caused by environmental contamination with fluorides. Molecules, 29(10), 2336.

IF_{2024} – 4.6; $MNiSW_{2024}$ – 140 pkt.

Publikacja 2.

Kamiński, **J**., & Piotrowicz-Cieślak, A.I. 2026. Effects of inorganic fluoride and the fluoroquinolone antibiotic pefloxacin on the growth and microbiome structure of *Eruca sativa* L. International Journal of Molecular Sciences, 27(7), 2931.

IF_{2026} – 5.6; $MNiSW_{2026}$ – 140 pkt.

Sumaryczny IF – 10.2

Sumaryczna punktacja MNiSW – 280 pkt.

WYKAZ ORYGINALNYCH PRAC NIEBĘDĄCYCH PRZEDMIOTEM ROZPRAWY DOKTORSKIEJ:

1. Kijowska-Oberc, J., Staszak, A. M., **Kamiński, J.**, Ratajczak, E. 2020. Adaptation of forest trees to rapidly changing climate. Forests, 11(2), 123. https://doi.org/10.3390/f11020123.

   IF_{2020} – 2.59; $MNiSW_{2020}$ – 100 pkt.

2. Michalczyk, D. J., Krupka, M., **Kamiński**, **J**., Wierzbicka, M., Floryańska, S., Kopeć, W., & Piotrowicz-Cieślak, A.I. 2023. Physiological and biochemical parameters of field bean (*Vicia faba* var. minor) seeds stored for 33 years. Agriculture, 13(10), 2012. https://doi.org/10.3390/agriculture13102012.

   IF_{2023} – 3.3; $MNiSW_{2023}$ – 100 pkt.

WYKAZ UDZIAŁU W KONFERENCJACH NAUKOWYCH:

XI Konferencja Polskiego Towarzystwa Biologii Eksperymentalnej Roślin – 19–22 września 2023, Poznań

STRESZCZENIE

W celu oceny skutków oddziaływania zanieczyszczeń glebowych związkami fluoru na rośliny wykorzystano wodne ekstrakty gleby pobranej w pobliżu fermy brojlerów, w której stosowano ciprofloksacynę – antybiotyk z grupy fluorochinolonów. Ekstrakty te zastosowano jako podłoże do uprawy roślin modelowych – rzęsy drobnej (*Lemna minor* L.). W celu wykluczenia wpływu innych potencjalnych zanieczyszczeń równolegle prowadzono hodowle *L. minor* na pożywkach Murashige i Skoog'a (MS), zawierających stężenia jonów fluoru odpowiadające wartościom oznaczonym w ekstraktach glebowych. Analizie poddano cechy morfologiczne roślin, zawartość chlorofilu oraz aktywność enzymów zaangażowanych w jego metabolizm. Dodatkowo przeprowadzono eksperyment *in vitro* polegający na inkubacji komercyjnego chlorofilu *a* z NaF w celu identyfikacji potencjalnych oddziaływań chemicznych między chlorofilem a jonami fluorkowymi.

Nie stwierdzono istotnych zmian morfologicznych ani u roślin uprawianych w ekstraktach glebowych, ani w warunkach kontrolnych. W obu wariantach zaobserwowano jednak wyraźny spadek zawartości chlorofilu oraz zaburzenia aktywności enzymów uczestniczących w jego metabolizmie, w tym dehydratazy kwasu δ-aminolewulinowego (enzymu biosyntezy chlorofilu) oraz chlorofilazy (enzymu odpowiedzialnego za jego degradację). Inkubacja chlorofilu *a* z NaF *in vitro* prowadziła do przesunięć maksimum absorbancji w pasmach Soreta i Qy. Obserwowane zmiany widmowe są zbliżone do opisanych w literaturze efektów substytucji fluoru przy atomie węgla 3^2 cząsteczki chlorofilu.

Rukola (*Eruca sativa* L.) to przykład powszechnie stosowanej rośliny spożywczej. Z tego względu stanowi aplikacyjny w kontekście epidemiologicznym model do badań nad zmianami mikrobiomu roślin pod wpływem zanieczyszczeń środowiskowych. W celu porównania wpływu jonów fluorkowych oraz fluorochinolonu (pefloksacyny) na mikrobiom roślin przeprowadzono czterotygodniową uprawę *E. sativa* na glebach wzbogaconych w NaF lub pefloksacynę. Zastosowano stężenia NaF odpowiadające wartościom środowiskowych stężeń F^- oraz równomolowe stężenia antybiotyku. Następnie przeprowadzono metabarcoding ukierunkowany na 16S rDNA, co umożliwiło analizę zmian w składzie mikrobiomu ryzosfery i fylosfery. NaF i pefloksacyna nie wywołały istotnych zmian morfologicznych u *E. sativa*. Obie substancje istotnie wpływały jednak na strukturę mikrobiomu zarówno w ryzosferze, jak i w fylosferze. Zmiany były bardziej wyraźne w obrębie fylosfery, szczególnie w odniesieniu do NaF, gdzie zaobserwowano większe wahania udziału poszczególnych taksonów. W obu wariantach doszło do zaniku grup

bakterii związanych ze wzrostem roślin oraz przyswajaniem azotu. W próbach z NaF odnotowano znaczący wzrost liczebności przedstawicieli rzędu Burkholderiales w fylosferze, natomiast we wszystkich wariantach badawczych zaobserwowano zanik rodzaju *Pedobacter.* Oba taksony obejmują liczne bakterie środowiskowe, wśród których występują również gatunki oportunistycznie patogenne oraz szczepy mogące stanowić rezerwuar genów oporności na antybiotyki.

Ponadto przeprowadzono profilowanie funkcjonalne mikrobiomu z wykorzystaniem narzędzia PICRUSt2 (Phylogenetic Investigation of Communities by Reconstruction of Unobserved States). Najbardziej istotne zmiany dotyczyły liczebności genów związanych ze szlakami metabolicznymi, w szczególności zaangażowanymi w metabolizm węgla, co wskazuje na istotne zaburzenia funkcjonowania centralnych procesów metabolicznych.

Na podstawie uzyskanych wyników można stwierdzić, że składowanie odchodów drobiu pochodzącego od zwierząt poddawanych antybiotykoterapii prowadzi do uwalniania związków fluoru w ilościach szkodliwych dla roślin. Negatywne efekty ich działania ujawniają się głównie na poziomie fizjologicznym i biochemicznym, co wskazuje, że ocena morfologiczna roślin bioindykatorowych jest niewystarczająca do pełnej oceny toksyczności tych zanieczyszczeń. Uzyskane wyniki sugerują ponadto możliwość bezpośrednich oddziaływań chemicznych jonów fluorkowych z chlorofilem. Zarówno pefloksacyna, jak i jony fluorkowe wywierają silną presję selekcyjną na mikrobiom roślinny, prowadząc do eliminacji mikroorganizmów korzystnych oraz selekcji taksonów potencjalnie patogennych i lekoopornych. Zaobserwowane zmiany w profilach funkcjonalnych mikrobiomu, szczególnie w obrębie metabolizmu węgla, wskazują na głęboki wpływ tych zanieczyszczeń na funkcjonowanie ekosystemów roślinnych.

ABSTRACT

To assess the effects of soil contamination with fluorine compounds on plants, aqueous extracts of soil collected near a broiler farm where ciprofloxacin – a fluoroquinolone antibiotic – had been used. These extracts were used as a growth medium for model plants – common duckweed (*Lemna minor* L.). To exclude the influence of other potential contaminants, parallel cultures of *L. minor* were grown on Murashige and Skoog (MS) media containing fluoride concentrations corresponding to those measured in the soil extracts. Morphological traits, chlorophyll content, and the activity of enzymes involved in its metabolism were analyzed. Additionally, an *in vitro* experiment was conducted in which commercial chlorophyll *a* was incubated with NaF to identify potential chemical interactions between chlorophyll and fluoride ions.

No significant morphological changes were observed either in plants grown in soil extracts or under control conditions. However, in both variants a clear decrease in chlorophyll content and disturbances in the activity of enzymes involved in its metabolism were detected, including δ-aminolevulinic acid dehydratase (an enzyme of chlorophyll biosynthesis) and chlorophyllase (responsible for its degradation). *In vitro* incubation of chlorophyll *a* with NaF resulted in a shift of absorbance maxima in Soret and Qy bands. The observed spectral changes are similar to those described in the literature for fluorine substitution at the carbon atom 3^2 of chlorophyll molecule.

Arugula (*Eruca sativa* L.) is a commonly consumed raw plant and thus represents a model useful in epidemiological context for studying microbiome changes under environmental contamination. To compare the effects of fluoride ions and a fluoroquinolone (pefloxacin) on the plant microbiome, a four-week cultivation of *E. sativa* was carried out on soils enriched with NaF or pefloxacin. NaF concentrations corresponding to environmental levels of F^- and equimolar concentrations of the antibiotic were used. 16S rDNA metabarcoding was performed to analyze changes in the composition of rhizosphere and phyllosphere microbiomes.

Neither NaF nor pefloxacin caused significant morphological changes in *E. sativa*. However, both substances significantly affected microbiome structure in both rhizosphere and phyllosphere. The changes were more pronounced in the phyllosphere, particularly for NaF, where greater fluctuations in the abundance of individual taxa were observed. In both variants, bacterial taxa associated with plant growth and nitrogen assimilation greatly reduced their abundance. In NaF-treated samples, a significant increase in representatives of the order Burkholderiales was observed in the phyllosphere, while in all experimental variants the genus *Pedobacter* disappeared.

Both taxa include microorganisms with pathogenic potential and the ability to transfer antibiotic resistance genes.

Additionally, functional profiling of the microbiome was performed using the PICRUSt2 (Phylogenetic Investigation of Communities by Reconstruction of Unobserved States) tool. The most significant changes concerned the abundance of genes associated with metabolic pathways, particularly those involved in carbon metabolism, indicating substantial disruption of central metabolic processes.

Based on the results obtained, it can be concluded that the storage of poultry manure from animals subjected to antibiotic therapy leads to the release of fluorine compounds in amounts harmful to plants. The negative effects of these compounds are manifested mainly at the physiological and biochemical levels, indicating that morphological assessment of bioindicator plants is insufficient for a full evaluation of their toxicity. The results also suggest the possibility of direct chemical interactions between fluoride ions and chlorophyll. Both pefloxacin and fluoride ions exert strong selective pressure on the plant microbiome, leading to the elimination of beneficial microorganisms and the selection of potentially pathogenic and antibiotic-resistant taxa. The observed changes in microbiome functional profiles, particularly in carbon metabolism, indicate a profound impact of these contaminants on the functioning of plant ecosystems.

STAN WIEDZY I UZASADNIENIE BADAŃ

Fluor jest trzynastym pod względem rozpowszechnienia pierwiastkiem w skorupie ziemskiej (Rudnick i Gao, 2014). Występuje w składzie wielu skał, takich jak granit, sjenit i gnejs (Alferyeva i in., 2011; Moine i in., 2019; Ozsvath, 2006; Taylor i Fallick, 1997). W środowisku naturalnym obecny jest zarówno w atmosferze w postaci gazowego fluorowodoru (HF), jak i w formie jonów fluorkowych (F^-) w glebie oraz wodach gruntowych i powierzchniowych (Kabir i in., 2020; Pyle i Mather, 2009; Sivasankar i in., 2016). Źródłem fluoru w atmosferze jest głównie aktywność wulkaniczna, natomiast w wodach pojawia się on przede wszystkim w wyniku chemicznego wietrzenia skał (Singh i in., 2018; Vithanage i Bhattacharya, 2015). Najwyższe zawartości fluoru odnotowuje się w glebach gliniastych, o niskiej wilgotności (Hong i in., 2016). Retencja F^- w glebie jest najwyższa w zakresie pH 5,0 – 6,5. W skrajnych wartościach pH mobilność jonów fluorkowych wzrasta, co sprzyja ich wymywaniu z gleb do wód gruntowych (Yadav i in., 2018). Obecność fluoru w minerałach ilastych wynika z jego wysokiego powinowactwa do glinu (Senkondo, 2017). Naturalnie podwyższone stężenia fluoru w wodach gruntowych występują przede wszystkim w regionach o wysokiej temperaturze i niskiej wilgotności, takich jak obszary północnej oraz środkowo-wschodniej Afryki, zachodnich Stanów Zjednoczonych, wschodniego wybrzeża Ameryki Południowej, Australii oraz centralnej i południowej Azji (Ali i in., 2016; Podgorski i Berg, 2022). W Afryce centralnej podwyższone stężenia fluoru wiążą się dodatkowo z aktywnością geologiczną w obrębie ryftu wschodnioafrykańskiego. Stosunkowo niskie w skali światowej stężenia rozpuszczalnego F zarejestrowano w zachodniej i centralnej Europie; przypadki jego podwyższonych zawartości dotyczą głównie warstw wodonośnych we wschodniej części kontynentu (Indermitte i in., 2009; Podgorski i Berg, 2022). W związku z tym obecność wysokich stężeń jonów fluorkowych w wodach powierzchniowych lub glebach na terenie Europy najczęściej wskazuje na jego antropogeniczne pochodzenie.

Do głównych antropogenicznych źródeł fluoru w środowisku należą procesy przemysłowe, takie jak produkcja aluminium (Cheng i in., 2020; Feng i in., 2003; Gautam i in., 2018), wytwarzanie ceramiki i cegieł (Fuge, 2019), spalanie węgla kamiennego (Choubisa, 2025), a także produkcja nawozów fosforanowych i antybiotyków (Ahmad i in., 2023; Mirlean i Roisenberg, 2007, Murphy, 2016). Istotną rolę w emisji fluoru odgrywa również rolnictwo. Szacuje się, że ponad połowa syntetycznych związków stosowanych w rolnictwie zawiera fluor, w tym nawozy fosforanowe, pestycydy, fumiganty oraz antybiotyki (Ogawa i in., 2020). Znaczną grupę fluorowanych antybiotyków stanowią fluorochinolony (Bhatt i Chatterjee, 2022), szeroko stosowane zarówno

w medycynie, jak i w chowie zwierząt. Związki te w dużym stopniu nie ulegają metabolizowaniu i są wydalane w formie niezmienionej (Frade i in., 2014). Konwencjonalne metody oczyszczania ścieków zazwyczaj nie zapewniają ich skutecznego usuwania, co prowadzi do ich przedostawania się do wód powierzchniowych. Dodatkowo ponowne wykorzystanie oczyszczonych ścieków do nawadniania pól sprzyja dalszemu rozprzestrzenianiu się tych związków w środowisku naturalnym (Frade i in., 2014; Gatica i Cytryn, 2013). Fluorochinolony charakteryzują się wysoką stabilnością chemiczną; ich degradacja zachodzi głównie poprzez odłączenie jonu fluorkowego od szkieletu węglowego, często pod wpływem promieniowania świetlnego (Murphy, 2016). Istotnym źródłem fluoru w glebie są także odchody zwierząt hodowlanych leczonych tymi antybiotykami. W dawkach subterapeutycznych antybiotyki działają jak promotory wzrostu u drobiu. Od połowy XX wieku, związki te są stosowane w tym celu na dużą skalę (Gouvêa i in., 2015).

Fluorochinolony należą do grup antybiotyków stosowanych w produkcji drobiarskiej. W przypadku takich substancji jak ciprofloksacyna, norfloksacyna, enrofloksacyna, sarafloksacyna czy ofloksacyna wykazano ich kumulację w tkankach mięśniowych ptaków (Hyung i in., 2017; Omotoso i Omojola, 2015; Peña i in., 2010; Pereira i in., 2018; Pugajeva i in., 2018; Widiastuti i in., 2022). W hodowli drobiu stosowane są liczne insektycydy zawierające fluor, które stanowią istotną część fluorowanych związków używanych w rolnictwie (Ogawa i in., 2020). Czynniki te wskazują na fermy drobiu jako potencjalnie istotne źródło fluoru w środowisku. Analiza składu chemicznego gleb w sąsiedztwie miejsc składowania odchodów drobiu może dostarczyć informacji na temat skali i zasięgu rozprzestrzeniania się fluoru.

W niskich stężeniach fluor wywiera korzystny wpływ na mineralizację szkliwa zębów u człowieka. Jego nadmiar wykazuje jednak działanie toksyczne wobec roślin i zwierząt (Banerjee i Roychoudhury, 2019; Barbier i in., 2010; Zuo i in., 2018). U ludzi przewlekła ekspozycja na stężenia fluoru w wodzie pitnej przekraczające 1,5 mg/L, wyznaczone jako dopuszczalne przez Światową Organizację Zdrowia (WHO) prowadzi m. in. do fluoroz zębów i kości, uszkodzeń narządów wewnętrznych oraz zaburzeń neurologicznych, szczególnie w okresie rozwoju prenatalnego (EFSA Scientific Commitee 2025; Li i in., 2020; Kabir i in., 2020; Tiwari i in., 2023). Problem nadmiernej ekspozycji dotyczy zwłaszcza regionów, w których wody gruntowe stanowią główne źródło wody pitnej, m. in. w Afryce Subsaharyjskiej oraz północno-zachodnich Indiach (Podgorski i Berg, 2022).

Fluor wywiera również istotny wpływ na rośliny. Poziom nagromadzenia F w tkankach roślin, powodujący toksyczne skutki może się bardzo różnić w zależności od gatunku. Stwierdzono przypadki tolerancji na stężenia 4000 µg/g tkanki, jednak większość roślin wykazywała objawy toksyczności poniżej 20 µg/g (Hong i in., 2016). Toksyczność F przejawia się na wielu poziomach

organizacji biologicznej – od zmian morfologicznych, przez zaburzenia struktury tkanek i organelli komórkowych, po zmiany biochemiczne. Fluor hamuje podziały komórkowe i wzrost roślin, prowadząc do deformacji tkanek, w tym komórek miękiszowych liści (Ahmed i in., 2020; Gomes i in., 2025; Luo i in., 2021; Rhimi i in., 2016; Singh i Verma, 2013). Zaburza również funkcjonowanie organelli, takich jak mitochondria, retikulum endoplazmatyczne czy tonoplast (Baunthiyal i Ranghar, 2014; Eleftheriou i Tsekos, 1991). Na poziomie biochemicznym powoduje stres oksydacyjny, zwiększając produkcję reaktywnych form tlenu (Benhamada i in., 2023; Sharma i Kaur, 2018) oraz modyfikując aktywność enzymów (Pelc i in., 2020; Zouari i in., 2017). Ponadto wiąże jony metali niezbędnych dla funkcjonowania enzymów (Gadi i in., 2021) oraz zakłóca procesy sygnalizacji komórkowej (Panda, 2015).

Jednym z najbardziej charakterystycznych objawów fitotoksyczności fluoru jest degradacja chlorofilu, prowadząca do występowania chlorozy (Gadi i in., 2021; Hong i in., 2016; Ram i in., 2014). Proces ten wiąże się z zaburzeniami fotosyntezy, szczególnie funkcjonowania fotosystemu II oraz transportu elektronów (Haddy i in., 2018; Verma i in., 2022). Fluor wpływa również na aktywność enzymów uczestniczących w asymilacji węgla, takich jak RuBisCo – karboksylazy/oksygenazy rybulozo-1,5-bisfosforanowej – kluczowego enzymu fotosyntezy. Pierwiastek ten ma istotne znaczenie także w metabolizmie węglowodanów (Baunthiyal i Ranghar, 2014; Singh i in., 2021). Mechanizmy bezpośrednich interakcji fluoru z cząsteczkami chlorofilu pozostają jednak w dużej mierze niepoznane. Z tego względu szczególnie istotne jest zbadanie mechanizmów utraty chlorofilu pod wpływem fluoru. Badania te mają znaczenie nie tylko poznawcze, ale także aplikacyjne, zwłaszcza w kontekście wykorzystania roślin w procesach bioremediacji. Rzęsa drobna (*Lemna minor* L.) jest organizmem modelowym o wysokim potencjale w tym zakresie, ze względu na jej szybki wzrost, łatwość hodowli oraz zdolność do akumulacji zanieczyszczeń (Ekperusi i in., 2019). Analiza jej reakcji na obecność fluorków może dostarczyć informacji o możliwości wykorzystania tego gatunku zarówno jako bioremediatora, jak i bioindykatora zanieczyszczeń.

Innym ważnym aspektem zagrożeń związanych z zanieczyszczeniem środowiska związkami fluoru jest wpływ na mikrobiom roślin. Mikroorganizmy kolonizujące glebę i tkanki roślin pełnią istotną rolę w przeżywalności roślin, ich odżywianiu, regulacji wzrostu oraz odporności na stresy biotyczne i abiotyczne (de Faria i in., 2021; Kim i in., 2024; Madhaiyan i in., 2015; Saleem i in., 2019; Xiong i in., 2023). Zmiany w strukturze mikrobiomu gleb osłabiają ich funkcjonalność metaboliczną, co powoduje zaburzenia obiegu pierwiastków w ekosystemie (Hartmann i Six, 2023; Huang i in., 2023). Zaburzenia flory bakteryjnej ryzosfery roślin mają istotny wpływ na ich zdolność przyswajania substancji mineralnych (Trivedi i in., 2020). Stwierdzono, że obecność jonów F^-

w glebie powoduje istotne zmiany w strukturach mikrobiomu roślin (Gan i in., 2021; Jiang i in., 2024; Martin-Pozas i in., 2025; Pramanik i in., 2025; Wang i in., 2024). Silnie elektroujemne atomy fluoru tworzą trwałe wiązania w cząsteczkach, dzięki czemu związki zawierające fluor są wysoce odporne na działanie czynników abiotycznych oraz procesy biodegradacji (Bhatt i Chatterjee, 2022). Spośród związków fluoru wchodzących w kontakt z roślinami, antybiotyki są szczególnie groźne dla mikrobiomu ze względu na ich stabilność w środowisku i wysoką aktywność biologiczną nawet w małych stężeniach (Cairns i in., 2018; Polianciuc i in., 2020; Yu i in., 2021).

Presja selekcyjna antybiotyków promuje rozprzestrzenianie opornych szczepów bakterii w środowisku (Pruden i in., 2013; Wu i in., 2023; Xie i in., 2018), co stwarza zagrożenie epidemiologiczne dla człowieka. Według ostatnich badań (Chen i in., 2019; Nithya i Babu, 2017; Rahman i Noor, 2012) zagrożenie to może dotyczyć mikrobiomu roślin spożywczych. Wykazano horyzontalny transfer genów lekooporności między mikrobiomem ryzosfery a mikrobiomem fylosfery roślin (Xu i in., 2021). Istnieją doniesienia o potencjalnie chorobotwórczych bakteriach, wykrywanych w fylosferze popularnych warzyw (Heaton i Jones 2008; Rosberg i in., 2021). Związane z tym ryzyko jest szczególnie istotne ze względu na panujący trend spożywania roślin na surowo. Dobrym przykładem jest tu rukola (*Eruca sativa* L.). W jej fylosferze wykryto bakterie z rodziny Enterobacteriaceae, będące nosicielami licznych genów oporności na antybiotyki (Cernava i in., 2019).

Pefloksacyna (Figura 1) to antybiotyk z grupy fluorochinolonów, który mimo powszechnego stosowania, nie został do tej pory zbadany jako czynnik zaburzający strukturę mikrobiomu roślin w warunkach laboratoryjnych. Badania nad zmianami w mikrobiomie *E. sativa* zachodzącymi pod wpływem pefloksacyny są użyteczne w ocenie zagrożenia, jakie stanowią te zmiany w kontekście ekologicznym i epidemiologicznym. Równoległe zbadanie zmian zachodzących pod wpływem jonów F^- o stężeniach odpowiadających stężeniom antybiotyku pozwoli określić, czy wpływ jonów fluorkowych na mikrobiom jest podobny do wpływu pefloksacyny. Na tej podstawie będzie można stwierdzić, jaka jest rola jonu F^- uwalnianego z pefloksacyny w jej oddziaływaniu z mikrobiomem.

Figura 1. Struktura chemiczna ciprofloksacyny (A) i pefloksacyny (B).



CEL PRACY

Celem pracy było kompleksowe wyjaśnienie ekologicznych i epidemiologicznych konsekwencji zanieczyszczenia środowiska związkami fluoru, ze szczególnym uwzględnieniem jonów fluorkowych oraz fluorowanych antybiotyków z grupy fluorochinolonów, poprzez analizę ich wpływu na fizjologię roślin oraz strukturę i funkcjonowanie mikrobiomów roślinnych. Badania koncentrowały się na identyfikacji mechanizmów odpowiedzi roślin i mikroorganizmów na stres fluorowy, ocenie potencjału roślin jako bioindykatorów i organizmów wykorzystywanych w procesach bioremediacji, a także określeniu znaczenia zmian mikrobiologicznych dla bezpieczeństwa środowiskowego i zdrowia publicznego.

Praca ma na celu również eksperymentalną weryfikację nowego, dotychczas niepotwierdzonego mechanizmu degradacji chlorofilu indukowanej obecnością związków fluoru. W przeciwieństwie do klasycznie postulowanego mechanizmu polegającego na oddziaływaniu jonów fluorkowych z jonem magnezu centralnie związanym w cząsteczce chlorofilu, badania podejmują próbę wykazania możliwości bezpośrednich interakcji fluorków ze szkieletem węglowym chlorofilu, prowadzących do destabilizacji barwnika bez odłączenia jonu Mg^{2+}.

Hipoteza 0: Zanieczyszczenia środowiska związkami fluoru, w tym fluorochinolonami, wywierają istotny wpływ na fizjologię roślin oraz strukturę i funkcjonowanie mikrobiomów roślinnych, prowadząc do zaburzeń metabolicznych oraz selekcji mikroorganizmów o zwiększonym potencjale patogennym i lekoopornym.

Hipoteza 1: Zanieczyszczenia gleb związkami fluoru pochodzącymi z przemysłu produkcji drobiu wywołują mierzalne zmiany fizjologiczne u badanych gatunków roślin, umożliwiające wykorzystanie ich jako bioindykatorów skażenia środowiska.

Hipoteza 2: Degradacja chlorofilu indukowana obecnością związków fluoru może zachodzić według dotychczas nieopisanego mechanizmu, niezwiązanego bezpośrednio z oddziaływaniem jonów fluorkowych na jon magnezu obecny w cząsteczce chlorofilu. Jony fluorkowe mogą oddziaływać bezpośrednio ze szkieletem węglowym chlorofilu, prowadząc do destabilizacji barwnika bez odłączenia Mg^{2+}.

Hipoteza 3: Wpływ związków fluoru na strukturę i funkcjonowanie mikrobiomów roślinnych różni się pomiędzy ryzosferą a fylosferą, co wynika ze złożoności i odmienności czynników środowiskowych kształtujących oba typy mikrobiomów.

MATERIAŁ I METODYKA BADAŃ

W celu oceny wpływu zanieczyszczeń glebowych związanych z chowem drobiu na rośliny pobrano próbki gleby z trzech stanowisk zlokalizowanych w różnej odległości od pryzmy odchodów brojlerów. Odchody pochodziły od ptaków leczonych ciprofloksacyną i były składowane na wolnym powietrzu. Z pobranych próbek przygotowano wodne ekstrakty glebowe, które następnie zastosowano jako medium hodowlane dla rzęsy drobnej (*Lemna minor*). Równolegle prowadzono hodowle kontrolne w płynnej pożywce Murashige i Skoog'a (MS), suplementowanej fluorkiem sodu (NaF) w stężeniach odpowiadających zawartości jonów fluorkowych (F^-) oznaczonych w ekstraktach glebowych. Po siedmiodniowej inkubacji materiał roślinny wykorzystano do analizy parametrów morfologicznych, oznaczenia zawartości chlorofilu oraz aktywności enzymów związanych z jego metabolizmem, tj. dehydratazy kwasu δ-aminolewulinowego, uczestniczącej w biosyntezie chlorofilu, oraz chlorofilazy, odpowiedzialnej za jego degradację.

W celu zbadania bezpośrednich interakcji chemicznych jonów fluorkowych z cząsteczką chlorofilu przygotowano serie roztworów fluorku sodu oraz komercyjnego chlorofilu *a* w metanolu. Zastosowane stężenia NaF odpowiadały stężeniom jonów fluoru oznaczonym w ekstraktach glebowych. Próbki inkubowano w warunkach ciemności, w temperaturze 4 °C, przez okres 21 tygodni. W trakcie inkubacji, w odstępach tygodniowych, prowadzono pomiary fluorymetryczne w celu wykrycia ewentualnego powstawania nowych form chemicznych.

Wpływ pefloksacyny oraz jonów fluorkowych na mikrobiom roślinny oceniano w doświadczeniu obejmującym czterotygodniową uprawę *E. sativa* w warunkach laboratoryjnych. Rośliny hodowano na glebie suplementowanej równomolowymi stężeniami NaF lub pefloksacyny. Zastosowane stężenia (10 µM i 20 µM) odpowiadały wartościom literaturowym, leżącym w zakresie zawartości jonów fluorkowych spotykanych w środowisku (Biglari i in., 2016; Malago i in., 2017; McMahon i in., 2020; Ozsvath, 2006; Walna i in., 2007; Yadav i in., 2018). Po zakończeniu eksperymentu przeprowadzono izolację bakteryjnego DNA z ryzosfery oraz fylosfery badanych roślin. Uzyskany materiał wykorzystano do analizy struktury mikrobiomu z zastosowaniem metabarkodowania opartego na 16S rDNA. Uzyskane warianty sekwencji amplikonów (ASV) sklasyfikowano na kolejnych poziomach taksonomicznych – od królestwa do gatunku. Dodatkowo przeprowadzono predykcję profilu funkcjonalnego mikrobiomu z wykorzystaniem narzędzia bioinformatycznego PICRUSt2 (Phylogenetic Investigation of Communities by Reconstruction of Unobserved States).

W pracy zastosowano następujące metody analityczne (Tabela 1).

Tabela 1. Wykaz zastosowanych w pracy metod badawczych.

L. p.	Parametr	Metoda	Publikacja nr
1.	Parametry fizyczne gleby	Dyfrakcja laserowa: Mastersizer 2000 (Malvern)	1
2.	Ekstrahowalna kwasowość	Metoda Kappen’a (Jaremko i Kalembasa, 2014)	1
3.	Wymienialne jony	Spektroskopia absorpcji atomowej (Jaremko i Kalembasa, 2014)	1
4.	pH gleby	Potencjometr (Jaremko i Kalembasa, 2014)	1
5.	Parametry morfologiczne	Program komputerowy ImageJ	1
6.	Pomiar suchej masy	ISTA (International Seed Testing Association)	1
7.	Pomiar zawartości białka	Metoda Bradford’a	1
8.	Aktywność dehydratazy kwasu δ-aminolewulinowego	Jiao i in., 2017	1
9.	Aktywność chlorofilazy	Zhang i in., 2011	1
10.	Zawartość chlorofilu	Lichtenthaler i Buschmann, 2001	1
11.	Degradacja chlorofilu *in vitro*	Pomiary fluorymetryczne	1
12.	Struktura metagenomu	Izolacja bakterii z tkanek roślinnych (Krupka i Piotrowicz-Cieślak, 2024)	2
13.	Struktura metagenomu	Izolacja DNA - zestaw DNeasy PowerSoil Pro Kit (Qiagen)	2
14.	Profil metaboliczny mikrobiomu	Narzędzie q2-picrust2 (QIIME2 wersja 2024.5)	2

WYNIKI I DYSKUSJA

Fermy brojlerów stanowią poważny problem środowiskowy nie tylko w Polsce, ale i na świecie (Bokkers i de Boer, 2009; Fisher i in., 2015; da Silva i in., 2014; Szablewski i in., 2022; Wychodnik i in., 2020; Yayli i Kilic, 2023). W badanej fermie brojlerów, w której na szeroką skalę stosowano ciprofloksacynę, odchody zwierzęce składowano w postaci pryzmy bezpośrednio na powierzchni gruntu, w warunkach otwartych i w kontakcie z glebą. Taki sposób magazynowania stanowi potencjalne źródło zanieczyszczenia środowiska, szczególnie gleby, związkami fluoru. W celu oceny wpływu tych zanieczyszczeń na fizjologię organizmów roślinnych pobrano próbki gleby z trzech stanowisk zlokalizowanych w rosnącej odległości od miejsca składowania odchodów, z których wyekstrahowano jony fluorkowe.

Analiza fizykochemiczna wykazała, że wszystkie badane gleby charakteryzowały się strukturą gliniastą oraz kwaśnym odczynem (pH ≤ 5,5). Zawartość wymienialnych jonów wapnia wynosiła około 3,5 cmol(+)/kg, natomiast zawartość glinu wynosiła około 5 g/kg. Parametry te mają istotne znaczenie dla zachowania rozpuszczalnego fluoru w glebie, ponieważ zarówno wapń, jak i glin wykazują wysokie powinowactwo do jonów fluorkowych (Harrington i in., 2003; He i in., 2016; Pickering, 1985; Ruan i in., 2004; Tang i in., 2009; Zhang i in., 2017), wpływając na ich retencję. Jednocześnie kwaśne środowisko zwiększa mobilność oraz biodostępność fluoru. Doniesienia literaturowe (Arnesen, 1997; Peng i in., 2021; Ruan i in., 2003) wskazują ponadto, że obecność glinu może sprzyjać pobieraniu fluoru przez rośliny, zwiększając tym samym jego potencjalną toksyczność.

Zawartość fluoru w pryzmie obornika wynosiła od 37 do 48 mg/kg, natomiast w ekstraktach glebowych mieściła się w zakresie 2,1–4,9 mg/kg i malała wraz ze wzrostem odległości od źródła zanieczyszczenia. Biorąc pod uwagę lokalizację stanowiska badawczego w regionie o niskim naturalnym poziomie fluorków w glebie, oddalonym od obszarów przemysłowych oraz naturalnych źródeł tego pierwiastka (np. terenów wulkanicznych; Bellomo i in., 2007; Cronin i in., 2003; Sawyer i Oppenheimer, 2006), można wnioskować, że podwyższone stężenia fluorków były bezpośrednio związane ze składowaniem odchodów.

Wpływ zanieczyszczeń na organizmy roślinne oceniono z wykorzystaniem rzęsy drobnej (*Lemna minor*) jako organizmu modelowego. Podłoże hodowlane stanowiły wodne ekstrakty glebowe. W celu określenia zmian morfologicznych i fizjologicznych wywołanych przez zanieczyszczenia inne niż jony fluorkowe przeprowadzono równolegle doświadczenia stosując pożywki Murashige i Skoog’a suplementowane fluorkiem sodu w stężeniach odpowiadających

poziomom jonów fluorkowych oznaczonym w ekstraktach. Dodatkowo zastosowano próbę kontrolną bez dodatku NaF oraz wariant o stężeniu 100-krotnie wyższym (210 mg/L), umożliwiający określenie zakresu odpowiedzi organizmu na wyższe dawki czynnika stresowego.

Po siedmiu dniach hodowli rzęsy drobnej, zarówno w przypadku ekstraktów glebowych, jak i pożywek syntetycznych, nie stwierdzono istotnych statystycznie zmian w parametrach morfologicznych roślin, takich jak liczba i powierzchnia frondów, ich zabarwienie lub świeża i sucha masa. Wyjątek stanowiła próba o najwyższym stężeniu NaF, w której zaobserwowano całkowite zahamowanie wzrostu, chlorozę oraz dezintegrację struktur roślinnych. Wyniki te wskazują, że poziomy fluoru emitowane przez badaną fermę nie powodują wyraźnych, makroskopowych zmian u *L. minor*.

W związku z tym przeprowadzono analizy na poziomie fizjologicznym i biochemicznym, obejmujące oznaczenie zawartości chlorofilu oraz aktywności enzymów związanych z jego metabolizmem: dehydratazy kwasu δ-aminolewulinowego (uczestniczącej w biosyntezie chlorofilu) oraz chlorofilazy (odpowiedzialnej za jego degradację). We wszystkich wariantach doświadczalnych odnotowano istotne zmiany tych parametrów, co wskazuje, że oddziaływanie fluoru ujawnia się przede wszystkim na poziomie molekularnym i metabolicznym, niewidocznym w obserwacjach morfologicznych. Podkreśla to konieczność stosowania czułych metod biochemicznych w ocenie wpływu zanieczyszczeń środowiskowych. Brak istotnych zmian morfologicznych u *L. minor* obserwowany w warunkach ekspozycji na ekstrakty glebowe może sugerować niską toksyczność zastosowanych stężeń fluoru. Wyniki przeprowadzonych analiz biochemicznych jednoznacznie wskazują, że ocena oparta wyłącznie na cechach makroskopowych prowadzi do niedoszacowania rzeczywistego wpływu zanieczyszczeń. Zmiany w zawartości chlorofilu oraz aktywności enzymów zaangażowanych w jego metabolizm świadczą o tym, że fluor oddziałuje na kluczowe procesy fizjologiczne roślin, nawet wówczas, gdy nie dochodzi do widocznego zahamowania wzrostu. Jest to zgodne z koncepcją, według której stres środowiskowy w pierwszej kolejności manifestuje się na poziomie molekularnym, a dopiero w dalszej perspektywie prowadzi do zmian fenotypowych (Chaerle i Van Der Straeten, 2000; Cooper i in., 2025; Velagaleti i in., 1990).

Dodatkowo stwierdzono, że po siedmiodniowej hodowli zawartość jonów fluorkowych w ekstraktach glebowych uległa obniżeniu o ponad 85%. W połączeniu z brakiem zahamowania wzrostu roślin sugeruje to zdolność *L. minor* do efektywnego usuwania fluoru ze środowiska wodnego. Wysoka efektywność usuwania jonów F^- sugeruje, że gatunek ten może odgrywać ważną rolę w naturalnych procesach samooczyszczania ekosystemów wodnych (Liu i in., 2017; Sarkheil i Safari, 2020; Sasmaz i in., 2015). Wskazuje to jednocześnie na możliwość jego praktycznego wykorzystania w technologiach bioremediacyjnych, szczególnie w przypadku wód

zanieczyszczonych związkami fluoru o niskich i umiarkowanych stężeniach. Należy jednak podkreślić, że proces ten wiąże się z akumulacją fluoru w tkankach roślinnych, co może mieć dalsze konsekwencje ekologiczne. *L. minor* stanowi pierwotne ogniwo wielu łańcuchów troficznych w ekosystemach wodnych, co może powodować gromadzenie zaabsorbowanych przez rośliny zanieczyszczeń w tkankach organizmów na wyższych szczeblach łańcucha i rozprzestrzenianie ich w środowisku (Kibet i in., 2019; Senkondo i in., 2018; Syamsuhaidi i in., 2025; Xue i in., 2018).

Uzupełniające badania nad mechanizmem oddziaływania fluoru na chlorofil przeprowadzono w warunkach *in vitro*, inkubując komercyjny chlorofil *a* w roztworze metanolowym z dodatkiem NaF w stężeniach odpowiadających poziomom zaobserwowanym w ekstraktach glebowych. Długotrwała inkubacja (21 tygodni) prowadziła do zmian w widmach absorpcyjnych barwnika, w tym efektu hipsochromowego w pasmach Soreta i Qy, co wskazuje na bezpośrednie oddziaływanie fluorków na strukturę cząsteczki chlorofilu. Wyniki te sugerują, że jony fluorkowe nie powodują całkowitej degradacji chlorofilu poprzez usunięcie centralnego jonu magnezu, lecz tworzą z nim związki kompleksowe zmieniające właściwości optyczne i funkcjonalne barwnika. Zaobserwowane przesunięcia maksimum absorbancji są zgodne z wynikami uzyskanymi przez Ogasawarę i współpracowników (2020), którzy wykazali, że analog chlorofilu *a* podstawiony 2 atomami fluoru w pozycji $C3^2$ charakteryzuje się przesunięciami maksimum absorbancji w pasmach Soreta i Qy w kierunku krótszych długości fal.

Przedstawione wyniki wpisują się w rosnącą liczbę doniesień (Chaney i Oliver, 1996; Huang i in., 1994; Rashid i in., 2023) wskazujących, że działalność rolnicza, mimo swojego „naturalnego" charakteru, może prowadzić do wprowadzania do środowiska istotnych ilości zanieczyszczeń chemicznych. Szczególnie problematyczne są sytuacje, w których substancje te nie wywołują natychmiastowych, widocznych efektów toksycznych, lecz oddziałują długofalowo, zaburzając funkcjonowanie organizmów na poziomie metabolicznym (Calfapietra i in., 2015; Minden i in., 2017; Wang i in., 2015). W takim kontekście kluczowe znaczenie ma rozwój metod diagnostycznych opartych na wskaźnikach biochemicznych i molekularnych, umożliwiających wczesne wykrywanie zmian środowiskowych.

Uzyskane wyniki wskazują, że fluor wprowadzany do środowiska wraz z odchodami zwierzęcymi może wywoływać istotne, choć często makroskopowo niewidoczne zmiany w funkcjonowaniu organizmów roślinnych. Jego działanie ma charakter wieloetapowy i obejmuje zarówno wczesne modyfikacje procesów biochemicznych, jak i późniejsze konsekwencje fizjologiczne. Granica między adaptacją a toksycznością jest przy tym płynna i zależy od stężenia czynnika oraz zdolności organizmu do kompensacji zaburzeń, co podkreśla znaczenie kompleksowej oceny wpływu praktyk rolniczych na środowisko.

Antybiotyki wprowadzane do środowiska stanowią istotny czynnik presji selekcyjnej, prowadzący do przekształceń strukturalnych i funkcjonalnych mikrobiomów glebowych poprzez preferencyjną proliferację szczepów opornych (Polianciuc i in., 2020). Proces ten skutkuje deregulacją kluczowych szlaków metabolicznych zachodzących w glebie oraz generuje potencjalne ryzyko epidemiologiczne związane z transmisją determinant oporności (Cycoń i in., 2019; Lucas i in., 2021). Szczególną grupę związków stanowią fluorochinolony, powszechnie wykorzystywane w terapii przeciwdrobnoustrojowej. Jednym z etapów ich transformacji środowiskowej jest uwalnianie jonów fluorkowych (F^-), które – niezależnie od cząsteczki macierzystej – wykazują zdolność do modulowania struktury mikrobiomów glebowych (Gan i in., 2021; Jiang i in., 2024; Martin-Pozas i in., 2025; Pramanik i in., 2025; Wang i in., 2024). Pefloksacyna, jako reprezentatywny fluorochinolon, nie została dotychczas kompleksowo scharakteryzowana pod kątem oddziaływania – wraz z uwalnianymi jonami F^- – na mikrobiom roślin w warunkach kontrolowanych.

E. sativa stanowi modelowy organizm roślinny o znaczeniu zarówno użytkowym, jak i eksperymentalnym. Wykazano, że ekstrakty z jej tkanek liściowych posiadają właściwości przeciwdrobnoustrojowe, co wskazuje na obecność bioaktywnych metabolitów wtórnych (Bassyouni i in., 2022; Driss, 2015; Nikaido i in., 2010; Poulaki i in., 2024; Rizwana i in., 2016; Qaddoumi i El-Banna, 2019). Jednocześnie raportowano obecność bakterii oportunistycznych oraz szczepów wielolekoopornych w obrębie jej fylosfery (Cernava i in., 2019). Ambiwalentny charakter interakcji roślina-mikrobiom predysponuje *E. sativa* do zastosowania jej jako systemu modelowego w badaniach nad wpływem kontaminantów środowiskowych na strukturę i funkcję mikrobiomu roślinnego.

Ocena wpływu pefloksacyny oraz jonów fluorkowych na *E. sativa* i związany z nią mikrobiom dostarczają istotnych informacji dotyczących ekologicznych i agronomicznych konsekwencji obecności tych zanieczyszczeń. Dysbioza mikrobiomu może prowadzić do obniżenia kondycji fizjologicznej roślin oraz zaburzeń funkcji biogeochemicznych gleby, co w konsekwencji przekłada się na spadek produktywności agroekosystemów oraz wzrost podatności roślin na stresy abiotyczne. Identyfikacja taksonów selektywnie promowanych lub hamowanych przez F^- i pefloksacynę ma kluczowe znaczenie dla opracowania strategii przeciwdziałania rozprzestrzenianiu się oporności na antybiotyki.

Eksperymenty przeprowadzono w warunkach kontrolowanych, stosując suplementację gleby pefloksacyną lub fluorkiem sodu (NaF) w stężeniach 10 µM oraz 20 µM. Zastosowane stężenia NaF znajdowały się w dolnej części zakresu wartości raportowanych dla środowisk skażonych związkami fluoru (Fung i in., 1999; Jha i in., 2008; Jiang i in., 2024; Kalinić i in., 2005; Pramanik i in., 2025;

Yi i in., 2017). Stężenia pefloksacyny dobrano w sposób molowo równoważny względem NaF, co umożliwiło rozdzielenie efektów wynikających z aktywności farmakologicznej antybiotyku od wpływu jonów F^- uwalnianych w procesach degradacyjnych. Fluorochinolony, mimo wysokiej stabilności chemicznej rdzenia węglowego, wykazują zdolność do stopniowego uwalniania fluoru w warunkach środowiskowych (Murphy, 2016).

Analiza parametrów morfologicznych po czterotygodniowej ekspozycji nie wykazała istotnych statystycznie różnic pomiędzy wariantami eksperymentalnymi a kontrolą. Sugeruje to niską czułość *E. sativa* jako bioindykatora w analizach makroskopowych, analogicznie do obserwacji dla *L. minor*. Pomimo braku istotnych statystycznie różnic, próby traktowane charakteryzują się znacznie większą wariancją od prób kontrolnych. Wskazuje to na indukcję odpowiedzi stresowej o charakterze subletalnym, niewykrywalnej na poziomie makroskopowych cech fenotypowych. Wyniki te podkreślają konieczność integracji analiz fizjologicznych i biochemicznych w badaniach bioindykacyjnych.

W celu charakterystyki mikrobiomu przeprowadzono izolację całkowitego DNA bakteryjnego z tkanek nadziemnych (fylosfera) oraz strefy korzeniowej (ryzosfera). Uzyskane ekstrakty poddano sekwencjonowaniu nowej generacji z wykorzystaniem metabarcodingu regionu V3-V4 16S rDNA. Warianty sekwencji amplikonów (ASV) przypisano taksonomicznie z wykorzystaniem referencyjnych baz danych, umożliwiając analizę zmian na różnych poziomach organizacji biologicznej.

W przeciwieństwie do stabilności parametrów morfologicznych, struktura mikrobiomu wykazała istotną podatność na działanie badanych kontaminantów. Analiza różnorodności wskazała na istotną przebudowę społeczności mikroorganizmów, przy czym skala obserwowanych zmian była znacznie większa w fylosferze, niż w ryzosferze. Dodatkowo, efekt ten był bardziej wyraźny w wariantach traktowanych NaF, niż pefloksacyną. Sugeruje to istotną rolę jonów fluorkowych jako niezależnego czynnika stresowego.

Zmiany w strukturze mikrobiomu były w dużej mierze determinowane wzrostem liczebności bakterii należących do rzędu Burkholderiales, wykazującym dodatnią korelację ze stężeniem roztworów NaF. Taksony te obejmują zarówno oportunistyczne patogeny, jak i organizmy będące rezerwuarami genów oporności (Kneis i in., 2024; Shmarina i in., 2024; Voronina i in., 2018). Na niższych poziomach taksonomicznych obserwowano zmiany w obrębie mikroorganizmów uczestniczących w cyklu azotowym oraz procesach odżywiania roślin, co wskazuje na potencjalne zakłócenia funkcji troficznych mikrobiomu.

Szczególnie istotny był całkowity zanik przedstawicieli rodzaju *Pedobacter* w próbach suplementowanych, pomimo ich obecności w próbach kontrolnych. Bakterie te, charakteryzujące się

szerokim spektrum oporności na antybiotyki (Viana i in., 2018), wykazały nieoczekiwaną wrażliwość zarówno na pefloksacynę, jak i jony fluorkowe. Obserwacja ta sugeruje możliwość wykorzystania tych czynników w selektywnej modulacji populacji mikroorganizmów wielolekoopornych.

Analiza predykcyjna potencjału funkcjonalnego mikrobiomu, przeprowadzona z wykorzystaniem narzędzia PICRUSt2, wykazała, że największe zmiany dotyczyły szlaków metabolicznych związanych z przemianami węgla, co wskazuje na wysoką podatność centralnych procesów metabolicznych bakterii na stres indukowany przez fluor. Zmiany te były szczególnie nasilone w mikrobiomie fylosfery, podczas gdy w ryzosferze nie obserwowano istotnej dywergencji funkcjonalnej pomiędzy wariantami eksperymentalnymi.

WNIOSKI

Na podstawie przeprowadzonych analiz sformułowano następujące wnioski:

1. Składowanie odchodów brojlerów po aplikacji ciprofloksacyny w bezpośrednim kontakcie z glebą prowadzi do uwalniania fluorków w ilościach szkodliwych dla roślin. W zastosowanym zakresie stężeń roztworów antybiotyku z grupy fluorochinolonów, efekty toksyczne w przypadku *L. minor* ujawniały się głównie na poziomie fizjologicznym i biochemicznym. Stosowany zakres stężeń roztworów ciprofloksacyny nie powoduje zmian morfologicznych badanych roślin. Ocena wizualna *L. minor* jest niewystarczająca w analizie ich przydatności jako bioindykatorów, kluczowe znaczenie mają badania fizjologiczne i biochemiczne.
2. Jony fluorkowe mogą bezpośrednio oddziaływać chemicznie z cząsteczką chlorofilu, przy czym proces ten nie wymaga usunięcia jonu magnezu z pierścienia porfirynowego.
3. Zarówno pefloksacyna, jak i jony fluorkowe wywierają istotną presję selekcyjną na mikrobiom *E. sativa.* Obserwowane zmiany obejmują zaburzenia liczebności mikroorganizmów istotnych dla funkcjonowania roślin, jak również wzrost udziału bakterii potencjalnie niebezpiecznych dla zdrowia człowieka, w tym nosicieli genów oporności na antybiotyki.
4. Większa zmienność mikrobiomu w obrębie fylosfery w porównaniu z ryzosferą wskazuje na większą złożoność czynników oddziałujących na mikroorganizmy zasiedlające nadziemne części roślin oraz podkreśla potrzebę dalszych badań w tym zakresie.
5. Zaobserwowane zmiany w profilach metabolicznych, szczególnie w obrębie szlaków metabolizmu związków węgla, świadczą o istotnym wpływie fluoru i pefloksacyny na podstawowe procesy metaboliczne bakterii. Wyniki te podkreślają konieczność uwzględniania aspektów mikrobiologicznych w ocenie wpływu zanieczyszczeń środowiskowych, zwłaszcza antybiotyków, na funkcjonowanie ekosystemów.

BIBLIOGRAFIA

Ahmad, N.; Usman, M.; Ahmad, H.R.; Sabir, M.; Farooqi, Z.U.R.; Shehzad, M.T. Environmental implications of phosphate-based fertilizer industrial waste and its management practices. Environ. Monit. Assess. 2023, 195(11), 1326.

Ahmed, S.; Karamat, M.; Haider, A.; Jabeen, F.; Ahmad, M.N.; Ansari, M.; Zulfiqar, A.; Jalal, A.; Nizam, A. Ameliorative effects of salicylic acid on dry biomass and growth of *Pisum sativum* L. under sodium fluoride stress. Fluoride 2020, 53, 335–355.

Alferyeva, Y.O.; Gramenitskii, E.N.; Shchekina, T.I. Experimental study of phase relations in a lithium-bearing fluorine-rich haplogranite and nepheline syenite system. Geochem. Int. 2011, 49(7), 676–690.

Ali, S.; Thakur, S.K.; Sarkar, A.; Shekhar, S. Worldwide contamination of water by fluoride. Environ. Chem. Lett. 2016, 14, 291–315.

Arnesen, A.K.M. Availability of fluoride to plants grown in contaminated soils. Plant Soil 1997, 191, 13–25.

Banerjee, A.; Roychoudhury, A. Fluorine: A biohazardous agent for plants and phytoremediation strategies for its removal from the environment. Biol. Plant. 2019, 63, 104–112.

Barbier, O.; Arreola-Mendoza, L.; Del Razo, L.M. Molecular mechanisms of fluoride toxicity. Chem. Biol. Interact. 2010, 188, 319–333.

Bassyouni, R.H.; Kamel, Z.; Algameel, A.A.; Ismail, G.; Gaber, S.N. In-vitro determination of antimicrobial activities of *Eruca sativa* seed oil against antibiotic-resistant gram-negative clinical isolates from neonates: A future prospect. BMC Complement. Med. Ther. 2022, 22, 229.

Baunthiyal, M.; Ranghar, S. Physiological and biochemical responses of plants under fluoride stress: An overview. Fluoride 2014, 47, 287–293.

Bellomo, S.; Aiuppa, A.; D'Alessandro, W.; Parello, F. Environmental impact of magmatic fluorine emission in the Mt. Etna area. J. Volcanol. Geotherm. Res. 2007, 165, 87–101.

Benhamada, O.; Benhamada, N.; Leghouchi, E. Oxidative stress induced by fluorine in *Xanthoria parietina* (L.) Th. Fr. Int. J. Second. Metab. 2023, 10(1), 124–136.

Bhatt, S.; Chatterjee, S. Fluoroquinolone antibiotics: Occurrence, mode of action, resistance, environmental detection, and remediation–A comprehensive review. Environ. Pollut. 2022, 315, 120440.

Biglari, H.; Chavoshani, A.; Javan, N.; Mahvi, A.H. Geochemical study of groundwater conditions with special emphasis on fluoride concentration, Iran. Desalin. Water Treat. 2016, 57(47), 22392–22399.

Bokkers, E.A.M.; de Boer, I.J.M. Economic, ecological, and social performance of conventional and organic broiler production in the Netherlands. Br. Poult. Sci. 2009, 50, 546–557.

Cairns, J.; Ruokolainen, L.; Hultman, J.; Tamminen, M.; Virta, M.; Hiltunen, T. Ecology determines how low antibiotic concentration impacts community composition and horizontal transfer of resistance genes. Commun. biol. 2018, 1(1), 35.

Calfapietra, C.; Peñuelas, J.; Niinemets, Ü. Urban plant physiology: Adaptation-mitigation strategies under permanent stress. Trends Plant Sci. 2015, 20, 72–75.

Cernava, T.; Erlacher, A.; Soh, J.; Sensen, C.W.; Grube, M.; Berg, G. Enterobacteriaceae dominate the core microbiome and contribute to the resistome of arugula (*Eruca sativa* Mill.). Microbiome 2019, 7, 13.

Chaerle, L.; Van Der Straeten, D. Imaging techniques and the early detection of plant stress. Trends Plant Sci. 2000, 5, 495–501.

Chaney, R.L.; Oliver, D.P. Sources, potential adverse effects and remediation of agricultural soil contaminants. In Contaminants and the soil environment in the Australasia-Pacific region: Proceedings of the first Australasia-Pacific conference on contaminants and soil environment in the Australasia-Pacific region, Adelaide, Australia, 18–23 February 1996; Springer: Dordrecht, The Netherlands, 1996; pp. 323–359.

Chen, Q.L.; Cui, H.L.; Su, J.Q.; Penuelas, J.; Zhu, Y.G. Antibiotic resistomes in plant microbiomes. Trends Plant Sci. 2019, 24(6), 530–541.

Cheng, K.; Zhang, J.; Yi, P.; Zhu, G.; Hao, W.; Ji, W.; Tian, H.; Wang, Y. Exploring the emission characteristics and reduction potential of air pollutants from Chinese aluminum industry: 2005–2025. Earth's Fut. 2020, 8(11), e2019EF001440.

Choubisa, S.L. Are coal-based thermal power plants safe for human health in case of fluoride poisoning in India? People need to be careful and alert. Clin. Med. Rev. Rep. 2025, 7(3).

Cooper, J.; Propst, K.; Hirsch, C.D. Current methods and future needs for visible and non-visible detection of plant stress responses. Front. Plant Sci. 2025, 16, 1585413.

Cronin, S.J.; Neall, V.E.; Lecointre, J.A.; Hedley, M.J.; Loganathan, P. Environmental hazards of fluoride in volcanic ash: A case study from Ruapehu volcano, New Zealand. J. Volcanol. Geotherm. Res. 2003, 121, 271–291.

Cycoń, M.; Mrozik, A.; Piotrowska-Seget, Z. Antibiotics in the soil environment–degradation and their impact on microbial activity and diversity. Front. Microbiol. 2019, 10, 338.

Driss, D. Antioxidant and antimicrobial activities of solvent extract obtained from rocket (*Eruca sativa* L.) flowers. Free Radic. Antioxid. 2015, 5(1).

EFSA Scientific Committee, Bennekou, S.H.; Allende, A.; Bearth, A.; Casacuberta, J.; Castle, L.; Coja, T.; Crepet, A.; Hoogenboom, R.; Knutsen, H.; Lambre, C.; Nielsen, S.S; Turck, D.; Civera, A.V.; Villa, R.; …; Halldorsson, T. Updated consumer risk assessment of fluoride in food and drinking water including the contribution from other sources of oral exposure. EFSA Journal 2025, 23(7), e9478.

Ekperusi, A.O.; Sikoki, F.D.; Nwachukwu, E.O. Application of common duckweed (*Lemna minor*) in phytoremediation of chemicals in the environment: State and future perspective. Chemosphere 2019, 223, 285–309.

Eleftheriou, E.P.; Tsekos, I. Fluoride effects on leaf cell ultrastructure of olive trees growing in the vicinity of the aluminum factory of Greece. Trees 1991, 5, 83–89.

de Faria, M.R.; Costa, L.S.A.S.; Chiaramonte, J.B.; Bettiol, W.; Mendes, R. The rhizosphere microbiome: Functions, dynamics, and role in plant protection. Trop. Plant Pathol. 2021, 46, 13–25.

Feng, Y.W.; Ogura, N.; Feng, Z.W.; Zhang, F.Z.; Shimizu, H. The concentrations and sources of fluoride in atmospheric depositions in Beijing, China. Water Air Soil Pollut. 2003, 145, 95–107.

Fisher, D.J.; Yonkos, L.T.; Staver, K.W. Environmental concerns of roxarsone in broiler poultry feed and litter in Maryland, USA. Environ. Sci. Technol. 2015, 49, 1999–2012.

Fung, K.F.; Zhang, Z.Q.; Wong, J.W.C.; Wong, M.H. Fluoride contents in tea and soil from tea plantations and the release of fluoride into tea liquor during infusion. Environ. Pollut. 1999, 104, 197–205.

Frade, V.M.F.; Dias, M.; Teixeira, A.C.S.C.; Palma, M.S.A. Environmental contamination by fluoroquinolones. Braz. J. Pharm. Sci. 2014, 50, 41–54.

Fuge, R. Fluorine in the environment, a review of its sources and geochemistry. J. Appl. Geochem. 2019, 100, 393–406.

Gadi, B.R.; Kumar, R.; Goswami, B.; Rankawat, R.; Rao, S.R. Recent developments in understanding fluoride accumulation, toxicity, and tolerance mechanisms in plants: An overview. J. Soil Sci. Plant Nutr. 2021, 21, 209–228.

Gan, C.D.; Jia, Y.B.; Yang, J.Y. Remediation of fluoride contaminated soil with nano-hydroxyapatite amendment: Response of soil fluoride bioavailability and microbial communities. J. Hazard. Mater. 2021, 405, 124694.
Gatica, J.; Cytryn, E. Impact of treated wastewater irrigation on antibiotic resistance in the soil microbiome. Environ. Sci. Pollut. Res. 2013, 20, 3529–3538.
Gautam, M.; Pandey, B.; Agrawal, M. Carbon footprint of aluminum production: Emissions and mitigation. In Environmental carbon footprints; Muthu, S.S.; Ed.; Butterworth-Heinemann, Oxford, UK, 2018; pp. 197–228.
Gomes, T.F.; Rezende, F.P.; Lima, A.M.; de Souza, G.A.; Miranda, J.D.B.; Barbosa, A.P.; da Silva, L.C. Morphoanatomical and metabolic changes in *Bixa orellana* L.(Bixaceae) exposed to atmospheric fluorine. Environ. Sci. Pollut. Res. 2025, 32(15), 9541–9554.
Gouvêa, R.; Dos Santos, F.F.; De Aquino, M.H.C. Fluoroquinolones in industrial poultry production, bacterial resistance and food residues: A review. Braz. J. Poult. Sci. 2015, 17, 1–10.
Haddy, A.; Lee, I.; Shin, K.; Tai, H. Characterization of fluoride inhibition in photosystem II lacking extrinsic PsbP and PsbQ subunits. J. Photochem. Photobiol. B. 2018, 185, 1–9.
Harrington, L.F.; Cooper, E.M.; Vasudevan, D. Fluoride sorption and associated aluminum release in variable charge soils. J. Colloid Interface Sci. 2003, 267, 302–313.
Hartmann, M.; Six, J. Soil structure and microbiome functions in agroecosystems. Nat. Rev. Earth Environ. 2023, 4, 4–18.
He, Z.; Lan, H.; Gong, W.; Liu, R.; Gao, Y.; Liu, H.; Qu, J. Coagulation behaviors of aluminum salts towards fluoride: Significance of aluminum speciation and transformation. Sep. Purif. Technol. 2016, 165, 137–144.
Heaton, J.C.; Jones, K. Microbial contamination of fruit and vegetables and the behaviour of enteropathogens in the phyllosphere: A review. J. Appl. Microbiol. 2008, 104, 613–626.
Hong, B.D.; Joo, R.N.; Lee, K.S.; Lee, D.S.; Rhie, J.H.; Min, S.W.; Song, S.G.; Chung, D.Y. Fluoride in soil and plant. Korean J. Agric. Sci. 2016, 43, 522–536.
Huang, J.; Gao, K.; Yang, L.; Lu, Y. Successional action of Bacteroidota and Firmicutes in decomposing straw polymers in a paddy soil. Environ. Microbiome 2023, 18, 76.
Huang, W.Y.; Beach, E.D.; Fernandez-Cornejo, J.; Uri, N.D. An assessment of the potential risks of groundwater and surface water contamination by agricultural chemicals used in vegetable production. Sci. Total Environ. 1994, 153, 151–167.
Hyung, S.W.; Lee, C.H.; Kim, B. Development of certified reference materials for accurate determination of fluoroquinolone antibiotics in chicken meat. Food Chem. 2017, 229, 472–478.
Indermitte, E.; Saava, A.; Karro, E. Exposure to high fluoride drinking water and risk of dental fluorosis in Estonia. Int. J. Environ. Res. Public Health 2009, 6, 710–721.
Jaremko, D.; Kalembasa, D. A comparison of methods for the determination of cation exchange capacity of soils/Porównanie metod oznaczania pojemności wymiany kationów i sumy kationów wymiennych w glebach. Ecol. Chem. Eng., S. 2014, 21, 487–498.
Jha, S.K.; Nayak, A.K.; Sharma, Y.K.; Mishra, V.K.; Sharma, D.K. Fluoride accumulation in soil and vegetation in the vicinity of brick fields. Bull. Environ. Contam. Toxicol. 2008, 80(4), 369–373.
Jiang, Y.; Zhang, D.; Zhang, S.; Li, T.; Wang, G.; Xu, X.; Pu, Y.; Nengzi, L. Interaction effects of different chemical fractions of lanthanum, cerium, and fluorine on the taxonomic composition of soil microbial community. BMC Microbiol. 2024, 24, 539.
Jiao, L.; Ding, H.; Wang, L.; Zhou, Q.; Huang, X. Bisphenol A effects on the chlorophyll contents in soybean at different growth stages. Environ. Pollut. 2017, 223, 426–434.
Kabir, H.; Gupta, A.K.; Tripathy, S. Fluoride and human health: Systematic appraisal of sources, exposures, metabolism, and toxicity. Crit. Rev. Environ. Sci. Technol. 2020, 50, 1116–1193.

Kalinić, N.; Hršak, J.; Vadjić, V.; Lambaša-Belak, Ž.; Mihelčić, V.; Perković, B. Fluoride content in soil and vegetation. Bull. Environ. Contam. Toxicol. 2005, 75.

Kibet, B.J.; Jackson, C.K.; Cheruiyot, M.Y.; Munyendo, W.L.; Ambrose, K.; Oindo, A.G. Assessment of fluoride and selected heavy metals in food chain around fluorspar mining plant, Kenya. Greener J. Environ. Manag. Public Saf. 2019, 8, 15–24.

Kim, H.S.; Kim, J.S.; Suh, M.K.; Eom, M.K.; Lee, J.; Lee, J.S. A novel plant growth-promoting rhizobacterium, *Rhizosphaericola mali* gen. nov., sp. nov., isolated from healthy apple tree soil. Sci. Rep. 2024, 14, 1038.

Kneis, D.; Tskhay, F.; de la Cruz Barron, M.; Berendonk, T.U. Bacteria of the order Burkholderiales are original environmental hosts of type II trimethoprim resistance genes (*dfrB*). ISME J. 2024, 18, wrae243.

Krupka, M.; Piotrowicz-Cieślak, A.I. Optimization of the method for isolating bacterial DNA from the aboveground part of lettuce. Int. J. Mol. Sci. 2024, 25, 8513.

Li, M.; Qu, X.; Miao, H.; Wen, S.; Hua, Z.; Ma, Z.; He, Z. Spatial distribution of endemic fluorosis caused by drinking water in a high-fluorine area in Ningxia, China. Environ. Sci. Pollut. Res. 2020, 27(16), 20281–20291.

Lichtenthaler, H.K.; Buschmann, C. Chlorophylls and carotenoids. Measurement and characterization by UV-VIS spectroscopy. Curr. Protoc. Food Anal. Chem. 2001, 1, F4–3.

Liu, C.; Dai, Z.; Sun, H. Potential of duckweed (*Lemna minor*) for removal of nitrogen and phosphorus from water under salt stress. J. Environ. Manag. 2017, 187, 497–503.

Lucas, J.M.; Sone, B.M.; Whitmore, D.; Strickland, M.S. Antibiotics and temperature interact to disrupt soil communities and nutrient cycling. Soil Biol. Biochem. 2021, 163, 108437.

Luo, J.; Ni, D.; Li, C.; Du, Y.; Chen, Y. The relationship between fluoride accumulation in tea plant and changes in leaf cell wall structure and composition under different fluoride conditions. Environ. Pollut. 2021, 270, 116283.

Madhaiyan, M.; Poonguzhali, S.; Senthilkumar, M.; Pragatheswari, D.; Lee, J.S.; Lee, K.C. *Arachidicoccus rhizosphaerae* gen. nov., sp. nov., a plant-growth-promoting bacterium in the family Chitinophagaceae isolated from rhizosphere soil. Int. J. Syst. Evol. Microbiol. 2015, 65, 578–586.

Malago, J.; Makoba, E.; Muzuka, A.N. Fluoride levels in surface and groundwater in Africa: A review. Am. J. Water Sci. Eng. 2017, 3(1), 1–17.

Martin-Pozas, T.; Ghezzi, D.; D'Angeli, I.M.; Madonia, G.; Chiarini, V.; Vattano, M.; de Waele, J.; Cappeletti, M.; Saiz-Jimenez, C.; Jurado, V. Microbial and geochemical variability in sediments and biofilms from Italian gypsum caves. Microb. Ecol. 2025, 88, 81.

McMahon, P.B.; Brown, C.J.; Johnson, T.D.; Belitz, K.; Lindsey, B.D. Fluoride occurrence in United States groundwater. Sci. Total Environ. 2020, 732, 139217.

Minden, V.; Deloy, A.; Volkert, A.M.; Leonhardt, S.D.; Pufal, G. Antibiotics impact plant traits, even at small concentrations. AoB Plants 2017, 9, plx010.

Mirlean, N.; Roisenberg, A. Fluoride distribution in the environment along the gradient of a phosphate-fertilizer production emission (southern Brazil). Environ. Geochem. Health. 2007, 29(3), 179–187.

Moine, B.; de Parseval, P.; Rakotondrazafy, M.; Ramambazafy, A. Fluorine-controlled composition of biotite in granulites of Madagascar: the effect of fluorine on thermometry of biotite–garnet gneisses. Contrib. Mineral. Petrol. 2019, 174(9), 75.

Murphy, C.D. Microbial degradation of fluorinated drugs. Appl. Microbiol. Biotechnol. 2016, 100, 2617–2627.

Nikaido, M.; Tonani, K.A.; Julião, F.C.; Trevilato, T.M.; Takayanagui, A.M.; Sanches, S.M.; Segura-Muñoz, S.I. Analysis of bacteria, parasites, and heavy metals in lettuce (*Lactuca sativa*) and rocket salad (*Eruca sativa* L.) irrigated with treated effluent from a biological wastewater treatment plant. Biol. Trace Elem. Res. 2010, 134, 342–351.

Nithya, A.; Babu, S. Prevalence of plant beneficial and human pathogenic bacteria isolated from salad vegetables in India. BMC microbiology 2017, 17(1), 64.
Ogasawara, S.; Nakano, K.; Tamiaki, H. Synthesis of fluorinated chlorophylls-a and their bio/physico-chemical properties. Eur. J. Org. Chem. 2020, 2020, 5537–5543.
Ogawa, Y.; Tokunaga, E.; Kobayashi, O.; Hirai, K.; Shibata, N. Current contributions of organofluorine compounds to the agrochemical industry. iScience 2020, 23, 101467.
Omotoso, A.B.; Omojola, A.B. Fluoroquinolone residues in raw meat from open markets in Ibadan, Southwest, Nigeria. Int. J. Health Animal Sci. Food Saf. 2015, 2, 32–40.
Ozsvath, D.L. Fluoride concentrations in a crystalline bedrock aquifer Marathon County, Wisconsin. Environ. Geol. 2006, 50, 132–138.
Panda, D. Fluoride toxicity stress: Physiological and biochemical consequences on plants. Int. J. Bio-Resource Environ. Agric. Sci. 2015, 1, 70–84.
Pelc, J.; Śnioszek, M.; Wróbel, J.; Telesiński, A. Effect of fluoride on germination, early growth and antioxidant enzymes activity of three winter wheat (*Triticum aestivum* L.) cultivars. Appl. Sci. 2020, 10(19), 6971.
Peña, A.; Silva, L.J.G.; Pereira, A.; Meisel, L.; Lino, C.M. Determination of fluoroquinolone residues in poultry muscle in Portugal. Anal. Bioanal. Chem. 2010, 397, 2615–2621.
Peng, C.Y.; Xu, X.F.; Ren, Y.F.; Niu, H.L.; Yang, Y.Q.; Hou, R.Y.; Cai, H.M. Fluoride absorption, transportation and tolerance mechanism in *Camellia sinensis*, and its bioavailability and health risk assessment: A systematic review. J. Sci. Food Agric. 2021, 101, 379–387.
Pereira, A.M.; Silva, L.J.; Rodrigues, J.; Lino, C.; Pena, A. Risk assessment of fluoroquinolones from poultry muscle consumption: Comparing healthy adult and pre-school populations. Food Chem. Toxicol. 2018, 118, 340–347.
Pickering, W.F. The mobility of soluble fluoride in soils. Environ. Pollut., Ser. B, Chem. Phys. 1985, 9, 281–308.
Podgorski, J.; Berg, M. Global analysis and prediction of fluoride in groundwater. Nat. Commun. 2022, 13, 4232.
Polianciuc, S.I.; Gurzău, A.E.; Kiss, B.; Ştefan, M.G.; Loghin, F. Antibiotics in the environment: Causes and consequences. Med. Pharm. Rep. 2020, 93, 231–240.
Poulaki, E.G.; Karamichali, I.; Lianos, O.; Alexopoulos, V.; Dimitrakas, V.; Amourgis, G.G.; Tjamos, S.E. Exploring the biocontrol potential of rocket (*Eruca sativa*) extracts and associated microorganisms against *Verticillium wilt*. J. Appl. Microbiol. 2024, 135, lxae070.
Pramanik, K.; Sen, A.; Dutta, S.; Mandal, G.S.; Paramanik, B.; Das, A.; Chatterjee, N.; Ghorai, A.K.; Ali, M.N. Microbial populations under fluoride stress: A metagenomic exploration from Indian soil. World J. Microbiol. Biotechnol. 2025, 41, 221.
Pruden, A.; Larsson, D.J.; Amézquita, A.; Collignon, P.; Brandt, K.K.; Graham, D.W.; Lazorchak, J.M; Suzuki, S.; Silley, P.; Snape, J.R.; Topp, E.; Zhang, T.; Zhu, Y.G. Management options for reducing the release of antibiotics and antibiotic resistance genes to the environment. Environ. Health Perspect. 2013, 121(8), 878.
Pugajeva, I.; Avsejenko, J.; Judjallo, E.; Bērzin, Š.A.; Bartkiene, E.; Bartkevics, V. High occurrence rates of enrofloxacin and ciprofloxacin residues in retail poultry meat revealed by an ultra-sensitive mass-spectrometric method, and antimicrobial resistance to fluoroquinolones in *Campylobacter* spp. Food Addit. Contam. Part A. 2018, 35, 1107–1115.
Pyle, D.M.; Mather, T.A. Halogens in igneous processes and their fluxes to the atmosphere and oceans from volcanic activity: A review. Chem. Geol. 2009, 263, 110–121.
Qaddoumi, S.; El-Banna, N. Antimicrobial activity of arugula (*Eruca sativa*) leaves on some pathogenic bacteria. Int. J. Biol. 2019, 11, 10–15.
Rahman, F.; Noor, R. Prevalence of pathogenic bacteria in common salad vegetables of Dhaka Metropolis. Bangladesh J. Bot. 2012, 41(2), 159–162.

Ram, A.; Verma, P.; Gadi, B.R. Effect of fluoride and salicylic acid on seedling growth and biochemical parameters of watermelon (*Citrullus lanatus*). Fluoride 2014, 47, 49–55.

Rashid, A.; Schutte, B.J.; Ulery, A.; Deyholos, M.K.; Sanogo, S.; Lehnhoff, E.A.; Beck, L. Heavy metal contamination in agricultural soil: Environmental pollutants affecting crop health. Agronomy 2023, 13, 1521.

Rhimi, N.; Ben Ahmed, C.; Elloumi, N.; Athar, H.R.; Noreen, S.; Ashraf, M.; Ben Abdallah, F.; Ben Nasri-Ayachi, M. Morpho-anatomical and physiological changes in grapevine leaves exposed to atmospheric fluoride and sulfur dioxide pollution. Appl. Ecol. Environ. Res. 2016, 14(5), 77–89.

Rizwana, H.; Alwhibi, M.S.; Khan, F.; Soliman, D.A. Chemical composition and antimicrobial activity of *Eruca sativa* seeds against pathogenic bacteria and fungi. J. Anim. Plant Sci. 2016, 26(6), 1859–1871.

Rosberg, A.K.; Darlison, J.; Mogren, L.; Alsanius, B.W. Commercial wash of leafy vegetables do not significantly decrease bacterial load but leads to shifts in bacterial species composition. Food Microbiol. 2021, 94, 103667.

Ruan, J.; Ma, L.; Shi, Y.; Han, W. Uptake of fluoride by tea plant (*Camellia sinensis* L.) and the impact of aluminium. J. Sci. Food Agric. 2003, 83, 1342–1348.

Ruan, J.; Ma, L.; Shi, Y.; Han, W. The impact of pH and calcium on the uptake of fluoride by tea plants (*Camellia sinensis* L.). Ann. Bot. 2004, 93, 97–105.

Rudnick, R.L.; Gao, S. Composition of the continental crust. In Treatise on Geochemistry, 2nd ed.; Holland, H.D., Turekian, K.K., Eds.; Elsevier: Amsterdam, The Netherlands, 2014; Volume 4, pp. 1–51.

Saleem, M.; Hu, J.; Jousset, A. More than the sum of its parts: Microbiome biodiversity as a driver of plant growth and soil health. Annu. Rev. Ecol. Evol. Syst. 2019, 50, 145–168.

Sarkheil, M.; Safari, O. Phytoremediation of nutrients from water by aquatic floating duckweed (*Lemna minor*) in rearing of African cichlid (*Labidochromis lividus*) fingerlings. Environ. Technol. Innov. 2020, 18, 100747.

Sasmaz, M.; Topal, E.I.A.; Obek, E.; Sasmaz, A. The potential of *Lemna gibba* L. and *Lemna minor* L. to remove Cu, Pb, Zn, and As in gallery water in a mining area in Keban, Turkey. J. Environ. Manag. 2015, 163, 246–253.

Sawyer, G.M.; Oppenheimer, C. Volcanic fluorine emissions: Observations by Fourier transform infrared spectroscopy. Adv. Fluorine Sci. 2006, 1, 165–185.

Senkondo, Y.H.; Mkumbo, S.; Sospeter, P. Fluorine and copper accumulation in lettuce grown on fluoride and copper contaminated soils. Commun. Soil Sci. Plant Anal. 2018, 49, 2638–2652.

Senkondo, Y. Immobilization of fluoride in soils through soil properties: A review. J. Exp. Agric. Int. 2017, 19, 1–8.

Sharma, R.; Kaur, R. Insights into fluoride-induced oxidative stress and antioxidant defences in plants. Acta Physiol. Plant. 2018, 40(10), 181.

Shmarina, G.; Pukhalskaya, D.; Shmarin, V.; Semykin, S.; Avakyan, L.; Krasovsky, S.; Goryainova, A.; Kostyuk, S.; Zinchenko, R.; Kashirskaya, N. *Burkholderia cepacia* in cystic fibrosis children and adolescents: Overall survival and immune alterations. Front. Cell. Infect. Microbiol. 2024, 14, 1374318.

da Silva, V.P.; van der Werf, H.M.; Soares, S.R.; Corson, M.S. Environmental impacts of French and Brazilian broiler chicken production scenarios: An LCA approach. J. Environ. Manag. 2014, 133, 222–231.

Singh, G.; Kumari, B.; Sinam, G.; Kumar, N.; Mallick, S. Fluoride distribution and contamination in the water, soil and plants continuum and its remedial technologies, an Indian perspective–A review. Environ. Pollut. 2018, 239, 95–108.

Singh, A.; Roychoudhury, A.; Samanta, S.; Banerjee, A. Fluoride stress-mediated regulation of tricarboxylic acid cycle and sugar metabolism in rice seedlings in absence and presence of exogenous calcium. J. Plant Growth Regul. 2021, 40(4), 1579–1593.

Singh, M.; Verma, K.K. Influence of fluoride-contaminated irrigation water on physiological responses of poplar seedlings (*Populus deltoides* clone-S7C15). Fluoride 2013, 46, 83–89.

Sivasankar, V.; Darchen, A.; Omine, K.; Sakthivel, R. Fluoride: A world ubiquitous compound, its chemistry, and ways of contamination. In Surface modified carbons as scavengers for fluoride from water; Sivasankar, V., Ed.; Springer: Cham, Switzerland, 2016; pp. 5–32.

Syamsuhaidi, U.A.; Purnamasari, D.K.; Putra, R.A. Adding duckweed (*Lemna minor*) to local duck diet: determined based on the performance and heavy metal concentration in their meat. Am. J. Anim. Vet. Sci. 2025, 20(1): 86.96

Szablewski, T.; Stuper-Szablewska, K.; Cegielska-Radziejewska, R.; Tomczyk, Ł.; Szwajkowska-Michałek, L.; Nowaczewski, S. Comprehensive assessment of environmental pollution in a poultry farm depending on the season and the laying hen breeding system. Animals 2022, 12, 740.

Tang, Y.; Guan, X.; Su, T.; Gao, N.; Wang, J. Fluoride adsorption onto activated alumina: Modeling the effects of pH and some competing ions. Colloids Surf. A: Physicochem. Eng. Asp. 2009, 337, 33–38.

Taylor, R.P.; Fallick, A.E. The evolution of fluorine-rich felsic magmas: source dichotomy, magmatic convergence and the origins of topaz granite. Terra Nova, 1997, 9(3), 105–108.

Tiwari, K.K.; Raghav, R.; Pandey, R. Recent advancements in fluoride impact on human health: A critical review. Environ. Sustain. Indic. 2023, 20, 100305.

Trivedi, P.; Leach, J.E.; Tringe, S.G.; Sa, T.; Singh, B.K. Plant-microbiome interactions: From community assembly to plant health. Nat. Rev. Microbiol. 2020, 18(11), 607–621.

Velagaleti, R.R.; Marsh, S.S.; Reichenbach, N.G.; Kramer, D.; Fleischman, D.E. Some approaches to rapid and pre-symptom diagnosis of chemical stress in plants. In Plants for Toxicity Assessment; ASTM International: West Conshohocken, PA, USA, 1990; pp. 333–345.

Verma, K.K.; Verma, P.; Singh, M.; Verma, C.L. Influence of fluoride phytotoxicity in germinating seedlings of *Pisum sativum*: Modeling of morpho-physiological traits. Vegetos 2022, 35, 736–746.

Viana, A.T.; Caetano, T.; Covas, C.; Santos, T.; Mendo, S. Environmental superbugs: The case study of *Pedobacter* spp. Environ. Pollut. 2018, 241, 1048–1055.

Vithanage, M.; Bhattacharya, P. Fluoride in the environment: Sources, distribution and defluoridation. Environ. Chem. Lett. 2015, 13, 131–147.

Voronina, O.L.; Kunda, M.S.; Ryzhova, N.N.; Aksenova, E.I.; Sharapova, N.E.; Semenov, A.N.; Gintsburg, A.L. On Burkholderiales order microorganisms and cystic fibrosis in Russia. BMC Genom. 2018, 19, 74.

Walna, B.; Kurzyca, I.; Siepak, J. Variations in the fluoride level in precipitation in a region of human impact. In Acid Rain-Deposition to Recovery; Brimblecombe, P., Hara, H., Houle, D., Novak, M., Eds.; Springer: Dordrecht, The Netherlands, 2007; pp. 33–40.

Wang, X.; Ryu, D.; Houtkooper, R.H.; Auwerx, J. Antibiotic use and abuse: A threat to mitochondria and chloroplasts with impact on research, health, and environment. BioEssays 2015, 37, 1045–1053.

Wang, M.; Chen, X.; Hamid, Y.; Yang, X. Evaluating the response of the soil bacterial community and lettuce growth in a fluorine and cadmium co-contaminated yellow soil. Toxics 2024, 12, 459.

Widiastuti, R.; Martindah, E.; Anastasia, Y. Detection and dietary exposure assessment of fluoroquinolones residues in chicken meat from the districts of Malang and Blitar, Indonesia. Trop. Anim. Sci. J. 2022, 45, 98–103.

Wu, J.; Wang, J.; Li, Z.; Guo, S.; Li, K.; Xu, P.; Ok, Y.; Jones, D.L.; Zou, J. Antibiotics and antibiotic resistance genes in agricultural soils: A systematic analysis. Crit. Rev. Environ. Sci. Technol. 2023, 53, 847–864.

Wychodnik, K.; Gałęzowska, G.; Rogowska, J.; Potrykus, M.; Plenis, A.; Wolska, L. Poultry farms as a potential source of environmental pollution by pharmaceuticals. Molecules 2020, 25, 1031.

Xie, W.Y.; Shen, Q.; Zhao, F.J. Antibiotics and antibiotic resistance from animal manures to soil: A review. Eur. J. Soil Sci. 2018, 69, 181–195.

Xiong, Q.; Yang, J.; Ni, S. Microbiome-mediated protection against pathogens in woody plants. Int. J. Mol. Sci. 2023, 24, 16118.

Xu, H.; Chen, Z.; Huang, R.; Cui, Y.; Li, Q.; Zhao, Y.; Wang, X.; Mao, D.; Luo, Y.; Ren, H. Antibiotic resistance gene-carrying plasmid spreads into the plant endophytic bacteria using soil bacteria as carriers. Environ. Sci. Technol. 2021, 55(15), 10462–10470.

Xue, Y.; Peijnenburg, W.J.; Huang, J.; Wang, D.; Jin, Y. Trophic transfer of Cd from duckweed (*Lemna minor* L.) to tilapia (*Oreochromis mossambicus*). Environ. Toxicol. Chem. 2018, 37(5), 1367–1377.

Yadav, N.; Rani, K.; Yadav, S.S.; Yadav, D.K.; Yadav, V.K.; Yadav, N. Soil and water pollution with fluoride, geochemistry, food safety issues and reclamation–A review. Int. J. Curr. Microbiol. Appl. Sci. 2018, 7, 1147–1162.

Yayli, B.Ü.Ş.R.A.; Kilic, I. Assessment of environmental impacts of broiler farms using different indicators. Int. J. Environ. Sci. Technol. 2023, 20, 125–134.

Yi, X.; Qiao, S.; Ma, L.; Wang, J.; Ruan, J. Soil fluoride fractions and their bioavailability to tea plants (*Camellia sinensis* L.). Eviron. Geochem. Hlth. 2017, 39(5), 1005–1016.

Yu, K.; Qiu, Y.; Shen, Y.; Gao, C.; Feng, R.; Zeng, X.; Wang, W.; Chen, L.; Huang, L.S. Environmental concentrations of antibiotics alter the zebrafish gut microbiome structure and potential functions. Environ. Pollut. 2021, 278, 116760.

Zhang, X.; Zhang, Z.; Li, J.; Wu, L.; Guo, J.; Ouyang, L.; Xia, Y.; Huang, X.; Pang, X. Correlation of leaf senescence and gene expression/activities of chlorophyll degradation enzymes in harvested Chinese flowering cabbage (*Brassica rapa* var. *parachinensis*). J. Plant Physiol. 2011, 168, 2081–2087.

Zhang, J.; Brutus, T.E.; Cheng, J.; Meng, X. Fluoride removal by Al, Ti, and Fe hydroxides and coexisting ion effect. J. Environ. Sci. 2017, 57, 190–195.

Zouari, M.; Elloumi, N.; Bellassoued, K.; Ahmed, C.B.; Krayem, M.; Delmail, D.; Elfeki, A.; Ben Rouina, B.; Ben Abdallah, F.; Labrousse, P. Enzymatic antioxidant responses and mineral status in roots and leaves of olive plants subjected to fluoride stress. S. Afr. J. Bot. 2017, 111, 44–49.

Zuo, H.; Chen, L.; Kong, M.; Qiu, L.; Lü, P.; Wu, P.; Chen, K. Toxic effects of fluoride on organisms. Life Sci. 2018, 198, 18–24.

PUBLIKACJE

PUBLIKACJA 1

Kamiński, J., Stachelska-Wierzchowska, A., Michalczyk, D. J., Klimkowicz-Pawlas, A., Olkowska, E., Wolska, L., & Piotrowicz-Cieślak, A. I. 2024. Changes in metabolism and content of chlorophyll in common duckweed (*Lemna minor* L.) caused by environmental contamination with fluorides. Molecules, 29(10), 2336.

molecules

MDPI

Article

Changes in Metabolism and Content of Chlorophyll in Common Duckweed (*Lemna minor* L.) Caused by Environmental Contamination with Fluorides

Jan Kamiński [1], Alicja Stachelska-Wierzchowska [2], Dariusz J. Michalczyk [1], Agnieszka Klimkowicz-Pawlas [3], Ewa Olkowska [4], Lidia Wolska [4] and Agnieszka I. Piotrowicz-Cieślak [1,*]

[1] Department of Plant Physiology, Genetics and Biotechnology, University of Warmia and Mazury, Oczapowskiego Str. 1A, 10-719 Olsztyn, Poland; darim@uwm.edu.pl (D.J.M.)
[2] Department of Physics and Biophysics, University of Warmia and Mazury, Oczapowskiego Str. 4, 10-719 Olsztyn, Poland; alicja.stachelska@uwm.edu.pl
[3] Department of Soil Science Erosion and Land Protection, Institute of Soil Science and Plant Cultivation—State Research Institute, Czartoryskich Str. 8, 24-100 Puławy, Poland; agnes@iung.pulawy.pl
[4] Department of Environmental Toxicology, Faculty of Health Sciences, Medical University of Gdansk, Dębowa Str. 23A, 80-204 Gdansk, Poland; ewa.olkowska@gumed.edu.pl (E.O.); lidiawolska@gumed.edu.pl (L.W.)
* Correspondence: acieslak@uwm.edu.pl

Abstract: The impact of fluorine on plants remains poorly understood. We examined duckweed growth in extracts of soil contaminated with fluorine leached from chicken manure. Additionally, fluorine levels were analyzed in fresh manure, outdoor-stored manure, and soil samples at varying distances from the manure pile. Fresh manure contained 37–48 mg $F^- \times kg^{-1}$, while soil extracts contained 2.1 to 4.9 mg $F^- \times kg^{-1}$. We evaluated the physiological effects of fluorine on duckweed cultured on soil extracts or in 50% Murashige–Skoog (MS) medium supplemented with fluorine concentrations matching those in soil samples (2.1 to 4.9 mg $F^- \times L^{-1}$), as well as at 0, 4, and 210 mg $\times L^{-1}$. Duckweed exposed to fluorine displayed similar toxicity symptoms whether in soil extracts or supplemented medium. Fluoride at concentrations of 2.1 to 4.9 mg $F^- \times L^{-1}$ reduced the intact chlorophyll content, binding the porphyrin ring at position 3^2 without affecting Mg^{2+}. This reaction resulted in *chlorophyll a* absorption peak shifted towards shorter wavelengths and formation of a new band of the F^--*chlorophyll a* complex at $\lambda = 421$ nm. Moreover, plants exposed to low concentrations of fluorine exhibited increased activities of aminolevulinic acid dehydratase and chlorophyllase, whereas the activities of both enzymes sharply declined when the fluoride concentration exceeded 4.9 mg $\times L^{-1}$. Consequently, fluorine damages *chlorophyll a*, disrupts the activity of chlorophyll-metabolizing enzymes, and diminishes the plant growth rate, even when the effects of these disruptions are too subtle to be discerned by the naked human eye.

Keywords: chlorophyllase; aminolevulinic acid dehydratase; fluoride; chlorophyll absorption spectra; intensive poultry farming

check for updates

Citation: Kamiński, J.; Stachelska-Wierzchowska, A.; Michalczyk, D.J.; Klimkowicz-Pawlas, A.; Olkowska, E.; Wolska, L.; Piotrowicz-Cieślak, A.I. Changes in Metabolism and Content of Chlorophyll in Common Duckweed (*Lemna minor* L.) Caused by Environmental Contamination with Fluorides. *Molecules* **2024**, *29*, 2336. https://doi.org/10.3390/molecules29102336

Received: 16 April 2024
Revised: 9 May 2024
Accepted: 12 May 2024
Published: 16 May 2024

Copyright: © 2024 by the authors. Licensee MDPI, Basel, Switzerland. This article is an open access article distributed under the terms and conditions of the Creative Commons Attribution (CC BY) license (https://creativecommons.org/licenses/by/4.0/).

1. Introduction

Many human activities result in environmental pollution with pesticides, herbicides, artificial fertilizers, antibiotics, and various other substances, which have toxic effects on animals and plants [1,2]. Equally harmful are some naturally occurring pollutants and human activities can increase their concentrations excessively. These environmental toxins include fluorine and its compounds [3].

Fluorine is the 13th most abundant element in the Earth's crust. Its average concentration in continental plates is as high 557 mg $\times kg^{-1}$ [4]. Fluorine anions and their compounds, fluorides, are commonly found in groundwater and soil, especially in clay soils. The bedrock can sometimes be a natural source of soil fluoride. Fluoride-containing

rocks include granite, syenites, gneisses, and hornblende [5–9]. The concentration of F^- in soil at the site of gneisses and granites exceeds 5000 mg $\times$ kg^{-1} [2]. Through weathering of fluoride-containing rocks, F^- enters soils and groundwater. Volcanic eruptions could be another natural source of F^- [2]; however, they do not occur at this site. Fluorine escapes from volcanoes as HF gas, which is partly adsorbed onto volcanic ash. Through the volcanic route, an estimated 0.5 $\pm$ 0.2 Mt of fluorine enters the atmosphere annually [10]. However, none of these factors were a source of fluoride in the analyzed soil.

Fluorine present in the environment has anthropogenic origins in addition to the natural ones. The production of aluminum is one of the most important anthropogenic sources [11–13]. The production of 1 tonne of aluminum results in the release of 0.5–0.6 kg F [14]. Coal combustion greatly contributes to the release of F to the atmosphere [15]. Hard coal contains fluorine in amounts ranging from 4 to 40 g $\times$ kg^{-1} [1]. Annual HF emissions from coal-fired power plants in 2001 were as high as 55.8 million tonnes [16]. The increased level of fluorine in the environment is also due to the production of bricks and ceramic tiles [15]. This sector of industrial production releases 1.8 million tonnes F annually [17].

Fluorine compounds have been detected in groundwater in widely varying amounts depending on the country and sampling location. Worldwide, its content can range from 0.01 to 48 mg $\times$ L^{-1} [18]. In many African countries, China, South Asia, and the Middle East, groundwater is one of the main sources of drinking water [2,19]. According to WHO, the highest acceptable level of F in drinking water is 1.5 mg $\times$ L^{-1}. Values above this level have been detected in many countries in North and South America and Eurasia. In Pakistan, the fluorine content is 7.85 mg $\times$ L^{-1} [20], 2.3 mg $\times$ L^{-1} in Algeria [21], about 5 mg $\times$ L^{-1} in Argentina [22], 1.38 mg $\times$ L^{-1} in Poland at an industrial waste site [23], 0.3–9.2 mg $\times$ L^{-1} in Greece at aluminum processing plants [24], 3.2 and 6.5 mg $\times$ L^{-1} in the USA at industrial sites in Pennsylvania, and 7 mg $\times$ L^{-1} in Estonia in aquifers of Silurian and Ordovician age [25].

Fluorine compounds are commonly used in agriculture. Fluorine-containing compounds constitute 53% of all agrochemicals and insecticides represent over 70% of them [26]. Some fluorinated insecticidal agents are widely used against flies or other insects in poultry houses. These include bifenthrin, indoxacarb [27,28], cyfluthrin, fipronil, and lambda-cyhalothrin [26,29,30].

Intensification of agricultural production plays a significant role in the increase in F^- content in soil and groundwater. The use of phosphate fertilizers [15], pesticides, fumigants, and fluoride-containing antibiotics increases the fluorine level in the environment [1,31,32]. Rainfall contaminated by emissions from phosphate fertilizer production contains more than 1 mg $\times$ L^{-1} of fluoride and this concentration is observed at a distance of up to 2 km from the emission source [33]. Fluoroquinolones are fluorine-containing antibiotics commonly used in poultry husbandry. The presence of fluoroquinolones has even been found in broiler meat. Of the fluoroquinolones analyzed (ciprofloxacin, norfloxacin, enrofloxacin, sarafloxacin, ofloxacin), ciprofloxacin was present in the highest amounts, exceeding 1 mg $\times$ kg^{-1} of poultry meat [34]. However, the content of other antibiotics can also be significant. The levels of enrofloxacin and norfloxacin in broiler meat exceeded 242 and 113 µg $\times$ kg^{-1}, respectively [32,35–38]. As can be seen above, agricultural production leads to fluorine contamination of soil, water, and fertilizers through various pathways.

Fluorine present in the environment has extensively documented phytotoxic properties. Fluoride affects plants on many levels, including external morphology, tissue structures, and intracellular structures. Fluorine decreases the rate of cell division and growth, which hampers the overall plant growth and development [39]. Cell growth was markedly inhibited, for instance, in *Arabidopsis thaliana* cell suspension treated with 1 mM NaF [40]. Internal structure of cells gradually deteriorates with exposure time. This involves expansion and aggregation of endoplasmic reticulum, mitochondria losing electron density of the matrix, and eventual breakdown of tonoplast. Cells lose their shape and eventually collapse [41–45]. Fluoride toxicity in plants is also manifested by damage of cell membranes [46]. Fluoride stress induces lipoxygenase activity, which oxidizes membrane

lipids and eventually causes electrolyte leakage. The significant role of membrane lipid oxidation in F stress is also indicated by increased malondialdehyde content [47,48] and increased amounts of small molecular antioxidants (ascorbate, GSH) were also detected in plants responding to the fluoride-induced stress [47,49–51].

Fluoride ions interact with proteins, binding to their amino acid side chains, interfering with protein folding, modifying the protein 3D structures, and disrupting their functions. Moreover, increase in ROS resulting from F-induced stress causes carbonylation of amino acids and permanently damages proteins. F^- ions form complexes with metal cations essential in enzyme function, like Mg, Mn, and Fe, which inhibits many enzymes [45]. Fluoride shows high affinity to Al, and F is often absorbed by plants in complexes with Al. It was shown that the AlF_4^- complex acts as an analogue of the phosphate anion, thus inhibiting enzymes involving PO_4^{3-}, like ATPases and G proteins [52]. It is important, as enzymes involving phosphate are essential in all aspects of cell biology, including energy metabolism, signaling, and biosynthesis of various substances. Metal complexation by F interferes with other aspects of physiology, like Ca-related signaling.

Loss of chlorophyll is another widely documented and often very noticeable symptom of fluoride stress. Chlorosis usually begins at the leaf margins, progressing between veins towards the leaf base [1,3]. Leaves exposed to gaseous HF also show tissue damage, progressing over exposure time. Fluoride-induced leaf damage first appears in the spongy mesophyll and lower epidermis, followed by chloroplast damage in the palisade parenchyma [45,53]. Chlorosis is among the most universal symptoms reported in plants exposed to F^- contamination [54,55]. The mechanism of chlorophyll loss due to F stress is poorly understood. Complexation of Fe by F impairs chlorophyll biosynthesis [54]. Gaseous HF produces an acidic environment, which dissociates magnesium from the chlorophyll porphyrin ring. Both *chlorophyll a* and *chlorophyll b* levels decrease as a result of stress. However, both in plants growing under optimum conditions and plants subjected to stress, *chlorophyll a* usually clearly predominates in quantity [56,57].

F stress and disturbances in structure and contents of chlorophyll resulting from it not only impair light absorption by the photosynthetic apparatus but they also affect the photosynthetic electron transport chain. Total quantum efficiency of PSII is reduced due to inhibited Hill reaction. Fluoride ions substitute Cl^- in PSII, which blocks water photolysis and generates ROS [58]. Fan et al. [59] explored electron transport chain efficiency in tall fescue under combined F and Al stress. The PSI saturation with electrons dropped, while transferring electrons from plastoquinone increased. Photosynthesis impairment is also related to lowered activity of carbon-fixing and sugar-processing enzymes, like rubisco, amylase, invertase, and sucrose synthase [41,46,54]. Virtually nothing is known about reactions of fluoride ions with the carbon skeleton of chlorophyll.

The aim of this study was to evaluate the impact of extracts of soil contaminated with manure from intensive poultry farming (and consequently contaminated with fluoride) on plant physiological state. Duckweed (*Lemna minor* L.) was used as a bioindicator plant and the following parameters were analyzed: fluoride and *chlorophyll a* content, rate of plant growth, activities of chlorophyllase, and aminolevulinic acid dehydratase. In addition, we studied the molecular mechanism of fluoride's effect on chlorophyll in plants. To the best of our knowledge, the detailed mechanism of fluoride-induced chlorophyll decay in plants has not been fully understood to date.

2. Results and Discussion

2.1. Effect of Soil Extracts on the Growth of Duckweed (Environmental Samples)

Fluoride content was determined in three soil samples from fields located different distances from the improperly managed poultry manure pile. The location of the sampling points is shown in Figure 1. Soil sampling point 3 was located closest to the place where the manure from the poultry house was stored. It was shown that the highest fluoride content was in soils 2 and 3 and was 4.19 and 4.9 mg $\times$ kg^{-1} soil, respectively. A twice lower content of 2.1 mg $\times$ kg^{-1} was found in soil 1, located at a considerable distance

from the manure pile (Table 1). The assessed soil composition (soils 1, 2, 3) did not differ significantly. Soils 1 and 2 were classified as sandy loam, while soil 3 was a loamy sand. More detailed data on soil properties are given in Table S1.

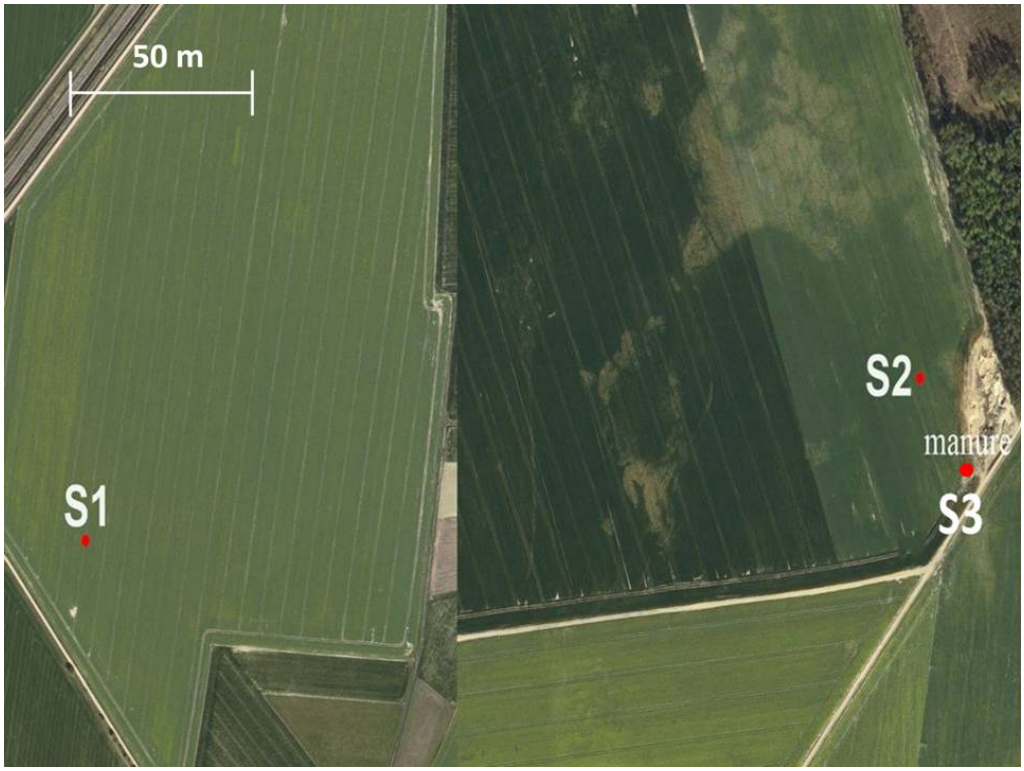


Figure 1. Place of sampling and location of manure pile.

Table 1. The content of fluoride ions, soil texture, extractable acidity, and exchangeable calcium cation content in the analyzed soils.

Soil	F^- Content mg × kg^{-1}	Sand, %	Silt, %	Clay, %	USDA Soil Texture Classes	pH_{KCl}	Hh cmol(+) × kg^{-1}	Al^{3+} g × kg^{-1}	Ca^{2+} cmol(+) × kg^{-1}
1	2.1	70.38	26.75	2.87	sandy loam	5.5	2.52	4.2	3.60
2	4.19	65.81	30.55	3.65	sandy loam	4.9	4.16	5.9	3.65
3	4.9	75.50	22.26	2.24	loamy sand	4.9	3.90	4.7	2.24

The fluoride content in manure collected from the inside of the poultry house was 37–48 mg × kg^{-1} and the F^- content in manure collected from the pile outside the chicken house was 1 mg × kg^{-1}.

The analyzed soils had a relatively low Ca^{2+} content, and total aluminum was at the level of 4.2, 5.9, and 4.7 g × kg^{-1} (in soils 1, 2, and 3, respectively). Ca^{2+} and Al^{3+} contents were analyzed because these cations have a high affinity for F^-, resulting in high F retention in clay soils rich in Al and Ca [15,17]. The fluorine content of the soil is also significantly affected by the soil pH. Under alkaline pH conditions, F mobility in the soil increases [60,61]; the same pattern (higher F solubility) is also observed at pH below 5 [62]. It should be emphasized that the soils analyzed were acidic (Table 1). In addition, fluoride-containing groundwater usually has a high pH and a high content of HCO_3^- and Na^+ [5,63–65]. The soil parameters analyzed (Table 1 and Supplementary Table S1) clearly indicate that the fluoride in analyzed samples was not a natural component of those soils but was leaked from the manure. Moreover, the manure stored inside the chicken house contained nearly fifty times more fluoride than the manure stored outside the chicken house. Apparently, much of the initial content of fluorides in manure is gradually leaked out due to atmospheric factors.

Selecting the location of sampling points, we ruled out areas located close to industrial centers, as Singh et al. [1] indicated that proximity to industrial plants can also be a source of soil fluoride. Only the manure pile could be the source of fluorides in the soil studied in this paper. It should be clearly stated that the source of fluoride ions in poultry excrement is unknown. One can speculate that they could originate either in preparations used to combat pests in broiler houses or medicinal substances containing fluorine.

Common duckweed was grown in soil extracts (samples taken from field at sites 1, 2, 3). We chose the duckweed as it is widely used as an indicator plant for the assessments of effects of chemical pollutants on plant physiology and biochemistry. Previous studies have mainly focused on heavy metal ions, especially Pb and Cd [66,67]. Common duckweed has not been investigated for responses to fluoride contamination to date.

Across all of the soil extracts analyzed, it was shown that the duckweed showed no morphological changes (Figure 2); the area of the shoots, their number, fresh and dry weight, and color showed no significant differences across the analyzed samples. However, with increased fluoride contents, there were significant decreases in chlorophyll content (Table 2) and activity of the enzymes: chlorophyllase (Chlase) and delta-aminolevulinic acid dehydratase (ALAD) (Figure 2H,I). The lowest ALAD value for soil 3 (fluoride level 4.9 mg × kg^{-1}) was 98 nmol of porphobililinogen produced per 1 g of fresh weight within 1 h, while the Chlase activity for plants growing in this soil was 0.11 mmol of chlorophyllide produced per 1 g of fresh weight within 1 h. A reduction in chlorophyll content was also observed in these samples.

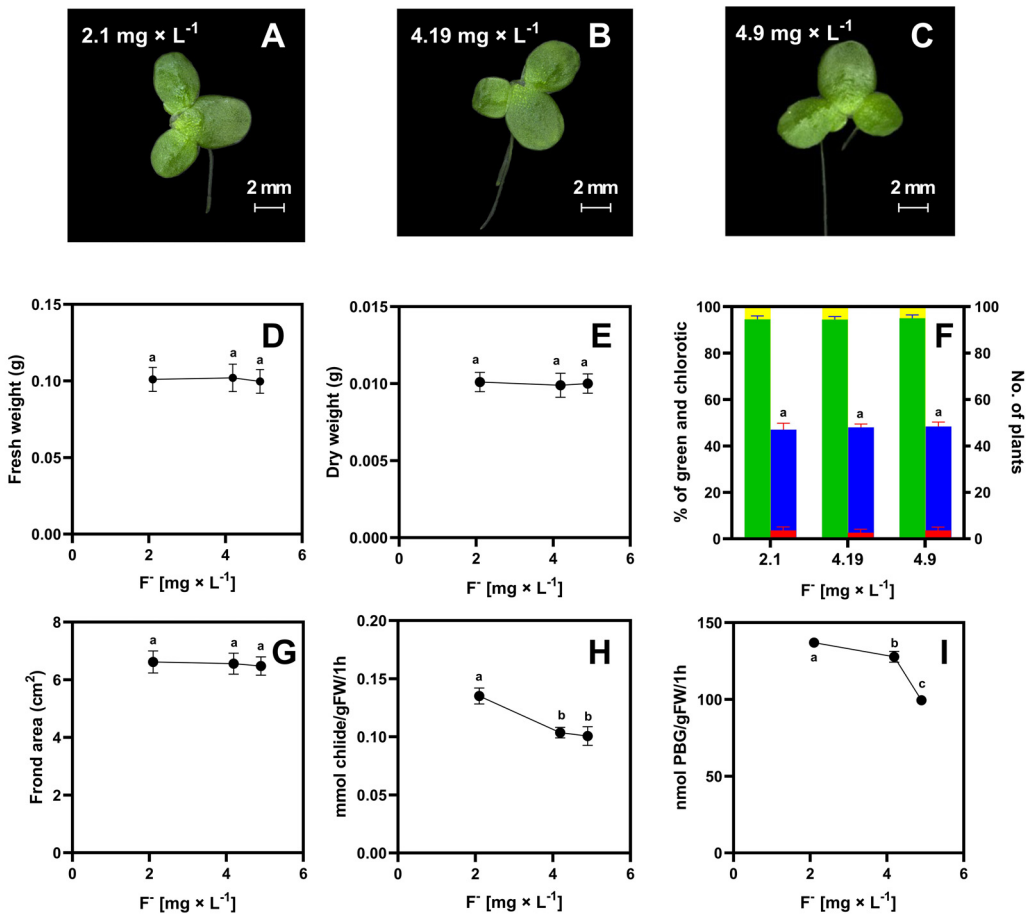


Figure 2. General appearance of plants after 7 days of growth in soil extracts (initial number of plants was ten)—(**A**–**C**); fresh weight [g]—(**D**); dry weight [g]—(**E**); percent frequency of green plants (green bar), percent frequency of yellow fronds (yellow bar), number of green plants (blue bar), number of yellow plants (red bar)—(**F**); surface area [cm^2]—(**G**); chlorophyllase activity [mmol of chlorophyllide

produced per 1 g of fresh weight within 1 h]—(**H**) and aminolevulinic acid dehydratase activity [as nmol of porphobilinogen produced per 1 g of fresh weight within 1 h]—(**I**). Tests were conducted in triplicates. The one-way analysis of variance (ANOVA) was carried out using Tukey's post hoc test ($p \leq 0.05$). Small letters represent groups of significant difference.

Table 2. Chlorophyll concentration in common duckweed growing in aqueous soil extracts. F^- [mg × L^{-1}], C [M] × 10^{-5} ± SD chlorophyll content. The one-way analysis of variance (ANOVA) was carried out using Tukey's post hoc test ($p \leq 0.05$). Small letters represent groups of significant difference.

	Chlorophyll a **Lambert–Beer Method**	***Chlorophyll a*** **Lichtenthaler, Buschmann Method**	***Chlorophyll b*** **Lichtenthaler, Buschmann Method**
Content F^- [mg × L^{-1}]	**C [M] × 10^{-5} ± SD**	**C [M] × 10^{-5} ± SD**	**C [M] × 10^{-5} ± SD**
2.10	6.24 ± 0.04 a	6.25 ± 0.03 a	1.82 ± 0.03 a
4.19	5.27 ± 0.03 b	5.27 ± 0.05 b	1.61 ± 0.04 b
4.90	2.68 ± 0.02 c	2.68 ± 0.01 c	0.89 ± 0.03 c

Chlorophyll absorption spectra and chlorophyll concentrations calculated from the Lambert–Beer law are shown in Supplementary Figure S1.

For soil 3, the chlorophyll content decreased by 57% relative to soil one (Table 2), but the reduction in chlorophyll content was not noticeable when visually comparing plant color (compare with Figure 2A–C). It should be noted that the amount of *chlorophyll a* was 3 to 4 times higher than *chlorophyll b* in all analyzed plants.

The F^- content in duckweed was also assessed before as well as after culture in the medium. It should be noted that the duckweed did take up F^- and its content in the surrounding medium decreased. The decrease in F^- content is shown in Table 3.

Table 3. Fluoride ion content before and after seven-day growth of the common duckweed. The one-way analysis of variance (ANOVA) was carried out using Tukey's post hoc test ($p \leq 0.05$). Small letters represent groups of significant difference.

Initial F^- Content [mg × L^{-1}]	**Final F^- Content [mg × L^{-1}]**	**Reduction in F^- [%]**
2.10	0.25 ± 0.01 a	88.0 a
4.19	0.19 ± 0.01 b	95.5 b
4.90	0.17 ± 0.004 b	96.5 b

2.2. Growth of Duckweed in Simulated Soil Extracts (50% MS Medium + F^-)

To eliminate the influence of potential soil contaminants or deficiencies, other than the presence of fluorine, some plants were grown in 50% MS medium supplemented with F^- at concentrations identical to those detected in the soil samples. It should be noted that 21 metals were detected in the analyzed soil, among them heavy metals, but none of them exceeded the permissible levels (Table S1). Additionally, a treatment was used in which the fluoride concentration was increased 100-fold compared to the soil with the lowest fluoride content and a concentration of 4 mg × L^{-1} was additionally applied; 50% Murashige–Skoog medium (50% MS) was used for duckweed, as it has been used successfully by other researchers to test various types of environmental contaminants [68–70].

Plants grown on F^--supplemented 50% MS media showed no morphological differences from plants grown on soil extracts with the same F^- concentrations; plant number, surface area, and fresh and dry weight were identical in both types of treatments. Different concentrations of fluorine also did not result in clear disturbances in plant appearance, except for the highest F^- concentration, which clearly caused plant death (Figure 3). At the highest fluorine concentration (210 mg × L^{-1}, not actually observed in studied soils), plants did not increase in number from the first day of culture, and their shoots disintegrated into

individual segments, which were totally chlorotic. Also, the ALAD and Chlase enzymes in plants grown in 50% MS medium + fluorine showed similar activity patterns to those from plants grown in soil extracts. An almost twofold increase in fluoride concentration from 2.10 to 4.19 or 4.90 mg × L^{-1} was not toxic to the plants. The only change that was observed was a reduction in chlorophyll content, but even these changes were not detectable visually but only by spectrophotometric determinations (Table 3).

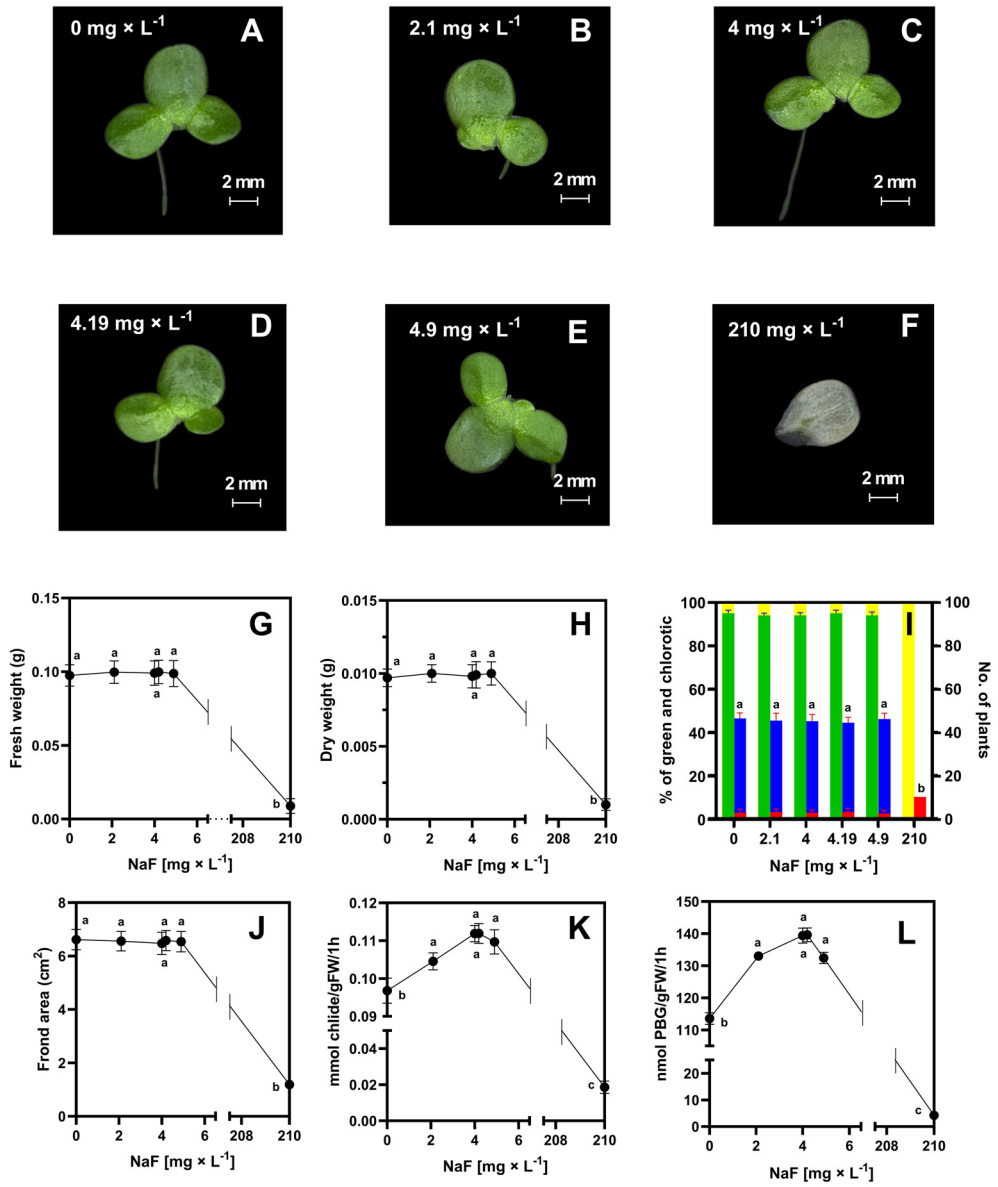


Figure 3. General appearance of plants after 7 days of growth in simulated soil extracts (50% MS medium + F^-)—(**A**–**F**); fresh weight [g]—(**G**); dry weight [g]—(**H**); percent frequency of green plants (green bar), percent frequency of yellow fronds (yellow bar), number of green plants (blue bar), number of yellow plants (red bar)—(**I**); surface area [cm^2]—(**J**); chlorophyllase activity [mmol of chlorophyllide produced per 1 g of fresh weight within 1 h]—(**K**) and aminolevulinic acid dehydratase activity [as nmol of porphobilinogen produced per 1 g of fresh weight within 1 h]—(**L**). Tests were conducted in triplicates. The one-way analysis of variance (ANOVA) was carried out using Tukey's post hoc test ($p \leq 0.05$). Small letters represent groups of significant difference.

The chlorophyll decay profile was identical in plants grown on soil extracts to the corresponding MS + fluorine plants with the same F^- concentration. At a fluoride ion dose of 210 mg × L^{-1}, chlorophyll was present in trace amounts (0.02 × 10^{-7} M) and a

reduction in chlorophyll content was visually apparent. Chlorophyll interactions with heavy metals have been studied repeatedly in terrestrial as well as aquatic plants [71–74]. An important feature of the action of metals, including heavy metals, is the substitution of Mg^{2+} ions in the porphyrin ring. Grajek et al. [71] indicated that after magnesium replacement with cadmium, a 50% decrease in chlorophyll content is observed due to the formation of the Cd-Chl complex. A decrease in fluorescence intensity and quenching by the Cd-Chl complex was also observed. Fluoride ions cannot replace Mg^{2+}, and therefore, no color change was observed.

Plants growing in 50% MS medium took up nearly 100% of F^- in the medium (Table 4), similar to plants grown in soil extracts. Only at the highest F^- concentration in 50% MS did the plants take up no more than 30% of F^- from the medium, and still it resulted in the death of the plants.

Table 4. Molar concentration of chlorophyll C [M] extracted from common duckweed growing in 50% Murashige–Skoog medium. Small letters represent groups of significant difference.

	Chlorophyll a **Lambert–Beer Method**	***Chlorophyll a*** **Lichtenthaler, Buschmann Method**	***Chlorophyll b*** **Lichtenthaler, Buschmann Method**
Initial F^- Content [mg× L^{-1}]	**C [M] × 10^{-5} ± SD**	**C [M] × 10^{-5} ± SD**	**C [M] × 10^{-5} ± SD**
0	12.25 ± 0.08 a	12.26 ± 0.08 a	3.19 ± 0.06 a
2.10	11.46 ± 0.08 b	11.48 ± 0.08 b	3.18 ± 0.06 b
4.00	11.23 ± 0.09 b	11.23 ± 0.10 b	3.04 ± 0.07 b
4.19	10.66 ± 0.02 c	10.66 ± 0.08 c	3.00 ± 0.08 b
4.90	6.51 ± 0.01 d	6.51 ± 0.08 d	1.80 ± 0.08 b
210	0 ± 0 e	0 ± 0 e	0 ± 0 e

2.3. Extracellular Reaction of Pure Chlorophyll a with Fluoride

In this section, we present the results of experiments on the effect of sodium fluoride on pure (commercial) chlorophyll using spectroscopic methods (absorption and fluorescence). Chlorophylls exhibit two main light absorption bands: the Soret band from 360 to 440 nm and the Q band consisting of Qy from 640 to 680 nm and Qx from 600 to 640 nm. The absorption and fluorescence measurement were carried out for a series of *chlorophyll a* solutions with a constant concentration of 1×10^{-5} M and sodium fluoride with concentrations corresponding to the fluorine content in the soil and Murashige and Skoog medium, and we additionally used a sodium fluoride concentration of 420 mg × L^{-1}. The experiment was conducted for 21 weeks. We used *chlorophyll a* in our studies because its content in plants is more than three times higher than that of *chlorophyll b* [75–79]; our results are shown in Tables 2 and 4. Figures 4 and 5 show selected absorption and fluorescence spectra of *chlorophyll a* with the addition of NaF at concentrations of 0, 0.021, 210, and 420 mg × L^{-1}. Figure 4A shows the results of *chlorophyll a* absorption tests without the addition of sodium fluoride. It can be seen that without the presence of NaF, the absorption value of *chlorophyll a* in the Q_y band at λ = 665 nm did not change. However, in the Soret band, the maximum chlorophyll absorption at λ = 433 nm increased slightly over the 21 weeks of the experiment. The fluorescence spectrum (Figure 4B) slightly shifted to the shortwave side after 21 weeks of storing the solutions at 4 °C and in the dark. The temperature of +4 °C was used in this study to minimize the degradation of *chlorophyll a*, and at the same time, not to significantly limit the rate of the reaction between *chlorophyll a* and sodium fluoride. It has been repeatedly shown that chlorophyll degradation is stimulated by light and temperature [56,57,80–82]. For short-term storage of chlorophyll (for 3–4 weeks), the recommended temperature is −20 °C, while for a longer storage, the recommended temperature is −70 °C, and it prevents a significant decrease in the concentration of *chlorophyll a* [83]. In vitro, chlorophyll molecules are not protected against photooxidation [84].

King et al. [85], however, showed that chlorophyll stored in vitro at temperatures close to 0 °C degrades much slower than at higher temperatures.

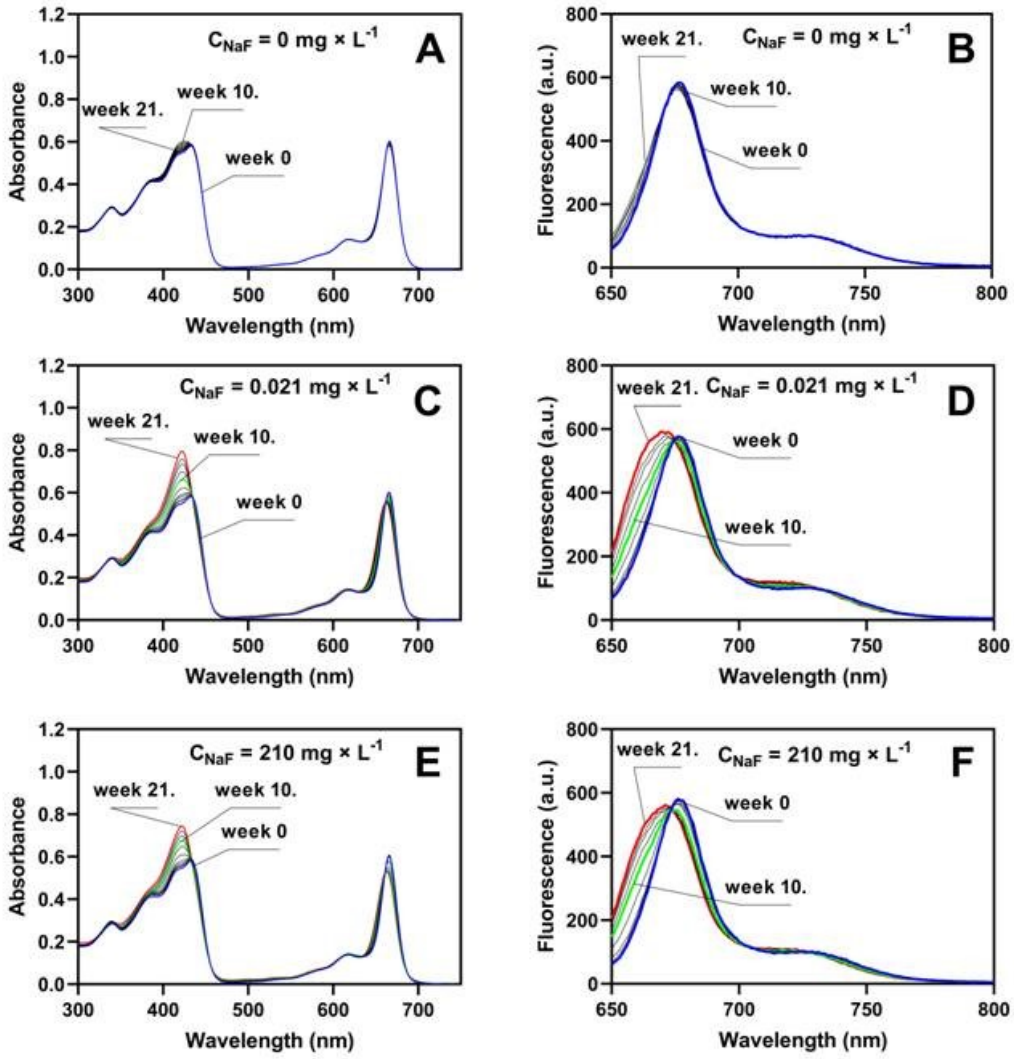


Figure 4. Absorption (**A**) and fluorescence (**B**) of *chlorophyll a* without NaF or with 0.021 mg × L^{-1} NaF (**C**,**D**), or with 210 mg × L^{-1} NaF (**E**,**F**). In the figures, the blue line marks the beginning of the reaction, the green line marks the 10th week, and the red line marks the 21st week of the reaction of chlorophyll with fluorine ions.

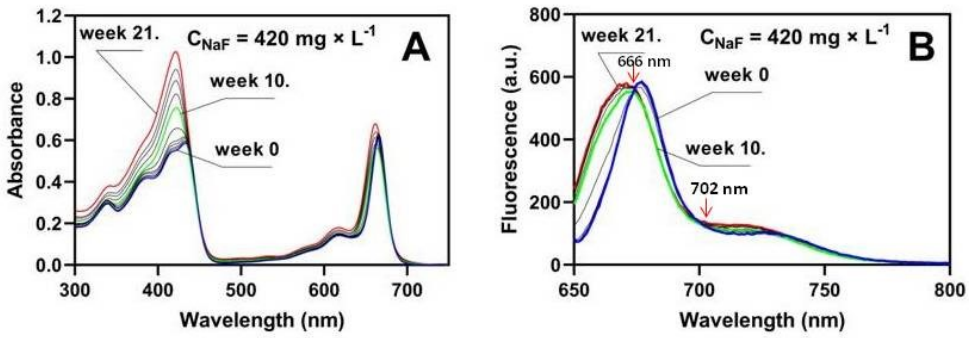


Figure 5. Absorption (**A**) and fluorescence (**B**) spectra of *chlorophyll a* after reaction with 420 mg × L^{-1} NaF. In the figures, the blue line marks the beginning of the reaction, the green line marks the 10th week, and the red line marks the 21st week of the reaction of chlorophyll with fluoride anions. The arrows show two isosbetic points at 666 and 702 nm.

In the case of treatment of chlorophyll with different doses of NaF, the absorbance value of *chlorophyll a* decreased within 10 weeks from A = 0.602 to A = 0.577 for C_{NaF} = 0.021 mg × L^{-1} (Figure 4C), and on the 10th week there was a shift in the absorption spectrum towards the shortwave. In the Soret band, there was also a shift in the absorption spectrum towards the short wavelength, and there was a large increase in the absorption of the newly created band: from the value of A = 0.582 to A = 0.796. Two isosbestic points were visible in the absorption spectra at wavelengths λ = 662 nm and λ = 435 nm, indicating the formation of a new chlorophyll–fluoride complex. For the maximum concentration, Figure 5 shows a fully developed spectrum of the complex (red line).

By carefully analyzing the Q_y band for the max dose of NaF (Figure 5A), we see that until the 10th week, the absorption band for chlorophyll decreases, and then this band shifts significantly to the shortwave direction, and an increase in the newly formed band at a wavelength of λ = 672 nm is observed. The value of this band reaches its maximum at a concentration of 420 mg × L^{-1}. The Soret band is changing significantly already in the 10th week. Its vibronic structure is lost and a new band of the complex is created at a wavelength of λ = 421 nm with a maximum of A = 1.026, for which the absorbance value in week 21 was almost twice as high as for *chlorophyll a* with C_{NaF} = 0.021 mg × L^{-1} (Figure 5).

The obtained results were fully confirmed by fluorescence tests. A strong shift of the fluorescence spectrum towards the shortwave region was observed. A new fluorescence band of the complex was created with a maximum at a wavelength of λ = 662 nm. A clear isosbestic point was visible at a wavelength of λ = 666 nm and 702 mn (Figure 5B). The reaction of HF with chlorophyll is known in the literature. However, this reaction causes the removal of magnesium and the introduction of hydrogen in its place [86,87]. In our case, we did not observe pheophytin production. The characteristic feature of the absorption spectrum of pheophytin is two absorption bands at wavelengths of 506 and 536 nm, distinguishing this compound from chlorophyll. There were no peaks at wavelengths of 506 and 536 nm, which clearly indicates the absence of pheophytin formation. Furthermore, using commercially highly purified pheophytin, we have shown that the presence of this compound does not shift the chlorophyll absorption band along the wavelength axis towards shorter wavelengths (Figure 6). We plotted pheophytin at two concentrations, *chlorophyll a*, and the new chlorophyll-fluoride complex on a single graph to compare the absorption spectra and demonstrate that there is no shift in absorption peaks concerning pheophytin.

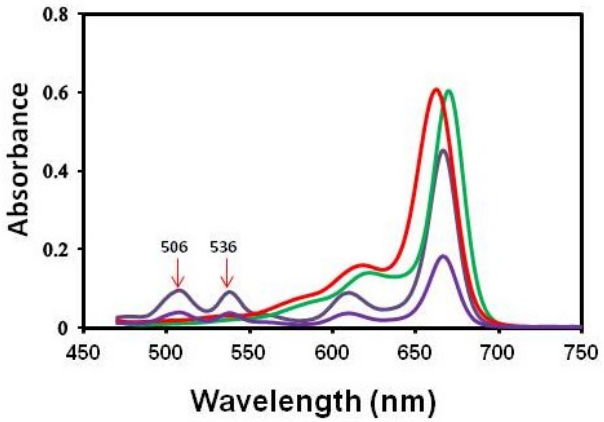


Figure 6. Absorption of chlorophyll (—), pheophytin in concentration 1 × 10^{-5} M (—), and a new product of chlorophyll reaction with fluoride (—). The arrows show two peaks characteristic for pheophytin at 506 and 536 nm.

The formation of pheophytin was observed during the reaction of tetracycline with chlorophyll, where tetracycline "extracted" magnesium from the porphyrin ring of chlorophyll, which resulted in a distinct color change chlorosis [88]. Formation of the $3F^2$ *chlorophyll a* complex was demonstrated by Ogasawara et al. [89], showing that the formation of such a complex causes a shift in the absorption spectrum by 3 nm. Our research also

shows a 3 nm shift in the absorption spectra, confirming the incorporation of fluorine in the same position. We also observed a significant shift in the fluorescence spectrum of the resulting complex compared to pure chlorophyll. The fluorescence spectrum of chemical compounds shifts only when the compound reacts and forms a complex [71]. In the analyzed solution, only two chemical compounds were present: chlorophyll and fluoride, from which a new complex compound was formed. The appearance of two isosbestic points (Figure 5B) at wavelengths 666 and 702 nm indicates the equilibrium between chlorophyll and $3F^2$-chlorophyll in the solution. Based on the results obtained by Ogasawara et al. [89], we suggest that in the new complex, fluorine was attached to the 3^2 position of chlorophyll. In our study, the formation of the fluorine derivative of chlorophyll occurred under different conditions and via a different mechanism than that observed by Ogasawara et al. [89]. In Ogasawara's study, the reaction was conducted using pheophytin as an intermediate product; however, as mentioned, this compound was undetectable in our case, and the reaction proceeded with completely different dynamics (products visible after 21 weeks). Spectroscopic analysis, however, suggests that the final product of the reaction observed in this study was the same as that observed by Ogasawara et al. [89].

Therefore, we suggest that fluorine forms a new complex with *chlorophyll a* (Figures 4 and 5); however, it does not knock out the magnesium (as is the case in plants responding to tetracycline; [88]) but it is linked to the carbon in position 3^2 in the porphyrin ring, which results in shifts of both the absorption and fluorescence spectra.

The paper confirms that antibiotics as environmental pollutants have a toxic effect on plant metabolism, and particularly on photosynthesis. In the case of some pharmaceuticals (e.g., tetracycline), these disorders are manifested by both restriction of growth rate and pronounced chlorosis. Our research shows that the mechanism of phytotoxic action of fluorides is different. As was found by many researchers [39–51], fluoride contamination results in a broad spectrum of disruptions in plants. However, the focus of this paper is on elucidating the mechanism of damage to chlorophyll molecules, as this aspect of fluorine phytotoxicity has been inadequately understood thus far. Among the analyzed F^- doses, only the highest concentration (210 mg $\times$ kg^{-1}) resulted in pronounced chlorosis and had a lethal effect on the plants. We showed that F^- even at low doses results in the formation of a fluorinated derivative of chlorophyll with F^- linked to the carbon in the porphyrin ring in position 3^2. We sought to investigate whether, at the highest dose of F^-, clearly phytotoxic, its interaction with chlorophyll remains consistent with that observed at lower doses. Our findings indicate that it does.

3. Materials and Methods

3.1. Collection of Soil and Manure Samples and Preparation of Extracts

Soil samples were taken directly from the surface layer (0–30 cm) of the arable lands in the Warmia and Masuria voivodeship in Poland in an early spring 2021. Soil 1 was from the arable field regularly fertilized with the manure and soils 2 and 3 were from the field in near the manure pile (See Figure 1). Additionally, manure samples were collected from the interior of the poultry houses and from the manure pile, located outdoors.

For each sampling site, six subsamples were collected from an area of 1 m^2, homogenized on the site after the removal of the upper layer of organic vegetative materials, and mixed to provide a bulked sample for each site. The soils were characterized in terms of their physicochemical properties (Table 1). Particle size distribution was measured by laser diffraction method, using the Mastersizer 2000 apparatus with Hydro UM attachment (Malvern Panalytical, Malvern, UK) [90]. The pH was measured potentiometrically in a suspension in KCl solution (1 mol $\times$ L^{-1}), extractable acidity was measured by Kappen method, and exchangeable cations by atomic absorption spectroscopy after soil extraction with 1 mol $\times$ L^{-1} CH_3COONH_4 [91].

In order to examine the effect of F pollution on common duckweed, water extracts were made from the examined soils and used as growth media. For this purpose, 100 g of each soil type was suspended in 100 mL of deionized water and shaken for 24 h on a Heidolph

Unimax 1010 shaker (Heidolph, Schwabach, Germany) at 80 rpm. The samples were filtered and the content of fluoride (F^-) in the soil extract was determined (see Section 3.3). The extracts were used as growth media for common duckweed.

3.2. Axenic Cultures of Duckweed (Lemna minor L.)

To eliminate other possible contaminants present in the soil, 50% Murashige and Skoog medium [92] was used as a simulated soil extract and the fluorine was added at the concentrations found in the soil extracts, at 2.1, 4.19, 4.9 mg × kg^{-1} of soil. Additionally, the content of F^- was increased 10 times compared to the lowest content detected in soil.

Axenic cultures of duckweed (*Lemna minor* L.), established at the Department of Plant Physiology, Genetics and Biotechnology of the University of Warmia and Mazury in Olsztyn, were used. Soil extract or 50% Murashige–Skoog (MS) medium (100 mL; supplemented with an appropriate amount of fluoride) was placed in a glass jar (a capacity of 250 mL) with 10 plants of duckweed, each with 3 visible fronds. The samples were incubated for 7 days at 16 h/8 h photoperiod and day/night temperatures of 25 °C/17 °C and with daytime light intensity of 3.4 klx (fluorescent lamp Osram L36W/77 Fluora, Osram, Munich, Germany). After 7 days of culture, plant material from each jar was tested for the activity of two enzymes: chlorophyllase (Chlase) and delta-aminolevulinic acid dehydratase (ALAD). Chlorophyll contents and morphological parameters of plants from each jar were also examined, including surface area of the fronds, fresh and dry weight, and severity of chlorosis. Chlorosis was visually assessed using a stereo microscope and by determining numbers of normal, green plants as opposed to the chlorotic plants. The experiment was carried out with three replications.

3.3. Fluoride Content

Deionized water (with electroconductivity 0.05 µS × cm^{-1}) from an R5 UV demineralizer (HydroLab, Straszyn, Poland) was used for preparation of fluoride standard solutions and the mobile phase. A 3.6 mM Na_2CO_3 solution was used as the eluent (99.95–100.05% ACS reagent, Sigma Aldrich, Buchs, Switzerland). Fluoride standards (1000 ± 2 mg × L^{-1}, TraceCERT® certified reference material) were obtained from Merck, Germany. Six-point linear calibration curves with three replicates were made using F^- standards in two ranges: 0.01–1 mg × L^{-1} and 1–40 mg × L^{-1}. Samples were filtered through 0.45 µm pore size 25 mm PVDF syringe filters (ALWSCI Technologies Co., Shaoxing, China).

An ion chromatography system with a conductometric detector (CDD-10 AVP), supplied by Shimadzu (Duisburg, Germany), was used to perform measurements. Eluent conductivity suppression was performed using a XAMS anion membrane suppressor with ASUREX-A100 automatic regenerator (Diduco AB, Umeå, Sweden). The Shodex SI-52 4E column (PEEK, 5 µm particle size, 4 mm ID × 250 mm length) from Showa Denko KK, Tokyo, Japan, was used. The eluent flow rate was 0.8 mL × min^{-1} with 30 min duration of analysis. The oven containing the column and suppressor was heated to 40 °C. The volume of each injected sample was 20 µL. The detection limit for F^- was 3.1 µg × L^{-1}. Calibration curves for both ranges showed good linearity (R^2 = 0.9996 and R^2 = 0.9998, respectively).

3.4. Aminolevulinic Acid Dehydratase Assay

The analysis was performed according to Jiao et al. [93]. Plant material, 0.1 g of fresh weight, was homogenized in 1 mL of 0.05 M Tris-HCl (pH 8.2) buffer containing 0.1 mM DTT. The homogenate was centrifuged at 6000× *g* for 0.5 h at 4 °C. The supernatant was used to measure enzymatic activity. Extract (1 mL) was added to 1.35 mL of 0.05 M Tris-HCl buffer (pH 8.2) containing 0.1 mM DTT, 0.08 mL of 0.2 M $MgCl_2$, and 0.27 mL of 1 mg × mL aminolevulinic acid solution. The mixture was incubated for 1 h at 37 °C. Subsequently, 0.3 mL of 3 M TCA was added to stop the reaction. The sample was centrifuged at 6000× *g* for 10 min. The supernatant was mixed with Ehrlich reagent added in 1:1 (*v*/*v*) ratio, and after 10 min, the absorbance was measured at 555 nm. The molar absorption coefficient for

PBG is 6.1 × 10^{-4}. The activity of the enzyme was expressed as nmol of porphobilinogen produced per 1 g of fresh weight within 1 h.

3.5. Chlorophyllase Assay

The analysis was carried out according to Zhang et al. [94]. The plant material was homogenized in a mortar in liquid nitrogen. Plant material (1 g of fresh weight) was added to 2 mL of extraction buffer composed of 0.1 M sodium-phosphate buffer (pH 6.0) with 0.2% (*v*/*v*) Triton X-100, 30 g × L^{-1} PVPP, 1 mM PMSF and 5 mM cysteine. The homogenate was centrifuged at 9000× *g*, 4 °C for 20 min. The supernatant was used to measure enzymatic activity. Plant extract (0.2 mL) was added to 1 mL of 0.1 M sodium-phosphate buffer (pH 7.0) with 0.15% Triton X-100 and 0.2 mL of *chlorophyll a* solution in acetone. The mixture was incubated for 1 h at 40 °C, after which the reaction was completed by adding 3 mL of hexane. The sample was stirred to produce an emulsion, after which 9000× *g* at 4 °C was centrifuged for 2 min. Chlorophyllase activity was tested by measuring the absorbance of the lower aqueous phase after centrifugation at 667 nm. The molar absorption coefficient for chlorophyllide in acetone is 76.79 mM^{-1} × cm^{-1}. The enzyme activity was expressed in mmol of chlorophyllide produced per 1 g of fresh weight within 1 h.

3.6. Chlorophyll Content Assay

Plants (fresh weight 300 mg) were homogenized in 5 mL methanol. The samples were centrifuged at 7000× *g* for 5 min. The supernatant was collected and diluted 5× in methanol. The absorbance of extract was determined using Cary 5000 UV-Vis NIR spectrophotometer. Chlorophyll concentrations were calculated based on the Lambert–Beer law, using the known molar extinction coefficient of *chlorophyll a* in methanol (ε = 66,600 $M^{-1}cm^{-1}$) [95]. Additionally, the content of *chlorophyll a* and *b* was determined using the formulas provided by Lichtenthaler and Buschmann [96] for methanol solutions of chlorophyll. However, absorbance values measured at A652 and 665 nm were substituted for A652.4 and A665.2, respectively, in the Lichtenthaler and Buschmann formulas. This discrepancy arose because our spectrophotometer was unable to set wavelength values containing fractions. The obtained values in μg × mL^{-1} were then converted to mol × L^{-1}.

$$\text{Chl a } (\mu g/mL) = 16.72\ A_{665.2} - 9.16\ A_{652.4}$$

$$\text{Chl b } (\mu g/mL) = 34.09\ A_{652.4} - 15.28\ A_{665.2}$$

3.7. Effect of Fluoride on Chlorophyll a

Chlorophyll a (Sigma) was dissolved in methanol (ChemPur, Karlsruhe, Germany) to the concentration of 1 × 10^{-5} M and one of 3 concentrations of NaF, matching those in previously tested soils and MS media. Samples were incubated at room temperature in darkness for 10 days. Each day, spectrophotometric assay was performed using Cary 5000 UV-Vis NIR spectrophotometer for absorbance measurements and Cary Eclipse spectrophotometer for fluorescence measurements. Similarly, pheophytin (from ChromaDex, Longmont, CO, USA) was dissolved in methanol at concentrations of 1 × 10^{-5} M and its absorption was measured. All measurements were performed at temperatures of 25 ± 1 °C. Absorbance was tested in the wavelength range from 310 to 750 nm, emission was tested from 600 to 800 nm, and excitation was tested from 300 to 750 nm.

3.8. Experimental Procedure and Data Presentation

Each experiment was repeated three times and involved three internal replications. The results were presented as means followed by standard deviations.

3.9. Statistics

The results were analyzed using the one-way ANOVA test, and differences between groups were analyzed using Tukey's post hoc test with probability $p \leq 0.05$. All analyses were carried out using Statistica program 11.

4. Conclusions

1. Manure resulting as a by-product of poultry production contains phytotoxic levels of fluorine.
2. Extracts of such contaminated soil clearly affect the growth rate rather than morphology of *Lemna minor* as an indicator plant.
3. *Chlorophyll a* turns out to be the target of phytotoxic action of fluorine on *Lemna* plants.
4. This paper postulates the molecular mechanism of chlorophyll damage induced by fluorine, which is fluorine entering the porphyrin ring at position 3^2, and leaving magnesium ion at its central position.
5. Aquatic plants can serve as indicators of environmental pollution with fluoride, but visual assessment of their condition is not sufficient for this purpose. It is necessary to use at least simple instrumental analyses to reveal chlorophyll damage or changes in the activity of enzymes associated with its biosynthesis and catabolism. It is necessary to use at least simple instrumental analyses to reveal chlorophyll damage or changes in the activity of enzymes associated with its biosynthesis and catabolism.

Supplementary Materials: The following supporting information can be downloaded at: https://www.mdpi.com/article/10.3390/molecules29102336/s1, Table S1: The content of fluoride ions and physicochemical properties of soil—A, macroelements—B and other metals—C, D; Figure S1: Absorption spectra of chlorophyll isolated from duckweed A—growing on soil extracts and—B in conditions simulating soil extracts (50% MS + F^- medium).

Author Contributions: Writing—Original Draft, A.I.P.-C., J.K., A.K.-P., E.O., A.S.-W., L.W. and D.J.M.; Writing—Review and Editing, L.W. and A.I.P.-C.; Conceptualization, A.I.P.-C.; Investigation, J.K., A.K.-P., E.O., A.S.-W. and D.J.M.; Formal analysis, J.K., E.O., A.K.-P., A.S.-W. and D.J.M.; Visualization, J.K.; Data curation, A.I.P.-C.; Project administration, A.I.P.-C. and L.W.; Supervision, A.I.P.-C. All authors have read and agreed to the published version of the manuscript.

Funding: This research was funded by a grant from the National Science Centre, Poland (Grant No. UMO-2019/35/B/NZ7/04394).

Institutional Review Board Statement: Not applicable.

Informed Consent Statement: Not applicable.

Data Availability Statement: The original contributions presented in the study are included in the article.

Conflicts of Interest: The authors declare no conflicts of interest.

References

1. Singh, G.; Kumari, B.; Sinam, G.; Kumar, N.; Mallick, S. Fluoride distribution and contamination in the water, soil and plants continuum and its remedial technologies, an Indian perspective—A review. *Environ. Pollut.* **2018**, *239*, 95–108. [CrossRef] [PubMed]
2. Vithanage, M.; Bhattacharya, P. Fluoride in the environment: Sources, distribution and defluoridation. *Environ. Chem. Lett.* **2015**, *13*, 131–147. [CrossRef]
3. Choudhary, S.; Rani, M.; Devika, O.S.; Patra, A.; Singh, R.K.; Prasad, S.K. Impact of fluoride on agriculture: A review on its sources, toxicity in plants and mitigation strategies. *Int. J. Chem. Stud.* **2019**, *7*, 1675–1680.
4. Rudnick, R.L.; Gao, S. Composition of the continental crust. In *Treatise on Geochemistry*, 2nd ed.; Holland, H.D., Turekian, K.K., Eds.; Elsevier: Amsterdam, The Netherlands, 2014; Volume 4, pp. 1–51.
5. Handa, B.K. Geochemistry and genesis of fluoride-containing ground waters in India. *Groundwater* **1975**, *13*, 275–281. [CrossRef]
6. Jones, B.F.; Eugster, H.P.; Rettig, S.L. Hydrochemistry of the lake Magadi basin, Kenya. *Geochim. Cosmochim. Acta* **1977**, *41*, 53–72. [CrossRef]

7. Kabir, H.; Gupta, A.K.; Tripathy, S. Fluoride and human health: Systematic appraisal of sources, exposures, metabolism, and toxicity. *Crit. Rev. Environ. Sci. Technol.* **2020**, *50*, 1116–1193. [CrossRef]
8. Ozsvath, D.L. Fluoride concentrations in a crystalline bedrock aquifer Marathon County, Wisconsin. *Environ. Geol.* **2006**, *50*, 132–138. [CrossRef]
9. Sivasankar, V.; Darchen, A.; Omine, K.; Sakthivel, R. Fluoride: A world ubiquitous compound, its chemistry, and ways of contamination. In *Surface Modified Carbons as Scavengers for Fluoride from Water*; Sivasankar, V., Ed.; Springer: Cham, Switzerland, 2016; pp. 5–32.
10. Pyle, D.M.; Mather, T.A. Halogens in igneous processes and their fluxes to the atmosphere and oceans from volcanic activity: A review. *Chem. Geol.* **2009**, *263*, 110–121. [CrossRef]
11. Feng, Y.W.; Ogura, N.; Feng, Z.W.; Zhang, F.Z.; Shimizu, H. The concentrations and sources of fluoride in atmospheric depositions in Beijing, China. *Water Air Soil Pollut.* **2003**, *145*, 95–107. [CrossRef]
12. Neal, C. Fluorine variations in Welsh streams and soil waters. *Sci. Total Environ.* **1989**, *80*, 213–223. [CrossRef]
13. Walna, B.; Kurzyca, I.; Siepak, J. Variations in the fluoride level in precipitation in a region of human impact. In *Acid Rain-Deposition to Recovery*; Brimblecombe, P., Hara, H., Houle, D., Novak, M., Eds.; Springer: Dordrecht, The Netherlands, 2007; pp. 33–40.
14. Tjahyono, N.; Gao, Y.; Wong, D.; Zhang, W.; Taylor, M.P. Fluoride emissions management guide (FEMG) for aluminium smelters. In *Light Metals*; Lindsay, S.J., Ed.; Springer: Cham, Switzerland, 2011; pp. 301–306.
15. Tylenda, C.A. *Toxicological Profile for Fluorides, Hydrogen Fluoride, and Fluorine*; DIANE Publishing: Collingdale, PA, USA, 2011; pp. 211–213.
16. Ranjan, R.; Ranjan, A. Sources of fluoride toxicity. In *Fluoride Toxicity in Animals*; Springer: Cham, Switzerland, 2015; pp. 11–20.
17. Fuge, R. Fluorine in the environment, a review of its sources and geochemistry. *J. Appl. Geochem.* **2019**, *100*, 393–406. [CrossRef]
18. Emamjomeh, M.M.; Sivakumar, M. Fluoride removal by a continuous flow electrocoagulation reactor. *J. Environ. Manag.* **2009**, *90*, 1204–1212. [CrossRef] [PubMed]
19. Ayoob, S.; Gupta, A.K. Fluoride in drinking water: A review on the status and stress effects. *Crit. Rev. Environ. Sci. Technol.* **2006**, *36*, 433–487. [CrossRef]
20. Naseem, S.; Rafique, T.; Bashir, E.; Bhanger, M.I.; Laghari, A.; Usmani, T.H. Lithological influences on occurrence of high-fluoride groundwater in Nagar Parkar area, Thar Desert, Pakistan. *Chemosphere* **2010**, *78*, 1313–1321. [CrossRef] [PubMed]
21. Messaïtfa, A. Fluoride contents in groundwaters and the main consumed foods (dates and tea) in Southern Algeria region. *Environ. Geol.* **2008**, *55*, 377–383. [CrossRef]
22. Kruse, E.; Ainchil, J. Fluoride variations in groundwater of an area in Buenos Aires Province, Argentina. *Environ. Geol.* **2003**, *44*, 86–89. [CrossRef]
23. Czarnowski, W.; Wrześniowska, K.; Krechniak, J. Fluoride in drinking water and human urine in northern and central Poland. *Sci. Total Environ.* **1996**, *191*, 177–184. [CrossRef] [PubMed]
24. Haidouti, C. Fluoride distribution in soils in the vicinity of a point emission source in Greece. *Geoderma* **1991**, *49*, 129–138. [CrossRef]
25. Indermitte, E.; Saava, A.; Karro, E. Exposure to high fluoride drinking water and risk of dental fluorosis in Estonia. *Int. J. Environ. Res. Public Health* **2009**, *6*, 710–721. [CrossRef]
26. Ogawa, Y.; Tokunaga, E.; Kobayashi, O.; Hirai, K.; Shibata, N. Current contributions of organofluorine compounds to the agrochemical industry. *iScience* **2020**, *23*, 101467. [CrossRef]
27. Abbas, N.; Ijaz, M.; Shad, S.A.; Binyameen, M. Assessment of resistance risk to fipronil and cross resistance to other insecticides in the *Musca domestica* L. (Diptera: Muscidae). *Vet. Parasitol.* **2016**, *223*, 71–76. [CrossRef] [PubMed]
28. Abbas, N.; Khan, H.A.A.; Shad, S.A. Resistance of the house fly *Musca domestica* (Diptera: Muscidae) to lambda-cyhalothrin: Mode of inheritance, realized heritability, and cross-resistance to other insecticides. *Ecotoxicology* **2014**, *23*, 791–801. [CrossRef] [PubMed]
29. Ong, S.Q.; Ahmad, H.; Jaal, Z.; Rus, A.C. Comparative effectiveness of insecticides for use against the house fly (Diptera: Muscidae): Determination of resistance levels on a Malaysian poultry farm. *J. Econ. Entomol.* **2016**, *109*, 352–359. [CrossRef]
30. Scott, J.G.; Alefantis, T.G.; Kaufman, P.E.; Rutz, D.A. Insecticide resistance in house flies from caged-layer poultry facilities. *Pest Manag. Sci.* **2000**, *56*, 147–153. [CrossRef]
31. Borah, J.; Saikia, D. Estimation of the concentration of fluoride in the ground water of Tinsukia Town master plan area of the Tinsukia district, Assam, India. *Arch. Appl. Sci. Res.* **2011**, *3*, 202–206.
32. Pena, A.; Silva, L.J.G.; Pereira, A.; Meisel, L.; Lino, C.M. Determination of fluoroquinolone residues in poultry muscle in Portugal. *Anal. Bioanal. Chem.* **2010**, *397*, 2615–2621. [CrossRef] [PubMed]
33. Mirlean, N.; Roisenberg, A. Fluoride distribution in the environment along the gradient of a phosphate-fertilizer production emission (southern Brazil). *Environ. Geochem. Health* **2007**, *29*, 179–187. [CrossRef] [PubMed]
34. Hyung, S.W.; Lee, C.H.; Kim, B. Development of certified reference materials for accurate determination of fluoroquinolone antibiotics in chicken meat. *Food Chem.* **2017**, *229*, 472–478. [CrossRef]
35. Omotoso, A.B.; Omojola, A.B. Fluoroquinolone residues in raw meat from open markets in Ibadan, Southwest, Nigeria. *Int. J. Health Animal Sci. Food Saf.* **2015**, *2*, 32–40. [CrossRef]

36. Pereira, A.M.; Silva, L.J.; Rodrigues, J.; Lino, C.; Pena, A. Risk assessment of fluoroquinolones from poultry muscle consumption: Comparing healthy adult and pre-school populations. *Food Chem. Toxicol.* **2018**, *118*, 340–347. [CrossRef]
37. Pugajeva, I.; Avsejenko, J.; Judjallo, E.; Bērziņš, A.; Bartkiene, E.; Bartkevics, V. High occurrence rates of enrofloxacin and ciprofloxacin residues in retail poultry meat revealed by an ultra-sensitive mass-spectrometric method, and antimicrobial resistance to fluoroquinolones in *Campylobacter* spp. *Food Addit. Contam.* **2018**, *35*, 1107–1115. [CrossRef] [PubMed]
38. Widiastuti, R.; Martindah, E.; Anastasia, Y. Detection and dietary exposure assessment of fluoroquinolones residues in chicken meat from the districts of Malang and Blitar, Indonesia. *Trop. Anim. Sci. J.* **2022**, *45*, 98–103. [CrossRef]
39. Ram, A.; Verma, P.; Gadi, B.R. Effect of fluoride and salicylic acid on seedling growth and biochemical parameters of watermelon (*Citrullus lanatus*). *Fluoride* **2014**, *47*, 49–55.
40. Pulyaevskaya, M.A.; Varakina, N.N.; Gamburg, K.Z.; Rusaleva, T.M.; Stepanov, A.V.; Voinikov, V.K.; Rikhvanov, E.G. Sodium fluoride inhibits HSP synthesis in heat-stressed cultured cells of *Arabidopsis thaliana*. *Russ. J. Plant Physiol.* **2011**, *58*, 589–596. [CrossRef]
41. Baunthiyal, M.; Ranghar, S. Physiological and biochemical responses of plants under fluoride stress: An overview. *Fluoride* **2014**, *47*, 287–293.
42. Eleftheriou, E.P.; Tsekos, I. Fluoride effects on leaf cell ultrastructure of olive trees growing in the vicinity of the aluminium factory of Greece. *Trees* **1991**, *5*, 83–89. [CrossRef]
43. Fornasiero, R.B. Phytotoxic effects of fluorides. *Plant Sci.* **2001**, *161*, 979–985. [CrossRef]
44. Luo, J.; Ni, D.; Li, C.; Du, Y.; Chen, Y. The relationship between fluoride accumulation in tea plant and changes in leaf cell wall structure and composition under different fluoride conditions. *Environ. Pollut.* **2021**, *270*, 116283. [CrossRef] [PubMed]
45. Panda, D. Fluoride toxicity stress: Physiological and biochemical consequences on plants. *Int. J. Bio-Resour. Environ. Agric. Sci.* **2015**, *1*, 70–84.
46. Verma, K.K.; Verma, P.; Singh, M.; Verma, C.L. Influence of fluoride phytotoxicity in germinating seedlings of *Pisum sativum*: Modeling of morpho-physiological traits. *Vegetos* **2022**, *35*, 736–746. [CrossRef]
47. Banerjee, A.; Roychoudhury, A. Fluorine: A biohazardous agent for plants and phyto remediation strategies for its removal from the environment. *Biol. Plant.* **2019**, *63*, 104–112. [CrossRef]
48. Junior, A.M.D.; Oliva, M.A.; Martinez, C.A.; Cambraia, J. Effects of fluoride emissions on two tropical grasses: *Chloris gayana* and *Panicum maximum* cv. Colonião. *Ecotoxicol. Environ. Saf.* **2007**, *67*, 247–253. [CrossRef] [PubMed]
49. Ahmed, S.; Karamat, M.; Haider, A.; Jabeen, F.; Ahmad, M.N.; Ansari, M.; Zulfiqar, A.; Jalal, A.; Nizam, A. Ameliorative effects of salicylic acid on dry biomass and growth of *Pisum sativum* L. under sodium fluoride stress. *Fluoride* **2020**, *53*, 335–355.
50. Doley, D.; Hill, R.J.; Riese, R.H. Environmental fluoride in Australasia: Ecological effects, regulation and management. *Clean Air Environ. Qual.* **2004**, *38*, 35–55.
51. Singh, M.; Verma, K.K. Influence of fluoride-contaminated irrigation water on physiological responses of poplar seedlings (*Populus deltoides* clone-S7C15). *Fluoride* **2013**, *46*, 83–89.
52. Barbier, O.; Arreola-Mendoza, L.; Del Razo, L.M. Molecular mechanisms of fluoride toxicity. *Chem. Biol. Interact.* **2010**, *188*, 319–333. [CrossRef] [PubMed]
53. Rhimi, N.; Mezghani, I.; Elloumi, N.; Nasri, M.; Ben Abdallah, F. Morphological and anatomical responses of pear and almond trees to fluoride air pollution. *Fluoride* **2016**, *49*, 156–164.
54. Gadi, B.R.; Kumar, R.; Goswami, B.; Rankawat, R.; Rao, S.R. Recent developments in understanding fluoride accumulation, toxicity, and tolerance mechanisms in plants: An overview. *J. Soil Sci. Plant Nutr.* **2021**, *21*, 209–228. [CrossRef]
55. Hong, B.D.; Joo, R.N.; Lee, K.S.; Lee, D.S.; Rhie, J.H.; Min, S.W.; Song, S.G.; Chung, D.Y. Fluoride in soil and plant. *Korean J. Agric. Sci.* **2016**, *43*, 522–536. [CrossRef]
56. Hosikian, A.; Lim, S.; Halim, R.; Danquah, M.K. Chlorophyll extraction from microalgae: A review on the process engineering aspects. *Int. J. Chem. Eng.* **2010**, *2010*, 391632. [CrossRef]
57. Manolopoulou, E.; Varzakas, T.; Petsalaki, A. Chlorophyll determination in green pepper using two different extraction methods. *Curr. Res. Nutr. Food Sci.* **2016**, *4*, 52–60. [CrossRef]
58. Haddy, A.; Lee, I.; Shin, K.; Tai, H. Characterization of fluoride inhibition in photosystem II lacking extrinsic PsbP and PsbQ subunits. *J. Photochem. Photobiol. B Biol.* **2018**, *185*, 1–9. [CrossRef] [PubMed]
59. Fan, J.; Chen, K.; Xu, J.; Khaldun, A.B.M.; Chen, Y.; Chen, L.; Yan, X. Physiological effects induced by aluminium and fluoride stress in tall fescue (*Festuca arundinacea* Schreb). *Ecotoxical. Environ. Saf.* **2022**, *231*, 113192. [CrossRef]
60. Saxena, V.; Ahmed, S. Dissolution of fluoride in groundwater: A water-rock interaction study. *Environ. Geol.* **2001**, *40*, 1084–1087. [CrossRef]
61. Saxena, V.; Ahmed, S. Inferring the chemical parameters for the dissolution of fluoride in groundwater. *Environ. Geol.* **2003**, *43*, 731–736. [CrossRef]
62. Kabata-Pendias, A. *Trace Elements in Soils and Plants*, 4th ed.; CRC Press: Boca Raton, FL, USA, 2011.
63. Guo, Q.; Wang, Y.; Ma, T.; Ma, R. Geochemical processes controlling the elevated fluoride concentrations in groundwaters of the Taiyuan Basin, Northern China. *J. Geochem. Explor.* **2007**, *93*, 1–12. [CrossRef]
64. Jacks, G.; Bhattacharya, P.; Chaudhary, V.; Singh, K.P. Controls on the genesis of some high-fluoride groundwaters in India. *J. Appl. Geochem.* **2005**, *20*, 221–228. [CrossRef]

65. Jacks, G.; Rajagopalan, K.; Alveteg, T.; Jönsson, M. Genesis of high-F groundwaters, southern India. *J. Appl. Geochem.* **1993**, *8*, 241–244. [CrossRef]
66. Ozyigit, I.I.; Arda, L.; Yalcin, B.; Yalcin, I.E.; Ucar, B.; Hocaoglu-Ozyigit, A. *Lemna minor*, a hyperaccumulator shows elevated levels of Cd accumulation and genomic template stability in binary application of Cd and Ni: A physiological and genetic approach. *Int. J. Phytoremediat.* **2021**, *23*, 1255–1269. [CrossRef]
67. Sobrino, A.S.; Miranda, M.G.; Alvarez, C.; Quiroz, A. Bio-accumulation and toxicity of lead (Pb) in *Lemna gibba* L. (duckweed). *J. Environ. Sci. Health-Toxic/Hazard. Subst. Environ. Eng.* **2010**, *45*, 107–110. [CrossRef]
68. Kim, Y.; Hyun, S.H.; Park, H.E.; Choi, H.K. Metabolic profiling, free-radical scavenging and tyrosinase inhibitory activities of *Lemna minor* whole plants cultivated in various concentrations of proline and sucrose. *Process Biochem.* **2012**, *47*, 62–68. [CrossRef]
69. Krupka, M.; Michalczyk, D.J.; Žaltauskaitė, J.; Sujetovienė, G.; Głowacka, K.; Grajek, H.; Wierzbicka, M.; Piotrowicz-Cieślak, A.I. Physiological and biochemical parameters of common duckweed *Lemna minor* after the exposure to tetracycline and the recovery from this stress. *Molecules* **2021**, *26*, 6765. [CrossRef] [PubMed]
70. Stefaniak, B.; Woźny, A.; Budna, I. Callus induction and plant regeneration in *Lemna minor* L. *Biol. Plant.* **2002**, *45*, 469–472. [CrossRef]
71. Grajek, H.; Rydzyński, D.; Piotrowicz-Cieślak, A.; Herman, A.; Maciejczyk, M.; Wieczorek, Z. Cadmium ion-chlorophyll interaction–Examination of spectral properties and structure of the cadmium-chlorophyll complex and their relevance to photosynthesis inhibition. *Chemosphere* **2020**, *261*, 127434. [CrossRef] [PubMed]
72. Küpper, H.; Küpper, F.; Spiller, M. Environmental relevance of heavy metal substituted chlorophylls using the example of water plants. *J. Exp. Bot.* **1996**, *47*, 259–266. [CrossRef]
73. Küpper, H.; Parameswaran, A.; Leitenmaier, B.; Trtílek, M.; Setlík, I. Cadmium-induced inhibition of photosynthesis and long-term acclimation to cadmium stress in the hyperaccumulator *Thlaspi caerulescens*. *New Phytol.* **2007**, *175*, 655–674. [CrossRef] [PubMed]
74. Paunov, M.; Koleva, L.; Vassilev, A.; Vangronsveld, J.; Goltsev, V. Effects of different metals on photosynthesis: Cadmium and zinc affect chlorophyll fluorescence in durum wheat. *Int. J. Mol. Sci.* **2018**, *19*, 787. [CrossRef] [PubMed]
75. Anderson, J.M.; Goodchild, D.J.; Boardman, N.K. Composition of the photosystems and chloroplast structure in extreme shade plants. *Biochim. Biophys. Acta Bioenerg.* **1973**, *325*, 573–585. [CrossRef] [PubMed]
76. Croce, R.; Canino, G.; Ros, F.; Bassi, R. Chromophore organization in the higher-plant photosystem II antenna protein CP26. *Biochemistry* **2002**, *41*, 7334–7343. [CrossRef]
77. Ghirardi, M.L.; Melis, A. Chlorophyll b deficiency in soybean mutants. I. Effects on photosystem stoichiometry and chlorophyll antenna size. *Biochim. Biophys. Acta Bioenerg.* **1988**, *932*, 130–137. [CrossRef]
78. Goodchild, D.J.; Park, R.B. Further evidence for stroma lamellae as a source of photosystem 1 fractions from spinach chloroplasts. *Biochim. Biophys. Acta Bioenerg.* **1971**, *226*, 393–399. [CrossRef] [PubMed]
79. Tanaka, R.; Koshino, Y.; Sawa, S.; Ishiguro, S.; Okada, K.; Tanaka, A. Overexpression of chlorophyllide a oxygenase (CAO) enlarges the antenna size of photosystem II in *Arabidopsis thaliana*. *Plant J.* **2001**, *26*, 365–373. [CrossRef] [PubMed]
80. Holm-Hansen, O.; Riemann, B. Chlorophyll a determination: Improvements in methodology. *Oikos* **1978**, *30*, 438–447. [CrossRef]
81. Schwartz, S.J.; Lorenzo, T.V. Chlorophyll stability during continuous aseptic processing and storage. *J. Food Sci.* **1991**, *56*, 1059–1062. [CrossRef]
82. Wasmund, N.; Topp, I.; Schories, D. Optimising the storage and extraction of chlorophyll samples. *Oceanologia* **2006**, *48*, 125–144.
83. Aminot, A.; Rey, F. Chlorophyll a: Determination by spectroscopic methods. *ICES Tech. Mar. Environ. Sci.* **2002**, *30*, 1–17.
84. Petrović, S.; Zvezdanović, J.; Marković, D. Chlorophyll degradation in aqueous mediums induced by light and UV-B irradiation: An UHPLC-ESI-MS study. *Radiat. Phys. Chem.* **2017**, *141*, 8–16. [CrossRef]
85. King, V.A.E.; Liu, C.F.; Liu, Y.J. Chlorophyll stability in spinach dehydrated by freeze-drying and controlled low-temperature vacuum dehydration. *Food Res. Int.* **2001**, *34*, 167–175. [CrossRef]
86. Cai, H.; Dong, Y.; Li, Y.; Li, D.; Peng, C.; Zhang, Z.; Wan, X. Physiological and cellular responses to fluoride stress in tea (*Camellia sinensis)* leaves. *Acta Physiol. Plant.* **2016**, *38*, 144. [CrossRef]
87. Sharma, R.; Kaur, R. Insights into fluoride-induced oxidative stress and antioxidant defences in plants. *Acta Physiol. Plant.* **2018**, *40*, 181. [CrossRef]
88. Rydzyński, D.; Piotrowicz-Cieślak, A.I.; Grajek, H.; Wasilewski, J. Investigation of chlorophyll degradation by tetracycline. *Chemosphere* **2019**, *229*, 409–417. [CrossRef] [PubMed]
89. Ogasawara, S.; Nakano, K.; Tamiaki, H. Synthesis of fluorinated chlorophylls-a and their bio/physico-chemical properties. *Eur. J. Org. Chem.* **2020**, *2020*, 5537–5543. [CrossRef]
90. Debaene, G.; Niedźwiecki, J.; Pecio, A.; Żurek, A. Effect of the number of calibration samples on the prediction several soil properties at the farm-scale. *Geoderma* **2014**, *214–215*, 114–115. [CrossRef]
91. Jaremko, D.; Kalembasa, D. A comparison of methods for the determination of cation exchange capacity of soils/Porównanie metod oznaczania pojemności wymiany kationów i sumy kationów wymiennych w glebach. *Ecol. Chem. Eng.* **2014**, *21*, 487–498. [CrossRef]
92. Murashige, T.; Skoog, F. A revised medium for the rapid growth and bioassay with tobacco tissue cultures. *Physiol. Plant.* **1962**, *15*, 473–497. [CrossRef]

93. Jiao, L.; Ding, H.; Wang, L.; Zhou, Q.; Huang, X. Bisphenol A effects on the chlorophyll contents in soybean at different growth stages. *Environ. Pollut.* **2017**, *223*, 426–434. [CrossRef] [PubMed]
94. Zhang, X.; Zhang, Z.; Li, J.; Wu, L.; Guo, J.; Ouyang, L.; Xia, Y.; Huang, X.; Pang, X. Correlation of leaf senescence and gene expression/activities of chlorophyll degradation enzymes in harvested Chinese flowering cabbage (*Brassica rapa* var. *parachinensis*). *J. Plant Physiol.* **2011**, *168*, 2081–2087. [CrossRef] [PubMed]
95. Seely, G.R.; Jensen, R.G. Effect of solvent on the spectrum of chlorophyll. *Spectrochim. Acta* **1965**, *21*, 1835–1845. [CrossRef]
96. Lichtenthaler, H.K.; Buschmann, C. Chlorophylls and carotenoids. Measurement and characterization by UV-VIS spectroscopy. *Curr. Protoc. Food Anal. Chem.* **2001**, *1*, F4-3. [CrossRef]

Disclaimer/Publisher's Note: The statements, opinions and data contained in all publications are solely those of the individual author(s) and contributor(s) and not of MDPI and/or the editor(s). MDPI and/or the editor(s) disclaim responsibility for any injury to people or property resulting from any ideas, methods, instructions or products referred to in the content.

Changes in Metabolism and Content of Chlorophyll in Common Duckweed (*Lemna minor* L.) Caused by Environmental Contamination with Fluorides

Jan Kamiński[1], Alicja Stachelska-Wierzchowska[2], Dariusz J. Michalczyk[1], Agnieszka Klimkowicz-Pawlas[3], Ewa Olkowska[4], Lidia Wolska[4], Agnieszka I. Piotrowicz-Cieślak[1,*]

[1] Department of Plant Physiology, Genetics and Biotechnology, University of Warmia and Mazury, Oczapowskiego Str. 1A, 10-719 Olsztyn, Poland
[2] Department of Physics and Biophysics, University of Warmia and Mazury, Oczapowskiego Str. 4, 10-719 Olsztyn, Poland
[3] Department of Soil Science Erosion and Land Protection, Institute of Soil Science and Plant Cultivation—State Research Institute, Czartoryskich Str. 8, 24-100 Puławy, Poland
[4] Department of Environmental Toxicology, Faculty of Health Sciences, Medical University of Gdansk, Dębowa Str. 23A, 80-204 Gdansk, Poland

*Correspondence: acieslak@uwm.edu.pl

Supplementary material

Table S1. The content of fluoride ions and physicochemical properties of soil – A, macroelements – B and other metals – C, D.

A

Soil	**F– Content** mg × kg^{-1}	pH_{H2O}	pH_{KCl}	Hh, cmol(+)×kg^{-1}	EC, mS×m^{-1}	Corg, %	TC, %	TN, %	CEC, cmol(+)×kg^{-1}
1	**2.1**	6.5	5.5	2.52	6.43	1.09	1.29	0.135	6.36
2	**4.19**	6.1	4.9	4.16	5.88	1.37	1.73	0.167	8.47
3	**4.9**	6.2	4.9	3.90	7.71	1.28	1.52	0.133	7.44

B

Soil	$N\text{-}NO_3$ mg×kg^{-1}	$N\text{-}NO_4$ mg×kg^{-1}	P, %	K, mg×kg^{-1}	Ca, mg×kg	Mg, mg×kg	Ca^{2+}, cmol(+)×kg^{-1}	Mg^{2+}, cmol(+)×kg^{-1}	K_2O mg×100g^{-1}	K^+, cmol(+)×kg^{-1}	P_2O_5 mg×100g^{-1}
1	4.27	5.06	0.062	1177.87	1249.26	975.91	2.77	0.45	38.4	0.61	24.8
2	3.48	3.03	0.110	1044.87	1302.09	1036.89	2.72	0.78	45.8	0.78	25.4
3	11.49	34.97	0.165	791.72	1602.95	766.83	2.40	0.45	43.2	0.67	40.4

C

Soil	Na^{+}, cmol(+)×kg^{-1}	Mo, mg×kg^{-1}	Li, µg×kg^{-1}	Be, µg×kg^{-1}	Co, µg×kg^{-1}	Cd, µg×kg^{-1}	La, µg×kg^{-1}	Hg, µg×kg^{-1}	V, mg×kg^{-1}	Mn, mg×kg^{-1}	Cr, mg×kg^{-1}
1	0.02	0.29	3.78	0.23	2.14	0.10	9.01	19.00	9.33	226.85	6.63
2	0.02	0.24	4.68	0.27	1.96	0.16	9.99	23.08	11.09	247.66	7.72
3	0.03	0.34	3.26	0.23	1.71	0.10	7.71	18.45	9.15	257.47	6.59

D

Soil	Ni,	Cu,	Zn,	As,	Se,	Sn,	Sr,	Ba,	Pb,	Na,	Fe,

	mg×kg^{-1}	mg×kg^{-1}	mg×kg^{-1}	mg×kg^{-1}	mg×kg^{-1}	mg×kg^{-1}	mg×kg^{-1}	mg×kg^{-1}	mg×kg^{-1}	mg×kg^{-1}	mg×kg^{-1}
1	4.46	5.05	31.43	1.89	0.15	0.99	6.21	29.80	9.40	60.27	5465.99
2	4.80	5.92	40.03	2.30	0.17	1.10	6.79	39.13	12.20	54.09	5751.74
3	3.81	4.08	27.74	1.97	0.14	0.69	5.29	28.00	13.63	85.89	4931.30

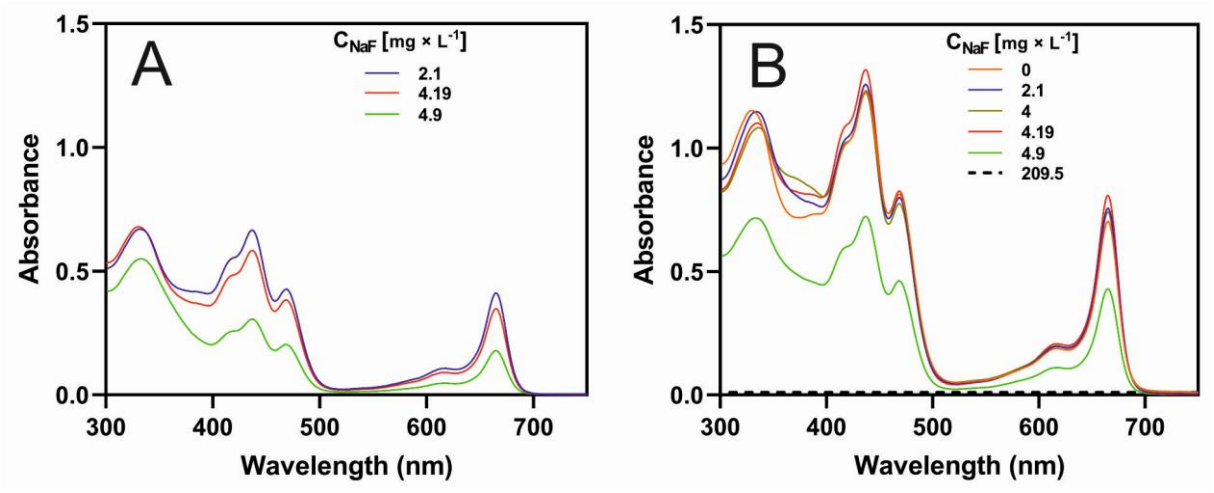


Figure S1. Absorption spectra of chlorophyll isolated from duckweed A – growing on soil extracts and – B in conditions simulating soil extracts (50% MS + F^- medium).

Olsztyn, 10 czerwca 2026
(miejscowość, data)

Jan Kamiński
(imię i nazwisko)

Nauki biologiczne
(dyscyplina naukowa)

Przewodniczący Rady Naukowej Dyscypliny Nauki Biologiczne
Uniwersytetu Warmińsko-Mazurskiego w Olsztynie
prof. dr hab. Nina Smolińska

OŚWIADCZENIE
autora rozprawy doktorskiej

Oświadczam, że w pracy pod tytułem **Kamiński, J.**, Stachelska-Wierzchowska, A., Michalczyk, D. J., Klimkowicz-Pawlas, A., Olkowska, E., Wolska, L., & Piotrowicz-Cieślak, A. I. (2024). Changes in Metabolism and Content of Chlorophyll in Common Duckweed (*Lemna minor* L.) Caused by Environmental Contamination with Fluorides. Molecules, 29(10), 2336. mój wkład merytoryczny w jej przygotowanie polegał na współautorstwie tekstu pracy, wykonaniu części eksperymentalnej, wizualizacji danych, analizie formalnej oraz opracowaniu i interpretacji wyników pracy.

Jan Kamiński
(podpis kandydata)

Olsztyn, 20 kwietnia 2026
(miejscowość, data)

dr Alicja Stachelska-Wierzchowska
(tytuł zawodowy/stopień/tytuł naukowy, imię i nazwisko)

Przewodniczący Rady Naukowej Dyscypliny Nauki Biologiczne
Uniwersytetu Warmińsko-Mazurskiego w Olsztynie
prof. dr hab. Nina Smolińska

OŚWIADCZENIE
współautora

Oświadczam, że w pracy pod tytułem:

Kamiński, J., Stachelska-Wierzchowska, A., Michalczyk, D. J., Klimkowicz-Pawlas, A., Olkowska, E., Wolska, L., & Piotrowicz-Cieślak, A. I. (2024). Changes in Metabolism and Content of Chlorophyll in Common Duckweed (*Lemna minor* L.) Caused by Environmental Contamination with Fluorides. Molecules, 29(10), 2336

mój wkład merytoryczny w jej przygotowanie polegał na pomocy w wykonaniu doświadczeń i opracowaniu wyników dotyczących widm absorpcji i fluorescencji.

Jednocześnie wyrażam zgodę na przedłożenie w/w pracy przez Jana Kamińskiego jako część rozprawy doktorskiej w formie spójnego tematycznie zbioru artykułów naukowych opublikowanych w czasopismach naukowych.

Oświadczam, iż samodzielna i możliwa do wyodrębnienia część ww. pracy wykazuje indywidualny wkład kandydata Jana Kamińskiego polegający na współautorstwie tekstu pracy, wykonaniu części eksperymentalnej, wizualizacji danych, analizie formalnej, opracowaniu i interpretacji wyników tej pracy.

A. Stachelska-Wierzchowska
.....
podpis

Olsztyn, 22 kwietnia 2026
(miejscowość, data)

dr Dariusz J. Michalczyk
(tytuł zawodowy/stopień/tytuł naukowy, imię i nazwisko)

Przewodniczący Rady Naukowej Dyscypliny Nauki Biologiczne
Uniwersytetu Warmińsko-Mazurskiego w Olsztynie
prof. dr hab. Nina Smolińska

OŚWIADCZENIE
współautora

Oświadczam, że w pracy pod tytułem:

Kamiński, J., Stachelska-Wierzchowska, A., Michalczyk, D. J., Klimkowicz-Pawlas, A., Olkowska, E., Wolska, L., & Piotrowicz-Cieślak, A. I. (2024). Changes in Metabolism and Content of Chlorophyll in Common Duckweed (*Lemna minor* L.) Caused by Environmental Contamination with Fluorides. Molecules, 29(10), 2336

mój wkład merytoryczny w jej przygotowanie polegał na pomocy w określeniu aktywności enzymów.

Jednocześnie wyrażam zgodę na przedłożenie w/w pracy przez Jana Kamińskiego jako część rozprawy doktorskiej w formie spójnego tematycznie zbioru artykułów naukowych opublikowanych w czasopismach naukowych.

Oświadczam, iż samodzielna i możliwa do wyodrębnienia część ww. pracy wykazuje indywidualny wkład kandydata Jana Kamińskiego polegający na współautorstwie tekstu pracy, wykonaniu części eksperymentalnej, wizualizacji danych, analizie formalnej, opracowaniu i interpretacji wyników tej pracy.

Michalczyk
.....
podpis

Puławy, 31 marca 2026
(miejscowość, data)

dr hab. Agnieszka Klimkowicz-Pawlas
(tytuł zawodowy/stopień/tytuł naukowy, imię i nazwisko)

Przewodniczący Rady Naukowej Dyscypliny Nauki Biologiczne
Uniwersytetu Warmińsko-Mazurskiego w Olsztynie
prof. dr hab. Nina Smolińska

OŚWIADCZENIE
współautora

Oświadczam, że w pracy pod tytułem:

Kamiński, J., Stachelska-Wierzchowska, A., Michalczyk, D. J., Klimkowicz-Pawlas, A., Olkowska, E., Wolska, L., & Piotrowicz-Cieślak, A. I. (2024). Changes in Metabolism and Content of Chlorophyll in Common Duckweed (*Lemna minor* L.) Caused by Environmental Contamination with Fluorides. Molecules, 29(10), 2336

mój wkład merytoryczny w jej przygotowanie polegał na analizie składu i właściwości próbek gleby.

Jednocześnie wyrażam zgodę na przedłożenie w/w pracy przez Jana Kamińskiego jako część rozprawy doktorskiej w formie spójnego tematycznie zbioru artykułów naukowych opublikowanych w czasopismach naukowych.

Oświadczam, iż samodzielna i możliwa do wyodrębnienia część ww. pracy wykazuje indywidualny wkład kandydata Jana Kamińskiego polegający na współautorstwie tekstu pracy, wykonaniu części eksperymentalnej, wizualizacji danych, analizie formalnej, opracowaniu i interpretacji wyników tej pracy.

Agnieszka Klimkowicz-Pawlas
.....
podpis

Gdańsk, 31 marca 2026
(miejscowość, data)

dr inż. Ewa Olkowska
(tytuł zawodowy/stopień/tytuł naukowy, imię i nazwisko)

Przewodniczący Rady Naukowej Dyscypliny Nauki Biologiczne
Uniwersytetu Warmińsko-Mazurskiego w Olsztynie
prof. dr hab. Nina Smolińska

OŚWIADCZENIE
współautora

Oświadczam, że w pracy pod tytułem:

Kamiński, J., Stachelska-Wierzchowska, A., Michalczyk, D. J., Klimkowicz-Pawlas, A., Olkowska, E., Wolska, L., & Piotrowicz-Cieślak, A. I. (2024). Changes in Metabolism and Content of Chlorophyll in Common Duckweed (*Lemna minor* L.) Caused by Environmental Contamination with Fluorides. Molecules, 29(10), 2336

mój wkład merytoryczny w jej przygotowanie polegał na analizie zawartości fluoru w ekstraktach glebowych.

Jednocześnie wyrażam zgodę na przedłożenie w/w pracy przez Jana Kamińskiego jako część rozprawy doktorskiej w formie spójnego tematycznie zbioru artykułów naukowych opublikowanych w czasopismach naukowych.

Oświadczam, iż samodzielna i możliwa do wyodrębnienia część ww. pracy wykazuje indywidualny wkład kandydata Jana Kamińskiego polegający na wpsółautorstwie tekstu pracy, wykonaniu części eksperymentalnej, wizualizacji danych, analizie formalnej, opracowaniu i interpretacji wyników tej pracy.

Ewa Olkowska
.....
podpis

Gdańsk, 31 marca 2026
(miejscowość, data)

prof. dr hab. Lidia Wolska
(tytuł zawodowy/stopień/tytuł naukowy, imię i nazwisko)

Przewodniczący Rady Naukowej Dyscypliny Nauki Biologiczne
Uniwersytetu Warmińsko-Mazurskiego w Olsztynie
prof. dr hab. Nina Smolińska

OŚWIADCZENIE
współautora

Oświadczam, że w pracy pod tytułem:

Kamiński, J., Stachelska-Wierzchowska, A., Michalczyk, D. J., Klimkowicz-Pawlas, A., Olkowska, E., Wolska, L., & Piotrowicz-Cieślak, A. I. (2024). Changes in Metabolism and Content of Chlorophyll in Common Duckweed (*Lemna minor* L.) Caused by Environmental Contamination with Fluorides. Molecules, 29(10), 2336

mój wkład merytoryczny polegał na opracowaniu koncepcji i zdefiniowaniu celu pracy.

Jednocześnie wyrażam zgodę na przedłożenie w/w pracy przez mgr. Jana Kamińskiego jako część rozprawy doktorskiej w formie spójnego tematycznie zbioru artykułów naukowych opublikowanych w czasopismach naukowych.

Oświadczam, iż samodzielna i możliwa do wyodrębnienia część ww. pracy wykazuje indywidualny wkład kandydata Jana Kamińskiego polegający na współautorstwie tekstu pracy, wykonaniu części eksperymentalnej, wizualizacji danych, analizie formalnej, opracowaniu i interpretacji wyników tej pracy.

Lidia Wolska
.....
podpis

Olsztyn, 8 czerwca 2026
(miejscowość, data)

prof. dr hab. Agnieszka I. Piotrowicz-Cieślak
(tytuł zawodowy/stopień/tytuł naukowy, imię i nazwisko)

Przewodniczący Rady Naukowej Dyscypliny Nauki Biologiczne
Uniwersytetu Warmińsko-Mazurskiego w Olsztynie
prof. dr hab. Nina Smolińska

OŚWIADCZENIE
współautora

Oświadczam, że w pracy pod tytułem:

Kamiński, J., Stachelska-Wierzchowska, A., Michalczyk, D. J., Klimkowicz-Pawlas, A., Olkowska, E., Wolska, L., & Piotrowicz-Cieślak, A. I. (2024). Changes in Metabolism and Content of Chlorophyll in Common Duckweed (*Lemna minor* L.) Caused by Environmental Contamination with Fluorides. Molecules, 29(10), 2336

mój wkład merytoryczny w powstanie publikacji obejmował opracowanie koncepcji, redakcję naukową tekstu oraz wsparcie merytoryczne w procesie przygotowania publikacji.

Jednocześnie wyrażam zgodę na przedłożenie w/w pracy przez Jana Kamińskiego jako część rozprawy doktorskiej w formie spójnego tematycznie zbioru artykułów naukowych opublikowanych w czasopismach naukowych.

Oświadczam, iż samodzielna i możliwa do wyodrębnienia część ww. pracy wykazuje indywidualny wkład kandydata Jana Kamińskiego polegający na współautorstwie tekstu pracy, wykonaniu części eksperymentalnej, wizualizacji danych, analizie formalnej, opracowaniu i interpretacji wyników tej pracy.

Agnieszka Piotrowicz-Cieślak
.....
podpis

PUBLIKACJA 2

Kamiński, **J**., & Piotrowicz-Cieślak, A.I. 2026. Effects of inorganic fluoride and the fluoroquinolone antibiotic pefloxacin on the growth and microbiome structure of *Eruca sativa* L. International Journal of Molecular Sciences, 27(7), 2931.

International Journal of Molecular Sciences

MDPI

Article

Effects of Inorganic Fluoride and the Fluoroquinolone Antibiotic Pefloxacin on the Growth and Microbiome Structure of *Eruca sativa* L.

Jan Kamiński and Agnieszka I. Piotrowicz-Cieślak *

Department of Plant Physiology, Genetics and Biotechnology, University of Warmia and Mazury in Olsztyn, 10-720 Olsztyn, Poland

* Correspondence: acieslak@uwm.edu.pl

Abstract

Environmental contamination with fluorinated compounds has increased markedly due to their widespread use in industry, medicine, and agriculture. Fluoride ions and fluoroquinolone antibiotics may enter soils through fertilizers, wastewater, and manure application, where they can interact with plant-associated microbial communities. In the present study, we investigated the effects of inorganic fluoride (applied as sodium fluoride, NaF) and the fluoroquinolone antibiotic pefloxacin on the growth and microbiome composition of *Eruca sativa* L. Plants were cultivated under controlled conditions and exposed for four weeks to NaF or pefloxacin at equimolar concentrations of 10 and 20 μM/kg soil. Morphological parameters, including biomass accumulation, root length, leaf dimensions, and leaf area, were not significantly affected by either treatment. Nevertheless, increased variability of growth traits was observed, particularly in plants exposed to NaF. High-throughput sequencing of the 16S rRNA gene revealed pronounced, treatment-specific alterations in both rhizosphere and phyllosphere bacterial communities. The rhizosphere microbiome was relatively stable at higher taxonomic levels but exhibited selective enrichment of Actinomycetota, including the class Thermoleophilia, under NaF exposure. In contrast, the phyllosphere microbiome showed strong sensitivity to fluoride, with a marked increase in Betaproteobacteria, dominated by Burkholderiales. Changes induced by pefloxacin were weaker and more diffuse. Our results demonstrate that plant-associated microbiomes respond to fluorinated compounds at concentrations that do not induce visible plant stress. The phyllosphere microbiome, in particular, represents a sensitive indicator of fluoride exposure and may serve as an early-warning system for environmental contamination.

Keywords: phyllosphere; rhizosphere; microorganism

Check for updates

Academic Editor: Daowan Lai

Received: 23 February 2026
Revised: 16 March 2026
Accepted: 17 March 2026
Published: 24 March 2026

Copyright: © 2026 by the authors. Licensee MDPI, Basel, Switzerland. This article is an open access article distributed under the terms and conditions of the Creative Commons Attribution (CC BY) license.

1. Introduction

Plant-associated microbiomes form complex and dynamic assemblages of microorganisms that colonize roots, aerial tissues, and surrounding soil. These microbial communities play essential roles in plant nutrition, growth regulation, pathogen suppression, and adaptation to abiotic stress [1–3]. The rhizosphere microbiome is largely shaped by root exudates and soil physicochemical properties, whereas the phyllosphere represents a nutrientlimited and highly variable environment exposed to ultraviolet radiation, desiccation, and atmospheric deposition [4–6].

Anthropogenic contamination has emerged as a major driver of microbiome alteration in terrestrial ecosystems. Among environmental contaminants,

antibiotics are of particular concern due to their persistence, biological activity at low concentrations, and ability to select for antibiotic-resistant bacteria [7–9]. Agricultural soils receive antibiotics through manure fertilization and irrigation with reclaimed water [10]. Numerous studies have demonstrated that antibiotic residues can alter soil microbial diversity, metabolic activity, and resistance gene pools, with potential consequences for ecosystem functioning and human health [11–13].

Fluoroquinolone antibiotics constitute a widely used class of synthetic antimicrobials characterized by the presence of a fluorine atom in their molecular structure. This substitution enhances antibacterial activity and stability but also contributes to environmental persistence [10,14]. Pefloxacin, a second-generation fluoroquinolone, is used in human medicine and has been detected in soils and sediments [15]. During environmental degradation processes, fluoroquinolones may release fluoride ions, introducing an additional stress factor for microbial communities [16].

Fluoride ions themselves are biologically active and can inhibit numerous enzymatic processes by forming complexes with metal cofactors or by interfering with phosphorylation reactions [17]. Although fluoride toxicity has been extensively studied in animals and humans, its effects on soil and plant-associated microbiomes remain poorly characterized. Importantly, fluoride may originate from multiple sources, including phosphate fertilizers, industrial emissions, and degradation of fluorinated organic compounds [18–20].

Leafy vegetables such as *Eruca sativa* L. (arugula) are particularly relevant models for studying microbiome responses to environmental contamination due to their short cultivation cycle and raw consumption. The microbiome of *E. sativa* has been shown to harbor diverse bacterial taxa, including potential human pathogens and antibiotic-resistant bacteria [21–23]. Alterations in the phyllosphere microbiome of edible plants may therefore have direct implications for food safety.

The objective of this study was to compare the effects of inorganic fluoride and an organic fluorine-containing antibiotic on the rhizosphere and phyllosphere microbiome of *E. sativa*. By applying equimolar concentrations of NaF and pefloxacin, we aimed to distinguish fluoride-specific effects from those associated with antibiotic activity and molecular structure.

2. Results

2.1. Morphological Response of Plants to Long-Term Soil Contamination

Four-week cultivation of *Eruca sativa* in uncontaminated horticultural soil resulted in homogeneous plant material with low variability of the analyzed morphological parameters. After this period, the mean fresh biomass was 1.0 ± 0.5 g, dry biomass approximately 0.10 ± 0.05 g, leaf length 6.0 ± 0.5 cm, root length 6.2 ± 1.0 cm, and leaf area approximately 5.0 ± 0.8 cm^2. The low variance of these parameters indicates stable growth conditions and the absence of environmental stress during the initial phase of the experiment.

After an additional four weeks of growth in control soil and soils contaminated with NaF and pefloxacin at concentrations of 10 and 20 μM/kg soil, no statistically significant differences were observed between the mean values of the analyzed morphological parameters (ANOVA, $p > 0.05$). Fresh biomass increased to a range of 2.0–5.0 g, while dry biomass ranged from 0.20 to 0.50 g (Figure 1A,D). Despite the lack of differences in mean values, a marked increase in variability was observed in contaminated soils, particularly in the NaF 20 μM/kg treatment, where the coefficient of variation for fresh biomass exceeded 35%, compared to approximately 15% in the control.

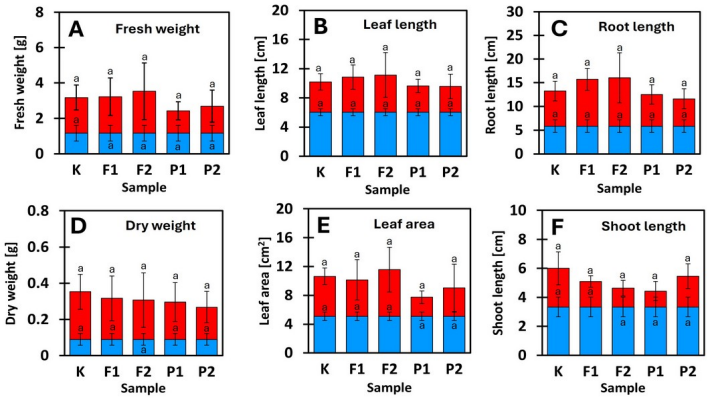


Figure 1. Morphology of *Eruca sativa* L. after 28 days—■, and 56 days—■ of growth. K—control (no fluoride addition); F1—sodium fluoride (NaF) at 10 µM/kg soil; F2—sodium fluoride (NaF) at 20 µM/kg soil; P1—pefloxacin at 10 µM/kg soil; P2—pefloxacin at 20 µM/kg soil. Panel (**A**) shows the mean fresh weight, panel (**B**) the mean leaf length, panel (**C**) the mean root length, panel (**D**) the dry weight, panel (**E**) leaf area, and panel (**F**) the mean shoot length of *E. sativa*. Data are presented as mean ± SD. Letters indicate statistically significant differences between groups (ANOVA, $p < 0.05$).

A similar pattern was observed for dimensional parameters. Leaf length increased to 8–15 cm, root length to 10–22 cm, and leaf area to 6–15 cm^2. The widest ranges of leaf length (8–15 cm) and root length (12–22 cm) were recorded in the NaF 20 µM/kg treatment, indicating increased inter-individual variability under fluoride exposure (Figure 1). Shoot length increased moderately from 3.5 ± 0.4 cm to 4–7 cm and was the only parameter for which variability remained comparable across all experimental variants.

2.2. Global Microbiome Restructuring in Response to Contamination

After 28 days of cultivation of *Eruca sativa* in soil supplemented with NaF and pefloxacin, the genomic structure of the rhizosphere and phyllosphere microbiomes was comprehensively characterized. Genomic DNA was isolated from soil and leaf samples collected from five experimental variants (control, 10 µM NaF, 20 µM NaF, 10 µM pefloxacin, 20 µM pefloxacin). Amplicon sequencing targeting the V3–V4 hypervariable region of the 16S rRNA gene was performed, and amplicon sequence variants (ASVs) were taxonomically assigned at the kingdom, phylum, class, order, family, genus, and species levels. Taxa representing less than 2% of ASVs within a given sample were grouped into a collective category designated as “Sparse.” Across all samples, both rhizospheric and phyllospheric, more than 99.8% of ASVs were assigned to Bacteria, with only a negligible fraction classified as Archaea (Supplementary Figure S1). This overwhelming bacterial dominance was consistent across all treatments. The genomic structure of both compartments comprised seven phyla: Bacteroidota, Pseudomonadota, Actinomycetota, Verrucomicrobiota, Myxococcota, Acidobacteriota, and Planctomycetota (Figure 2A,D).

In the rhizosphere, Bacteroidota, Acidobacteriota and Planctomycetota displayed relatively uniform abundances of approximately 6%, with variation not exceeding two percentage points between treatments. Actinomycetota accounted for approximately 12% in the control and both pefloxacin treatments, whereas their abundance increased markedly under NaF exposure, reaching 18% at 10 µM and 30% at 20 µM. Pseudomonadota constituted approximately 38% in the control, 20 µM NaF, and 20 µM pefloxacin, and approximately 47% in 10 µM NaF and 10 µM pefloxacin; these fluctuations did not show a clear dose-dependent relationship. Verrucomicrobiota were absent from NaF-treated samples. In the control group and at 10 µM pefloxacin, they accounted for approximately 7%, whereas at 20 µM

they accounted for approximately 10%. Planctomycetota were not detected in 10 µM pefloxacin, while Acidobacteriota were absent in the control and 20 µM pefloxacin treatments (Figure 2A).

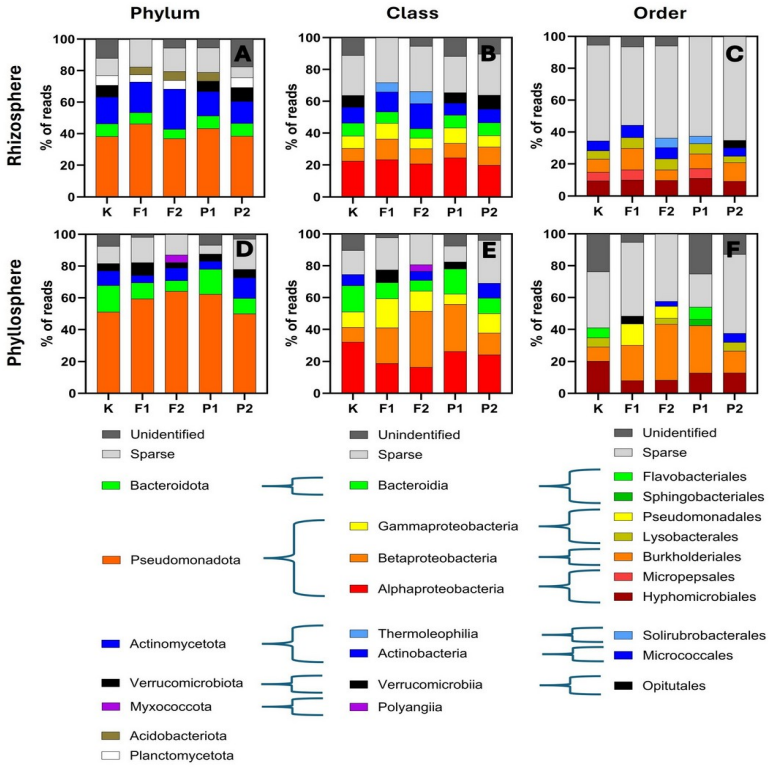


Figure 2. Relative abundance of amplicon sequence variants (ASVs) classified as unidentified (■), sparse (■), and assigned to major bacterial phyla (Bacteroidota (■), Pseudomonadota (■), Actinomycetota (■), Verrucomicrobiota (■), Myxococcota (■), Acidobacteriota (■), and Planctomycetota (□)), with further subdivision into classes and orders, in the rhizosphere and phyllosphere of *Eruca sativa*. Sample designations used in the figure: K—control without F-ions; F1—NaF at 10 µM/kg; F2—NaF at 20 µM/kg; P1—pefloxacin at 10 µM/kg; P2—pefloxacin at 20 µM/kg. ((**A**) Relative abundance of bacterial phyla in the rhizosphere; (**B**) relative abundance of bacterial classes in the rhizosphere; (**C**) relative abundance of bacterial orders in the rhizosphere; (**D**) relative abundance of bacterial phyla in the phyllosphere; (**E**) relative abundance of bacterial classes in the phyllosphere; (**F**) relative abundance of bacterial orders in the phyllosphere.

In contrast, the phyllosphere exhibited substantially greater variability (Figure 2D). Pseudomonadota increased progressively with rising NaF concentration, from 50% in the control to approximately 60% at 10 µM and 65% at 20 µM NaF. In 10 µM pefloxacin, their abundance resembled that observed in 20 µM NaF, whereas in 20 µM pefloxacin it approximated control levels. Conversely, Bacteroidota declined linearly with increasing NaF, decreasing from 15% in the control to 6% at 20 µM NaF. Their abundance in 10 µM pefloxacin was comparable to the control, and 9% in 20 µM pefloxacin. Actinomycetota and Verrucomicrobiota showed treatment-dependent changes without a consistent trend. Notably, Acidobacteriota and Planctomycetota were absent from the phyllosphere, whereas Myxococcota (6%) were detected exclusively in the 20 µM NaF treatment (Figure 2D). Class-level analysis refined the phylum-level observations (Figure 2B,E). In the rhizosphere, Bacteroidota were represented by Bacteroidia; Pseudomonadota by Alpha-, Beta-, and Gammaproteobacteria; Actinomycetota by Thermoleophilia and Actinobacteria; Verrucomicrobiota by Verrucomicrobiia; and Myxococcota by Polyangiia. No classes exceeding the Sparse threshold were identified within Acidobacteriota or Planctomycetota (Figure 2B). Verrucomicrobiia occurred in the same treatments as

Verrucomicrobiota and at comparable abundances. Thermoleophilia were detected exclusively under NaF exposure (~5%). Bacteroidia were present in all samples (~5%). Gammaproteobacteria accounted for ~7% in the control and high-concentration treatments (20 µM NaF and 20 µM pefloxacin), and 10% at 10 µM of both compounds. Alphaproteobacteria remained stable at ~20% across all treatments. Betaproteobacteria constituted ~10%, with minor variation. Actinobacteria declined under pefloxacin (8%) relative to the control (10%) but increased in a NaF dose-dependent manner (13% and 16% at 10 and 20 µM NaF, respectively) (Figure 2B).

In the phyllosphere, all classes displayed pronounced treatment-dependent variation (Figure 2E). Betaproteobacteria increased dramatically with NaF concentration, from 8% in the control to 20% at 10 µM and 34% at 20 µM NaF. Under pefloxacin, they accounted for 28% (10 µM) and 12% (20 µM). Alphaproteobacteria decreased progressively with increasing NaF (32%, 18%, and 15%), while representing 25% and 23% in 10 and 20 µM pefloxacin, respectively. Gammaproteobacteria varied between 6% and 18% without a clear concentration-dependent pattern. Bacteroidia declined with increasing NaF concentrations, from 16% in the control to 10% and 5% at higher exposure levels. Thermoleophilia were not detected in the phyllosphere; however, Polyangiia (4%) were observed exclusively at 20 µM NaF. Verrucomicrobiia appeared in 10 µM NaF (8%) and 10 µM pefloxacin (4%). Actinobacteria were detected in the control (7%), 20 µM NaF (6%), and 20 µM pefloxacin (10%) (Figure 2E). At the order level, the contribution of the Sparse category and Unidentified ASVs increased substantially (Figure 2C,F). In the rhizosphere, Sparse represented approximately 60% of ASVs, while Unidentified did not exceed 6%. Opitutales, Solirubrobacterales, and Micropepsales each accounted for ~5% but occurred selectively across treatments. Hyphomicrobiales (~9%) and Lysobacterales (~6%, except 2% at 20 µM pefloxacin) were present in all samples. Burkholderiales varied between 5% and 13% without correlation to treatment. Micrococcales comprised ~5% in the control and 20 µM pefloxacin and ~8% in NaF-treated samples (Figure 2C).

In the phyllosphere, Sparse constituted ~36% in the control and NaF treatments, 20% in 10 µM pefloxacin, and 50% in 20 µM pefloxacin (Figure 2F). The proportion of Unidentified ASVs declined sharply with increasing NaF (24%, 5%, 0%), paralleling the increase in Burkholderiales, whose abundance closely mirrored that of Betaproteobacteria at the class level. Hyphomicrobiales represented 20% in the control, 8% in NaF treatments, and 14% in pefloxacin treatments. Micropepsales and Solirubrobacterales were absent from the phyllosphere. Pseudomonadales, Flavobacterales, and Sphingobacterales were detected but showed no consistent concentration-dependent patterns (Figure 2F).

2.3. Variability at the Family and Genus Levels

At the family level, Sparse increased to levels up to approximately 70% of ASVs, and Incertae sedis taxa appeared for the first time (Figure 3). In both compartments, the combined proportion of Sparse and Incertae sedis was at least 50%.

In the rhizosphere, Sparse exceeded 70% and Incertae sedis accounted for ~10% (Figure 3A,B). Identified families included Microbacteriaceae, 67-14 (an unnamed family within Solirubrobacterales), Chitinophagaceae, Rhodanobacteraceae, Micropepsaceae, and Xanthobacteraceae, each contributing approximately 5–7% with relatively consistent representation across treatments. Certain families were treatment-specific, such as Opitutaceae (20 µM pefloxacin), 67-14 (20 µM NaF), Microbacteriaceae (10 µM NaF), and Chitinophagaceae (control and 10 µM pefloxacin). In the phyllosphere, the

combined proportion of Sparse and Incertae sedis ranged between 60% and 80%, with Incertae sedis varying markedly (7–50%) independently of treatment (Figure 3C). Identified families included Opitutaceae, Comamondaceae, Pseudomonadaceae, Rhodanobacteraceae, Oxalobacteraceae, Rhizobiaceae, Caulobacteraceae, and Beijerinckiaceae. Comamondaceae were present in all treatments and displayed a pattern closely paralleling that observed for Burkholderiales and Betaproteobacteria. Beijerinckiaceae were detected exclusively in the control (7%) (Figure 3C,D).

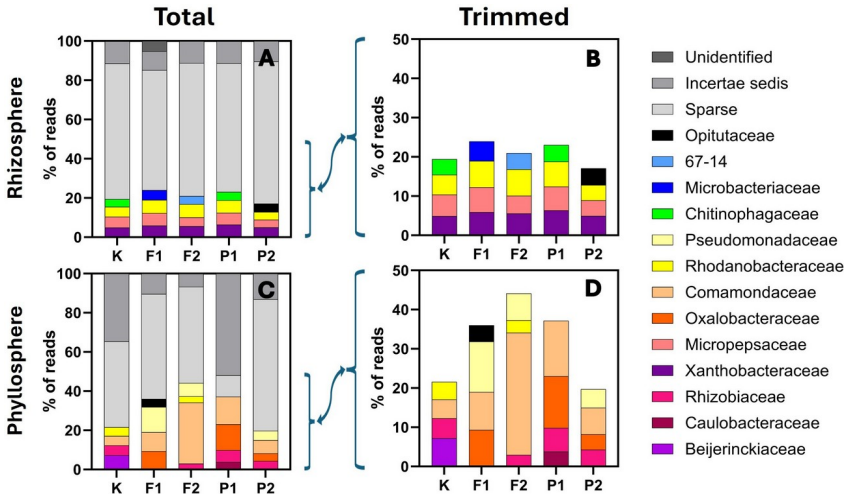


Figure 3. Percentage contribution of amplicon sequence variants (ASVs) assigned to unclassified (■), Incertae sedis (■), sparse (■), Opitutaceae (■), 67-14 (■), Microbacteriaceae (■), Chitinophagaceae (■), Pseudomonadaceae (■), Rhodanobacteraceae (■), Comamonadaceae (■), Oxalobacteraceae (■), Micropepsaceae (■), Xanthobacteraceae (■), Rhizobiaceae (■), Caulobacteraceae (■), and Beijerinckiaceae (■) families in the rhizosphere and the phyllosphere of *Eruca sativa*. Panel (**A**)—total rhizosphere reads; Panel (**B**)—rhizosphere reads rarefied to 50% of the total read count shown in Panel (**A**); Panel (**C**)—total phyllosphere reads; Panel (**D**)—phyllosphere reads rarefied to 50% of the total read count shown in Panel (**C**). Sample designations used in the figure: K—control without F-ions; F1—NaF at 10 μM/kg; F2—NaF at 20 μM/kg; P1—pefloxacin at 10 μM/kg; P2—pefloxacin at 20 μM/kg.

At the genus level, taxa other than Sparse and Incertae sedis accounted for less than 20% of ASVs in the rhizosphere and less than 40% in the phyllosphere (Figure 4). In the rhizosphere, Incertae sedis comprised ~37% and Sparse ~50%. Detected genera included Pseudonocardia, Mucilaginibacter (2% in control), Rhodanobacter, Opitutus, Burkholderia, Pseudolabrys, Roseateles, Micropepsis, and Massilia (Figure 4A,B).

In the phyllosphere, Mucilaginibacter, Micropepsis, Pseudonocardia, Burkholderia, and Opitutus were absent, whereas Pedobacter (3% in control), Flavobacterium, Chryseobacterium, Methylorubrum (4% in control), Asticcacaulis, Devosia, Pseudomonas, and Roseateles were identified (Figure 4C,D). Roseateles was particularly prominent at 20 μM NaF (25%), accounting for a substantial proportion of Comamondaceae (35%) in this treatment (Figures 3C,D and 4C,D).

No species-level taxa exceeded the Sparse threshold applied during downstream filtering of low-abundance features (Figure 5). Amplicon sequence variants (ASVs) were inferred using the DADA2 algorithm, which models sequencing errors and does not rely on sequence similarity clustering. Taxonomic assignments were performed using a Naive Bayes classifier trained on the SILVA 138.2 database. In the rhizosphere, Sparse and Unidentified accounted for ~34% and ~40% in the control and pefloxacin treatments,

whereas under NaF Unidentified declined to 22% and Sparse increased to 50%. Uncultured bacterium comprised approximately 20% across all treatments. The "Metagenome" category remained below 10% (7% in control, 5% under NaF, 6% and 9% in 10 and 20 µM pefloxacin, respectively) (Figure 5A,B).

In the phyllosphere, Unidentified represented 20% in the control and ~40% in NaF and 20 µM pefloxacin treatments. Sparse exhibited an inverse trend (60% in control and 10 µM pefloxacin; 40% in the remaining treatments). Uncultured bacterium accounted for 10% in the control and NaF treatments, 5% in 10 µM pefloxacin, and 15% in 20 µM pefloxacin. The "Metagenome" fraction increased under NaF exposure (4% in control to 7% and 6%) and measured 3% and 6% in 10 and 20 µM pefloxacin, respectively (Figure 5C,D). Collectively, these results demonstrate pronounced compartment-specific responses of the microbiome associated with *Eruca sativa*. The rhizosphere exhibited comparatively stable taxonomic composition with limited and non-linear treatment effects. In contrast, the phyllosphere displayed marked variability and clear NaF dose-dependent shifts, particularly within Betaproteobacteria, Burkholderiales, Comamondaceae, and the genus Roseateles (Figures 2–4). These findings indicate distinct ecological dynamics and differential sensitivity of aboveground and belowground microbial communities to soil-applied chemical stressors.

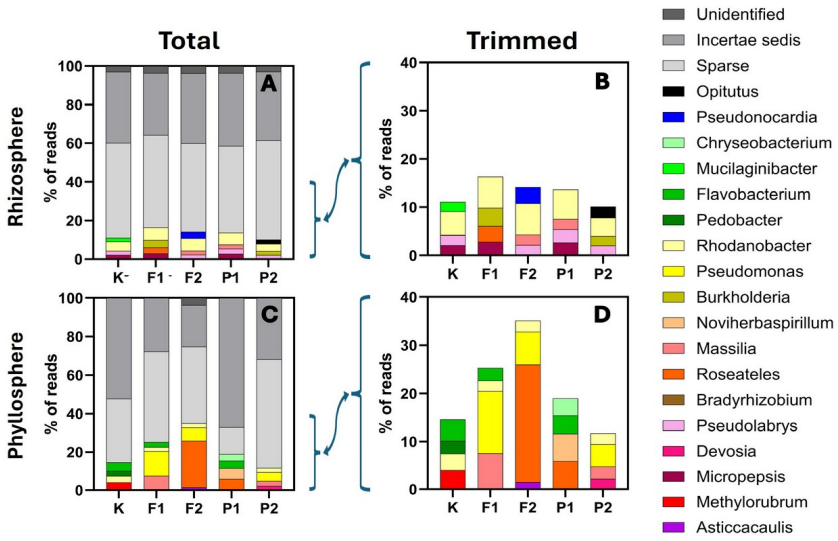


Figure 4. Percentage contribution of amplicon sequence variants (ASVs) assigned to unclassified (■), *Incertae sedis* (■), sparse (■), *Opitutus* (■), *Pseudomonocardia* (■), *Chryseobacterium* (■), *Mucilaginibacter* (■), *Flavobacterium* (■), *Pedobacter* (■), *Rhodanobacter* (■), *Pseudomonas* (■), *Burkholderia* (■), *Noviherbaspirillum* (■), *Massilia* (■), *Roseateles* (■), *Bradyrhizobium* (■), *Pseudolabrys* (■), *Devosia* (■), *Micropepsis* (■), *Methylorubrum* (■), and *Asticcacaulis* (■) genera in the rhizosphere and phyllosphere of *Eruca sativa*. Panel (**A**)—total rhizosphere reads; Panel (**B**)—rhizosphere reads rarefied to 40% of the total read count shown in Panel (**A**); Panel (**C**)—total phyllosphere reads; Panel (**D**)—phyllosphere reads rarefied to 40% of the total read count shown in Panel (**C**). Sample designations used in the figure: K—control without F-ions; F1—NaF at 10 µM/kg; F2—NaF at 20 µM/kg; P1—pefloxacin at 10 µM/kg; P2—pefloxacin at 20 µM/kg.

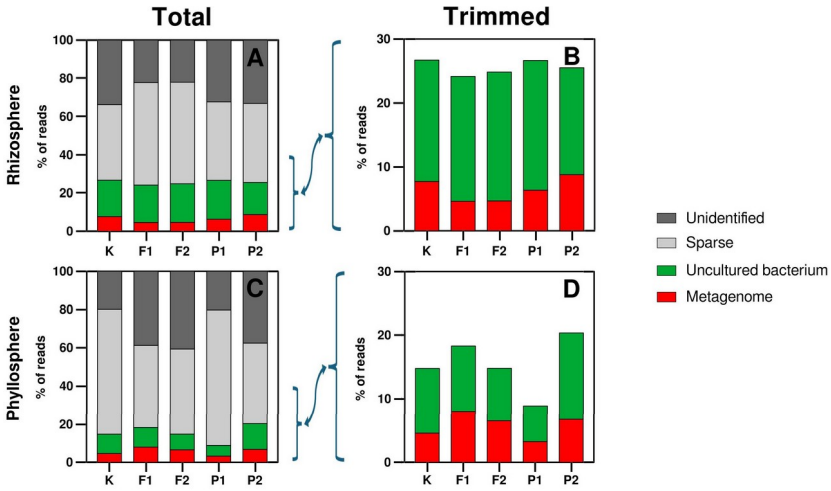


Figure 5. Percentage contribution of amplicon sequence variants (ASVs) assigned to unclassified (■), Sparse (■), Uncultured bacteria (■), Metagenome (■) genera in the rhizosphere and phyllosphere of *Eruca sativa*. Panel (**A**)—total rhizosphere reads; Panel (**B**)—rhizosphere reads rarefied to 30% of the total read count shown in Panel (**A**); Panel (**C**)—total phyllosphere reads; Panel (**D**)—phyllosphere reads rarefied to 30% of the total read count shown in Panel (**C**). Sample designations used in the figure: K—control without F-ions; F1—NaF at 10 μM/kg; F2—NaF at 20 μM/kg; P1—pefloxacin at 10 μM/kg; P2—pefloxacin at 20 μM/kg.

2.4. Functional Analysis of the Genomes

In this study, microbial genes and metabolites were assigned to fifteen functional categories, including central carbon metabolism, carbohydrate metabolism, amino acid biosynthesis and degradation, lipid and fatty acid metabolism, nucleotide metabolism, vitamin and cofactor biosynthesis, cell wall and envelope biosynthesis, secondary metabolite biosynthesis, aromatic compound degradation, fermentation, nitrogen and sulfur metabolism, polyamine metabolism, and translation and protein biosynthesis. The functional categorization (Table S1) allows a structured overview of microbial metabolic capabilities, facilitates comparison across environmental conditions (e.g., fluoride and pefloxacin exposure), and provides a framework for interpreting metabolomic and genomic data in a biologically meaningful context.

Significant functional changes in microbial metabolic pathways in response to fluoride (NaF) and pefloxacin (both at 20 μM/kg soil) were primarily observed in the phyllosphere (Figure 6) whereas the rhizosphere (Figure 7) remained largely stable under the same conditions. Among the analyzed pathways, the highest number of gene-level alterations occurred in nucleotide metabolism, central carbon metabolism, amino acid degradation, and vitamin and cofactor biosynthesis, indicating that these functional categories are particularly sensitive to chemical stressors at the higher exposure levels. In contrast, exposure to NaF at 10 μM/kg soil resulted in markedly fewer gene-level changes, with alterations in all pathways being even less than those observed in the untreated control, suggesting a threshold effect for fluoride-induced metabolic perturbations.

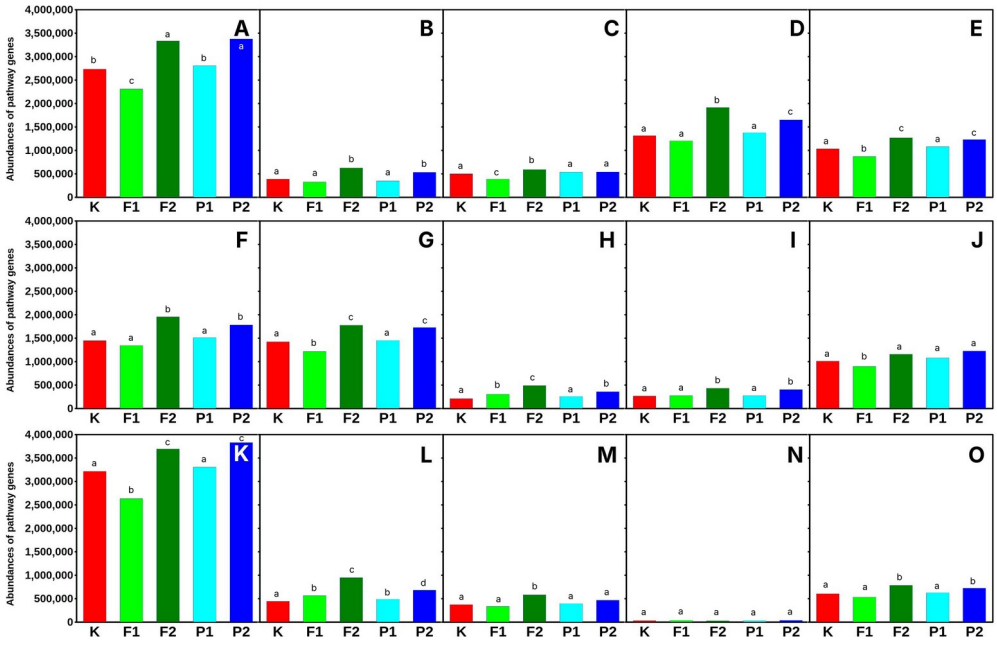


Figure 6. Functional categorization of microbial metabolic pathways in phyllosphere of *Eruca sativa*. of *Eruca sativa*. Fifteen biochemical pathways were analyzed, including: (**A**)—central carbon metabolism, (**B**)—carbohydrate metabolism, (**C**)—amino acid biosynthesis, (**D**)—amino acid degradation, (**E**)—lipid and fatty acid metabolism, (**F**)—nucleotide metabolism, (**G**)—vitamin and cofactor biosynthesis, (**H**)—cell wall and envelope biosynthesis, (**I**)—secondary metabolite biosynthesis, (**J**)—aromatic compound degradation, (**K**)—fermentation, (**L**)—nitrogen metabolism, (**M**)—sulfur metabolism, (**N**)—polyamine metabolism, and (**O**)—translation and protein biosynthesis. Sample designations used in the figure: **K**—control without F-ions; **F1**—NaF at 10 µM/kg; **F2**—NaF at 20 µM/kg; **P1**—pefloxacin at 10 µM/kg; **P2**—pefloxacin at 20 µM/kg. Different letters above bars indicate statistically significant differences between groups.

Overall, these findings indicate that microorganisms in the rhizosphere undergo dose-dependent metabolic adjustments in response to fluoride and pefloxacin, with high concentrations triggering substantial reprogramming in key functional categories. The phyllosphere-associated communities, however, remained relatively stable, highlighting the habitat-specific sensitivity of microbial metabolic networks. The differential responses of nucleotide metabolism, central carbon metabolism, amino acid degradation, and vitamin and cofactor biosynthesis underscore the importance of these pathways as metabolic hubs responsive to chemical stress in soil microbial communities.

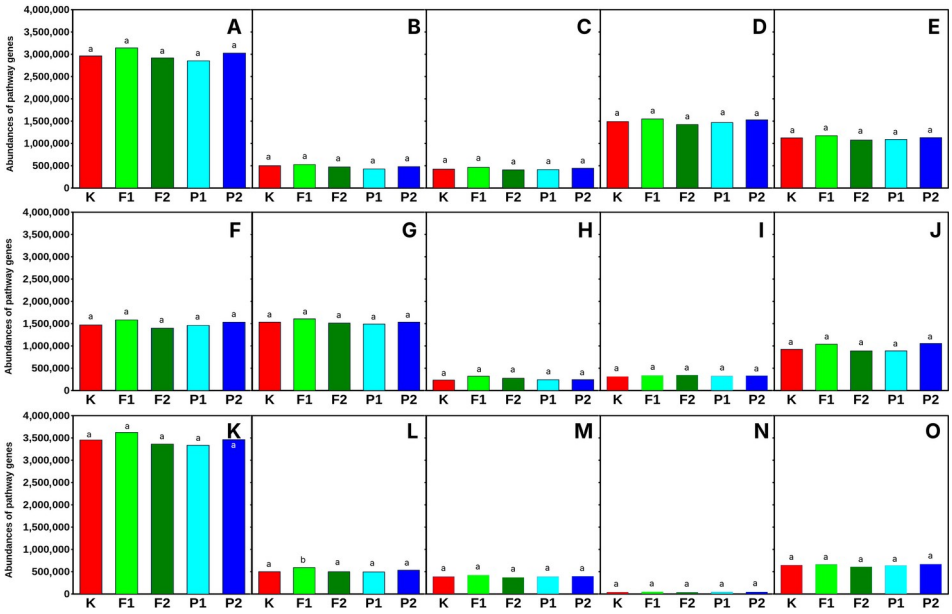


Figure 7. Functional categorization of microbial metabolic pathways in the rhizosphere of *Eruca sativa*. Fifteen biochemical pathways were analyzed, including: (**A**)—central carbon metabolism, (**B**)—carbohydrate metabolism, (**C**)—amino acid biosynthesis, (**D**)—amino acid degradation, (**E**)—lipid and fatty acid metabolism, (**F**)—nucleotide metabolism, (**G**)—vitamin and cofactor biosynthesis, (**H**)—cell wall and envelope biosynthesis, (**I**)—secondary metabolite biosynthesis, (**J**)—aromatic compound degradation, (**K**)—fermentation, (**L**)—nitrogen metabolism, (**M**)—sulfur metabolism, (**N**)—polyamine metabolism, and (**O**)—translation and protein biosynthesis. Sample designations used in the figure: K—control without F-ions; F1—NaF at 10 μM/kg; F2—NaF at 20 μM/kg; P1—pefloxacin at 10 μM/kg; P2—pefloxacin at 20 μM/kg. Different letters above bars indicate statistically significant differences between groups.

2.5. Quantitative Summary and Biological Implications

The applied concentrations of NaF and pefloxacin (10 and 20 μM/kg soil) did not result in statistically significant changes in mean morphological parameters of *Eruca sativa* but led to a pronounced increase in inter-individual variability, reaching 20–30% compared to the control. At the same time, both contaminants induced substantial microbiome restructuring, with shifts in the relative abundance of dominant phyla and classes reaching 15–20 percentage points, particularly in the phyllosphere.

The rhizosphere exhibited relative quantitative and qualitative stability, whereas the phyllosphere responded rapidly and selectively, indicating its high sensitivity to sublethal chemical pressure. These results suggest that microbiome analysis, particularly of leaf-associated communities, may reveal environmental stress effects earlier than conventional plant growth parameters.

3. Discussion

The aim of the present study was to evaluate the effects of fluorine-containing compounds—sodium fluoride and the fluoroquinolone antibiotic pefloxacin—on the structure of the rhizosphere and phyllosphere microbiome of *Eruca sativa*, with particular emphasis on changes in the abundance and relative proportions of bacterial taxa. After four weeks of cultivation on contaminated soils, immediately prior to genomic DNA isolation, plant morphological parameters were assessed, including fresh and dry biomass, shoot and root length, and leaf length and width. One-way analysis of variance ($p < 0.05$) did not reveal statistically significant differences between treatments for any of the measured traits; however, a pronounced increase in result dispersion was observed in contaminated variants compared to the control (Figure 1). This indicates increased

individual variability in plant responses under chemical stress. The applied concentrations of NaF and pefloxacin were below the levels that induce visible morphological changes in *E. sativa*, confirming that the observed microbial effects occurred under subtoxic conditions for the host plant. The use of equimolar concentrations of NaF and pefloxacin allowed discrimination between effects attributable to fluoride ions and those potentially associated with the intact fluoroquinolone molecule. This approach is methodologically important, as previous studies have demonstrated that the fluorine moiety of fluoroquinolones may dissociate from the carbon skeleton and undergo independent environmental dispersion [16]. The obtained results clearly demonstrate that both compounds exert a significant influence on the plant-associated microbiome; however, the direction and magnitude of these effects depend on the ecological niche (rhizosphere vs. phyllosphere), contaminant concentration, and taxonomic resolution level (Figure 2). Taxonomic identification at the family and genus levels revealed a high contribution of taxa belonging to the "sparse" group, defined as accounting for less than 2% of total reads. This pattern indicates a high microbial diversity in both the rhizosphere and phyllosphere, which persisted even under NaF and pefloxacin exposure (Figures 3 and 4). In the rhizosphere, taxa exceeding the sparse threshold collectively accounted for approximately 20% of all reads, whereas in the phyllosphere this proportion reached nearly 40%. This difference was largely attributable to the family Comamonadaceae within the order Burkholderiales (Figure 3C,D). At the order level, Burkholderiales accounted for approximately 40% of all phyllosphere reads (Figure 2F). The relative abundance of Comamonadaceae increased linearly with increasing NaF concentration. Although Comamonadaceae also increased in pefloxacin-treated samples, this effect was less pronounced than in fluoride-treated variants (Figure 3C,D). At the phylum levels, both rhizosphere and phyllosphere microbiomes were dominated by Pseudomonadota (ranging from approximately 40% to 60% of reads), Bacteroidota (~10–20%), Actinomycetota (~10–30%), Planctomycetota, and Verrucomicrobiota. This composition is consistent with previous reports on soil and plant-associated microbiomes, including those of leafy vegetables [24–29]. Despite the apparent stability of dominant phyla, the presence of NaF and pefloxacin resulted in substantial shifts in their relative proportions, highlighting the functional plasticity of microbial communities in response to chemical stress. In the rhizosphere, Verrucomicrobiota exhibited a particularly pronounced response. Their abundance dropped below Sparse threshold in the presence of NaF, whereas in pefloxacin-treated samples it remained comparable to the control at the lower concentration and increased at the higher concentration. This divergent response suggests that fluoride ions exert a stronger selective pressure on Verrucomicrobiota than fluorine bound within an organic antibiotic molecule. Similar patterns were reported by Jiang et al. [24], who observed an increase in Verrucomicrobiota at low fluoride concentrations and a decline at higher levels, interpreted as exceeding a tolerance threshold. In the present study, the applied concentrations were considerably lower, which may partially explain the differences in response patterns observed among treatments. Planctomycetota decreased from approximately 6% in the control to 4% in the presence of NaF, were not detected at 10 μM pefloxacin, and remained unaffected at 20 μM pefloxacin. Planctomycetota are considered relatively resistant to environmental stressors, including heavy metals and inorganic pollutants, which may explain their ecological success under fluoride exposure [30,31]. The absence of a response to pefloxacin suggests that the antibiotic exerts a more selective influence on the rhizosphere microbiome rather than a broad-spectrum effect across

dominant bacterial groups. Phyllosphere-derived samples displayed a distinctly different response pattern, emphasizing the importance of plant microhabitats in shaping microbial community structure. A notable observation was the decline of Actinomycetota at lower NaF concentrations followed by a marked increase at higher concentrations; a similar non-linear response was observed in pefloxacin-treated samples. Such concentration-dependent responses are well documented and are often interpreted as the result of niche replacement following the elimination of more sensitive taxa [24–29]. The increased abundance of Actinomycetota at higher contaminant levels may reflect their adaptive capacity or their ability to exploit resources released by dying microorganisms. One of the most striking changes at lower taxonomic levels was the substantial increase in Burkholderiales abundance in phyllosphere samples. In NaF-treated variants, this order accounted for up to 40–50% of total reads, while in pefloxacin-treated samples its abundance was lower but still markedly higher than in the control. In NaF 10 and 20 μM/kg variants, Comamonadaceae was the dominant family within Burkholderiales, reaching up to 30% of all reads. This family has been identified as a primary environmental reservoir of the trimethoprim resistance gene *dfrB* [32], suggesting that fluoride stress may promote the selection of bacteria involved in the dissemination of antibiotic resistance genes. Moreover, Burkholderiales include numerous opportunistic human pathogens capable of causing severe infections, particularly in immunocompromised individuals and patients with cystic fibrosis [33], which confers additional public health relevance to the observed shifts. In the rhizosphere, a notable phenomenon was the disappearance of Chitinophagaceae (Bacteroidota) in NaF (10 and 20 μM/kg soil) and pefloxacin (20 μM/kg soil) variants. This family plays an important role in plant growth promotion and nitrogen assimilation [34–36], and its elimination may indicate a weakening of beneficial plant–microbiome interactions under chemical stress. Similarly, Microbacteriaceae (Actinomycetota), which also contribute to plant growth promotion [37], were detected exclusively in the rhizosphere of the NaF 10 μM/kg variant, indicating high sensitivity to both fluoride ions and pefloxacin. Beijerinckiaceae and Caulobacteraceae represent an interesting example of copiotrophic bacteria capable of rapidly increasing in abundance under conditions of reduced microbial diversity [38,39]. In the present study, Beijerinckiaceae were detected exclusively in the control phyllosphere and declined to sparse levels in all contaminated variants. Caulobacteraceae exceeded the sparse threshold only in the phyllosphere under low pefloxacin concentration, suggesting colonization of niches vacated by antibiotic-sensitive taxa. Importantly, Caulobacteraceae are recognized as significant environmental carriers of antibiotic resistance genes, often linked to nitrogen metabolism pathways [40]. From the perspective of antibiotic resistance ecology, one of the most significant findings was the complete disappearance of the genus *Pedobacter* in all NaF- and pefloxacin-treated samples. In the control phyllosphere, *Pedobacter* accounted for approximately 2% of total reads, whereas in all contaminated variants it declined to sparse levels. *Pedobacter* species are considered “superbugs”, exhibiting resistance to multiple antibiotic classes, including aminoglycosides, β-lactams, colistin, and ciprofloxacin, with resistance genes constituting up to 6–8% of their genome [41]. The disappearance of *Pedobacter* in pefloxacin-treated samples suggests sensitivity to this fluoroquinolone despite its structural similarity to ciprofloxacin. The lack of prior reports on *Pedobacter* susceptibility to pefloxacin underscores the novelty and ecological relevance of this finding. At the genus level, several taxa with documented roles in plant growth promotion and nitrogen assimilation were identified, including *Mucilaginibacter* [42], *Rhodanobacter* [43], *Micropepsis* [44],

Methylorubrum [45], *Asticcacaulis* [46], and *Devosia* [47]. Changes in their abundance between control and contaminated variants indicate that fluoride and antibiotic stress may modify the functional potential of the microbiome even without complete elimination of specific taxa. The increased abundance of some of these genera in NaF- and pefloxacin-treated samples may be attributed to the high nitrogen content of the horticultural soil and the capacity of these bacteria to rapidly exploit available resources.

Central carbon metabolism (Figures 6 and 7) constitutes a fundamental metabolic network in microorganisms, integrating pathways responsible for energy production, redox balance, and the generation of biosynthetic precursors. Consequently, perturbations in these pathways may reflect metabolic adaptations of microorganisms to environmental stressors, including exposure to antimicrobial compounds. Fluoride is known to interfere with bacterial metabolism, particularly by targeting enzymes involved in glycolysis. One of the primary mechanisms of fluoride action is the inhibition of enolase, a key glycolytic enzyme responsible for the conversion of 2-phosphoglycerate to phosphoenolpyruvate. This inhibition reduces glycolytic flux and affects carbohydrate metabolism and ATP generation in bacterial cells [48,49]. Moreover, the reduction in phosphoenolpyruvate availability may disrupt the phosphotransferase system responsible for carbohydrate transport, thereby affecting both glucose uptake and central carbon metabolism [50]. Antibiotics may also influence central carbon metabolism in microorganisms. Increasing evidence suggests that antibiotic exposure induces metabolic reprogramming, particularly affecting pathways associated with energy production and respiration. For example, bactericidal antibiotics have been shown to stimulate metabolic activity and alter carbon flux through central metabolic pathways such as glycolysis and the tricarboxylic acid (TCA) cycle [51]. These metabolic changes may increase cellular respiration and promote the generation of reactive oxygen species, which contribute to antibiotic-induced bacterial cell death. Furthermore, antibiotic stress can lead to broader metabolic adjustments, including shifts in carbon utilization and alterations in metabolic intermediates linked to central carbon metabolism. Such metabolic responses may represent adaptive mechanisms that enable microorganisms to maintain energy balance and survive under antimicrobial pressure [52]. Taken together, these findings suggest that both fluoride and antibiotic exposure may significantly affect central carbon metabolism in microorganisms. As central carbon metabolism functions as a metabolic hub connecting numerous biochemical pathways (Table S3), its perturbation may lead to widespread metabolic reorganization and influence microbial adaptation to antimicrobial stress. Alterations in nucleotide metabolism suggest that fluoride and pefloxacin may interfere with DNA and RNA synthesis, potentially impacting replication and repair processes [52]. Similarly, changes in amino acid degradation could reflect shifts in protein turnover and nitrogen balance under stress conditions [53]. The observed effects on vitamin and cofactor biosynthesis indicate that essential coenzymes required for enzymatic activity may be limited, which could further constrain metabolic capacity [54].

Interestingly, the phyllosphere communities remained relatively stable, highlighting a habitat-specific sensitivity of microbial metabolism. These findings suggest that soil-associated microorganisms in the rhizosphere are more responsive to chemical stress, possibly due to higher exposure or metabolic flexibility required for survival in nutrient-rich and competitive environments.

Study Limitations and Future Directions

A limitation of the present study is the lack of direct measurements of fluoride ion concentrations in soil and plant tissues during the experiment, which would allow a more precise assessment of exposure dynamics. In addition, the applied 16S rRNA gene metabarcoding approach does not provide information on the functional potential of the microbiome, including antibiotic resistance genes or metabolic pathways involved in fluoride tolerance. Future studies combining quantitative fluoride analyses with shotgun metagenomics or metatranscriptomics would enable a more comprehensive evaluation of the functional consequences of fluoride and antibiotic-driven microbial selection in the rhizosphere and phyllosphere.

4. Materials and Methods

4.1. Cultivation Conditions of Eruca sativa

Eruca sativa was cultivated in horticultural soil (see Table S2 for soil composition), with 120 g of soil placed in 8 × 8 × 8 cm pots. Two to three seeds were sown per pot. Plants were grown for 4 weeks at 25 °C under a photoperiod of 18 h light and 6 h darkness. After this period, basic plant morphological parameters were measured, and the soil was supplemented with either NaF (Chempur, Piekary Śląskie, Poland) or pefloxacin (mesylate salt; $C_{17}H_{20}FN_3O_3$, Merck, Darmstadt, Germany) at concentrations of 10 and 20 µM/kg of soil. Cultivation was then continued for an additional 4 weeks under the same conditions, after which plant morphological parameters were assessed again.

4.2. Measurement of Morphological Parameters

The following parameters were evaluated: fresh and dry biomass, root length, leaf length and width, and leaf surface area. Dry biomass was determined after drying cleaned plant material at 40 °C for 24 h. Leaf surface area was measured using ImageJ software v.1.54m, while the remaining measurements were performed using millimeter paper. Differences between experimental groups were analyzed using one-way analysis of variance (ANOVA) with a significance level of $\alpha = 0.05$.

4.3. Isolation of Genomic DNA

4.3.1. Rhizosphere

Bacterial genomic DNA from the rhizosphere of *E. sativa* was isolated using the DNeasy PowerSoil Pro Kit (Qiagen, Hilden, Germany), according to the manufacturer's instructions.

4.3.2. Phyllosphere

Bacteria from *E. sativa* leaf tissues were isolated according to the protocol described by Krupka and Piotrowicz-Cieślak (2024), with minor modifications [55]. Leaves (5 g) were placed in 50 mL of sterile phosphate buffer (0.01 M, pH 7.4), subjected to sonication for 7 min, and subsequently shaken for 1 h at 180 rpm and 30 °C. The suspension was filtered through sterile gauze, and bacteria were collected on a PVDF membrane with a pore size of 0.22 µm. The membranes were stored at −80 °C prior to DNA isolation, which was also performed using the DNeasy PowerSoil Pro Kit.

4.3.2. Microbiome Metabarcoding

DNA sequencing and taxonomic identification of bacteria from the rhizosphere and phyllosphere were outsourced to Genomed S.A. (Warsaw, Poland). DNA libraries were prepared by amplification of the hypervariable

V3–V4 regions of the 16S rRNA gene, and sequencing was performed on the MiSeq platform (Illumina, San Diego, CA, USA) using paired-end reads method. Bacterial taxa were identified based on sequence comparison of the V3–V4 regions.

4.3.3. Library Preparation

Microbial DNA isolated from phyllosphere and rhizosphere of *Eruca sativa* was used for preparation of DNA libraries for metabarcoding analysis. Libraries were generated using a two-step PCR protocol targeting the V3–V4 hypervariable region of the bacterial 16S rRNA gene. In the first PCR reaction, the V3–V4 fragment was amplified using locus-specific primers containing Illumina overhang adapters. The primers used were:

Forward primer (5′ → 3′): CCTACGGGNGGCWGCAG
Reverse primer (5′ → 3′): GACTACHVGGGTATCTAATCC

PCR amplification conditions for the first stage are presented in Table S3. In the second PCR step, unique dual indices and sequencing adapters were attached to the amplicons using index primers (Table S4).

4.3.4. NGS Sequencing

Indexed libraries containing amplified V3–V4 fragments of the 16S rRNA gene were subjected to next-generation sequencing using a paired-end sequencing approach on an AVITI™ platform (Element Biosciences, San Diego, CA, USA).

4.3.5. Bioinformatical Analysis

Raw sequencing reads were demultiplexed and converted to FASTQ format using the MiSeq Reporter v2.6 software. Downstream bioinformatic analysis was performed using QIIME2 (version 2024.5) [56].

Primer and adapter sequences were removed using Cutadapt (version 4.7) [57]. Quality filtering was applied to remove low-quality reads (Phred score < 30) and very short sequences.

Denoising, error correction, and inference of amplicon sequence variants (ASVs) were performed using the DADA2 algorithm [58] implemented within QIIME2. During this step, paired-end reads were merged into full-length V3–V4 sequences, and reads that could not be successfully merged were discarded. Chimeric sequences were identified and removed as part of the DADA2 pipeline.

Taxonomic classification of the resulting ASVs was performed using the SILVA reference database (release 138.2) [59]. A hybrid classification strategy was applied:

1. Initial taxonomic assignment using VSEARCH 2.30.0 [60] based on sequence similarity against the reference database.
2. ASVs that could not be confidently classified in the first step were further assigned using a Naive Bayes classifier trained on the SILVA 138.2 database with a minimum confidence threshold of 0.7.

Multiple sequence alignment of representative ASVs was performed using MAFFT [61]. A phylogenetic tree was subsequently constructed using FastTree [62]. Both tools are implemented within the QIIME2 framework.

4.3.6. Functional Profiling of ASV Data

Functional potential of microbial communities was inferred using PICRUSt2, implemented through the q2-picrust2 plugin within the QIIME2

environment. This approach was used to predict the abundance of metabolic pathways based on the identified ASVs.

4.4. Statistical Analyses

All experiments were conducted with five biological replicates. One-way ANOVA with Tukey's post hoc test was used to assess the differences in DNA concentration between extraction methods. Statistical analyses were performed using GraphPad Prism 8.0.1.

5. Conclusions

In summary, the results of this study demonstrate that both fluoride ions and pefloxacin exert strong selective pressure on the microbiome of *Eruca sativa*, leading to substantial alterations in the structure of rhizosphere and phyllosphere bacterial communities. These changes include the elimination of beneficial plant-associated taxa, selection of potentially resistant bacteria, and shifts among groups of ecological and health relevance. The findings contribute to a deeper understanding of the mechanisms by which fluorinated compounds influence environmental microbiomes and underscore the necessity of incorporating microbiome-level processes into environmental risk assessments related to antibiotic use. The results indicate that carbon metabolism was the most strongly affected metabolic category under the studied conditions. The highest number of alterations was observed in pathways associated with carbon processing, suggesting substantial changes in central metabolic functions. These findings highlight the key role of carbon metabolism in the organism's response and suggest that shifts in carbon-related pathways may be an important component of the overall metabolic adaptation.

Supplementary Materials: The following supporting information can be downloaded at: https://www.mdpi.com/article/10.3390/ijms27072931/s1.

Author Contributions: Conceptualization, A.I.P.-C.; and methodology, J.K.; software, J.K.; validation, J.K.; formal analysis, J.K.; investigation, A.I.P.-C.; writing—original draft preparation, A.I.P.-C. and J.K.; writing—review and editing, A.I.P.-C.; visualization, J.K.; supervision, A.I.P.-C.; project administration, A.I.P.-C.; funding acquisition, A.I.P.-C. All authors have read and agreed to the published version of the manuscript.

Funding: This research was funded by a grant from the National Science Centre, Poland (Grant No. UMO-2019/35/B/NZ7/04394).

Institutional Review Board Statement: Not applicable.

Informed Consent Statement: Not applicable.

Data Availability Statement: The original contributions presented in this study are included in the article/Supplementary Material. Further inquiries can be directed to the corresponding author.

Conflicts of Interest: The authors declare no conflicts of interest.

References

1. Saleem, M.; Hu, J.; Jousset, A. More than the sum of its parts: Microbiome biodiversity as a driver of plant growth and soil health. *Annu. Rev. Ecol. Evol. Syst.* **2019**, *50*, 145–168. [CrossRef]
2. de Faria, M.R.; Costa, L.S.A.S.; Chiaramonte, J.B.; Bettiol, W.; Mendes, R. The rhizosphere microbiome: Functions, dynamics, and role in plant protection. *Trop. Plant Pathol.* **2021**, *46*, 13–25. [CrossRef]
3. Xiong, Q.; Yang, J.; Ni, S. Microbiome-mediated protection against pathogens in woody plants. *Int. J. Mol. Sci.* **2023**, *24*, 16118. [CrossRef] [PubMed]
4. Sohrabi, R.; Paasch, B.C.; Liber, J.A.; He, S.Y. Phyllosphere microbiome. *Annu. Rev. Plant Biol.* **2023**, *74*, 539–568. [CrossRef] [PubMed]

5. Berg, G.; Erlacher, A.; Grube, M. The edible plant microbiome: Importance and health issues. In *Principles of Plant–Microbe Interactions: Microbes for Sustainable Agriculture*; Lugtenberg, B., Ed.; Springer: Cham, Switzerland, 2014; pp. 419–426.
6. Compant, S.; Samad, A.; Faist, H.; Sessitsch, A. A review on the plant microbiome: Ecology, functions, and emerging trends in microbial application. *J. Adv. Res.* **2019**, *19*, 29–37. [CrossRef] [PubMed]
7. Polianciuc, S.I.; Gurzău, A.E.; Kiss, B.; Ş tefan, M.G.; Loghin, F. Antibiotics in the environment: Causes and consequences. *Med. Pharm. Rep.* **2020**, *93*, 231–240. [CrossRef]
8. Xie, W.Y.; Shen, Q.; Zhao, F.J. Antibiotics and antibiotic resistance from animal manures to soil: A review. *Eur. J. Soil Sci.* **2018**, *69*, 181–195. [CrossRef]
9. Wu, J.; Wang, J.; Li, Z.; Guo, S.; Li, K.; Xu, P.; Ok, Y.; Jones, D.L.; Zou, J. Antibiotics and antibiotic resistance genes in agricultural soils: A systematic analysis. *Crit. Rev. Environ. Sci. Technol.* **2023**, *53*, 847–864. [CrossRef]
10. Frade, V.M.F.; Dias, M.; Teixeira, A.C.S.C.; Palma, M.S.A. Environmental contamination by fluoroquinolones. *Braz. J. Pharm. Sci.* **2014**, *50*, 41–54. [CrossRef]
11. Tyrrell, C.; Burgess, C.M.; Brennan, F.P.; Walsh, F. Antibiotic resistance in grass and soil. *Biochem. Soc. Trans.* **2019**, *47*, 477–486. [CrossRef]
12. Liu, L.; Mi, J.; Wang, Y.; Zou, Y.; Ma, B.; Liao, X.; Liang, J.; Wu, Y. Different methods of incorporating ciprofloxacin in soil affect microbiome and degradation of ciprofloxacin residue. *Sci. Total Environ.* **2018**, *619*, 1673–1681. [CrossRef]
13. Gatica, J.; Cytryn, E. Impact of treated wastewater irrigation on antibiotic resistance in the soil microbiome. *Environ. Sci. Pollut. Res.* **2013**, *20*, 3529–3538. [CrossRef] [PubMed]
14. Redgrave, L.S.; Sutton, S.B.; Webber, M.A.; Piddock, L.J. Fluoroquinolone resistance: Mechanisms, impact on bacteria, and role in evolutionary success. *Trends Microbiol.* **2014**, *22*, 438–445. [CrossRef] [PubMed]
15. Li, J.; Wang, T.; Shao, B.; Shen, J.; Wang, S.; Wu, Y. Plasmid-mediated quinolone resistance genes and antibiotic residues in wastewater and soil adjacent to swine feedlots: Potential transfer to agricultural lands. *Environ. Health Perspect.* **2012**, *120*, 1144. [CrossRef] [PubMed]
16. Murphy, C.D. Microbial degradation of fluorinated drugs. *Appl. Microbiol. Biotechnol.* **2016**, *100*, 2617–2627. [CrossRef]
17. Strunecká, A.; Blaylock, R.L.; Patocka, J. Aluminofluoride complexes: Phosphate analogues and a hidden hazard for living organisms. *Curr. Inorg. Chem.* **2012**, *2*, 8–18. [CrossRef]
18. Vithanage, M.; Bhattacharya, P. Fluoride in the environment: Sources, distribution and defluoridation. *Environ. Chem. Lett.* **2015**, *13*, 131–147. [CrossRef]
19. Gadi, B.R.; Kumar, R.; Goswami, B.; Rankawat, R.; Rao, S.R. Recent developments in understanding fluoride accumulation, toxicity, and tolerance mechanisms in plants: An overview. *J. Soil Sci. Plant Nutr.* **2021**, *21*, 209–228. [CrossRef]
20. Fuge, R. Fluorine in the environment, a review of its sources and geochemistry. *Appl. Geochem.* **2019**, *100*, 393–406. [CrossRef]
21. Cernava, T.; Erlacher, A.; Soh, J.; Sensen, C.W.; Grube, M.; Berg, G. Enterobacteriaceae dominate the core microbiome and contribute to the resistome of arugula (*Eruca sativa* Mill.). *Microbiome* **2019**, *7*, 13. [CrossRef]
22. Rosberg, A.K.; Darlison, J.; Mogren, L.; Alsanius, B.W. Commercial wash of leafy vegetables do not significantly decrease bacterial load but leads to shifts in bacterial species composition. *Food Microbiol.* **2021**, *94*, 103667. [CrossRef]
23. Heaton, J.C.; Jones, K. Microbial contamination of fruit and vegetables and the behaviour of enteropathogens in the phyllosphere: A review. *J. Appl. Microbiol.* **2008**, *104*, 613–626. [CrossRef]
24. Jiang, Y.; Zhang, D.; Zhang, S.; Li, T.; Wang, G.; Xu, X.; Pu, Y.; Nengzi, L. Interaction effects of different chemical fractions of lanthanum, cerium, and fluorine on the taxonomic composition of soil microbial community. *BMC Microbiol.* **2024**, *24*, 539. [CrossRef] [PubMed]
25. Pramanik, K.; Sen, A.; Dutta, S.; Mandal, G.S.; Paramanik, B.; Das, A.; Chatterjee, N.; Ghorai, A.K.; Ali, M.N. Microbial populations under fluoride stress: A metagenomic exploration from Indian soil. *World J. Microbiol. Biotechnol.* **2025**, *41*, 221. [CrossRef] [PubMed]
26. Wang, X.; Wang, X.J.; Jiang, W.; Sun, Y.K.; Bian, T.; Mao, H. Plant-microbial community-perfluorinated compound response relationships in river sediments under hydrodynamic conditions. *ACS EST Water* **2025**, *5*, 6732–6744. [CrossRef]
27. Gan, C.D.; Jia, Y.B.; Yang, J.Y. Remediation of fluoride contaminated soil with nano-hydroxyapatite amendment: Response of soil fluoride bioavailability and microbial communities. *J. Hazard. Mater.* **2021**, *405*, 124694. [CrossRef]
28. Wang, M.; Chen, X.; Hamid, Y.; Yang, X. Evaluating the response of the soil bacterial community and lettuce growth in a fluorine and cadmium co-contaminated yellow soil. *Toxics* **2024**, *12*, 459. [CrossRef]
29. Martin-Pozas, T.; Ghezzi, D.; D'Angeli, I.M.; Madonia, G.; Chiarini, V.; Vattano, M.; De Waele, J.; Cappelletti, M.; Saiz-

Jimenez, C.; Jurado, V. Microbial and geochemical variability in sediments and biofilms from Italian gypsum caves. *Microb. Ecol.* **2025**, *88*, 81. [CrossRef]
30. Li, J.; Zheng, Q.; Liu, J.; Pei, S.; Yang, Z.; Chen, R.; Ma, L.; Niu, J.; Tian, T. Bacterial–fungal interactions and response to heavy metal contamination of soil in agricultural areas. *Front. Microbiol.* **2024**, *15*, 1395154. [CrossRef]
31. Nikolova, R.; Gatev, E.; Kenarova, A.; Petkova, M.; Dinev, N.; Baldrian, P.; Radeva, G. Selective pressure of heavy metals on soil microbial taxa near a smelting area. *Toxics* **2025**, *13*, 1025. [CrossRef]
32. Kneis, D.; Tskhay, F.; de la Cruz Barron, M.; Berendonk, T.U. Bacteria of the order Burkholderiales are original environmental hosts of type II trimethoprim resistance genes (*dfrB*). *ISME J.* **2024**, *18*, wrae243. [CrossRef] [PubMed]
33. Shmarina, G.; Pukhalskaya, D.; Shmarin, V.; Semykin, S.; Avakyan, L.; Krasovsky, S.; Goryainova, A.; Kostyuk, S.; Zinchenko, R.; Kashirskaya, N. *Burkholderia cepacia* in cystic fibrosis children and adolescents: Overall survival and immune alterations. *Front. Cell. Infect. Microbiol.* **2024**, *14*, 1374318. [CrossRef] [PubMed]
34. Kim, H.S.; Kim, J.S.; Suh, M.K.; Eom, M.K.; Lee, J.; Lee, J.S. A novel plant growth-promoting rhizobacterium, *Rhizosphaericola mali gen. nov.*, sp. *nov.*, isolated from healthy apple tree soil. *Sci. Rep.* **2024**, *14*, 1038. [CrossRef] [PubMed]
35. Madhaiyan, M.; Poonguzhali, S.; Senthilkumar, M.; Pragatheswari, D.; Lee, J.S.; Lee, K.C. Arachidicoccus rhizosphaerae gen. nov., sp. nov., a plant-growth-promoting bacterium in the family Chitinophagaceae isolated from rhizosphere soil. *Int. J. Syst. Evol. Microbiol.* **2015**, *65*, 578–586. [CrossRef]
36. Huang, J.; Gao, K.; Yang, L.; Lu, Y. Successional action of Bacteroidota and Firmicutes in decomposing straw polymers in a paddy soil. *Environ. Microbiome* **2023**, *18*, 76. [CrossRef]
37. Cordovez, V.; Schop, S.; Hordijk, K.; Dupré de Boulois, H.; Coppens, F.; Hanssen, I.; Raaijmakers, J.M.; Carrión, V.J. Priming of plant growth promotion by volatiles of root-associated *Microbacterium* spp. *Appl. Environ. Microbiol.* **2018**, *84*, e01865-18. [CrossRef]
38. Wang, J.; Xie, J.; Li, L.; Effah, Z.; Xie, L.; Luo, Z.; Zhou, Y.; Jiang, Y. Fertilization treatments affect soil CO_2 emission through regulating soil bacterial community composition in the semiarid Loess Plateau. *Sci. Rep.* **2022**, *12*, 20123. [CrossRef]
39. Chiba, A.; Uchida, Y.; Kublik, S.; Vestergaard, G.; Buegger, F.; Schloter, M.; Schulz, S. Soil bacterial diversity is positively correlated with decomposition rates during early phases of maize litter decomposition. *Microorganisms* **2021**, *9*, 357. [CrossRef]
40. Wang, Y.; Cai, J.; Chen, X.; Guo, B.; Liu, J.; Qiu, G.; Li, H. The connection between the antibiotic resistome and nitrogen-cycling microorganisms in paddy soil is enhanced by application of chemical and plant-derived organic fertilizers. *Environ. Res.* **2024**, *243*, 117880. [CrossRef]
41. Viana, A.T.; Caetano, T.; Covas, C.; Santos, T.; Mendo, S. Environmental superbugs: The case study of *Pedobacter* spp. *Environ. Pollut.* **2018**, *241*, 1048–1055. [CrossRef]
42. Fan, D.; Smith, D.L. *Mucilaginibacter* sp. *K* improves growth and induces salt tolerance in nonhost plants via multilevel mechanisms. *Front. Plant Sci.* **2022**, *13*, 938697. [CrossRef] [PubMed]
43. Woo, H.; Kim, I.; Chhetri, G.; Park, S.; Lee, H.; Yook, S.; Seo, T. Two novel bacterial species, *Rhodanobacter lycopersici* sp. *nov.* and *Rhodanobacter geophilus* sp. *nov.*, isolated from the rhizosphere of *Solanum lycopersicum* with plant growth-promoting traits. *Microorganisms* **2024**, *12*, 2227. [CrossRef] [PubMed]
44. Huang, Z.; Ruan, S.; Sun, Y.; Cheng, X.; Dai, J.; Gui, P.; Yu, M.; Zhong, Z.; Wu, J. Bacterial inoculants improved the growth and nitrogen use efficiency of *Pyrus betulifolia* under nitrogen-limited conditions by affecting the native soil bacterial communities. *Appl. Soil Ecol.* **2022**, *170*, 104285. [CrossRef]
45. Zhang, C.; Zhou, D.F.; Wang, M.Y.; Song, Y.Z.; Zhang, C.; Zhang, M.M.; Sun, J.; Yao, L.; Mo, X.H.; Ma, Z.X.; et al. Phosphoribosylpyrophosphate synthetase as a metabolic valve advances *Methylobacterium/Methylorubrum* phyllosphere colonization and plant growth. *Nat. Commun.* **2024**, *15*, 5969. [CrossRef]
46. Okazaki, K.; Tsurumaru, H.; Hashimoto, M.; Takahashi, H.; Okubo, T.; Ohwada, T.; Minamisawa, K.; Ikeda, S. Community analysis-based screening of plant growth-promoting bacteria for sugar beet. *Microbes Environ.* **2021**, *36*, ME20137.
47. Chhetri, G.; Kim, I.; Kang, M.; Kim, J.; So, Y.; Seo, T. *Devosia rhizoryzae* sp. *nov.*, and *Devosia oryziradicis* sp. *nov.*, novel plant growth promoting members of the genus *Devosia*, isolated from the rhizosphere of rice plants. *J. Microbiol.* **2022**, *60*, 1–10.
48. Guha-Chowdhury, N.; Clark, A.G.; Sissons, C.H. Inhibition of purified enolases from oral bacteria by fluoride. *Oral. Microbiol. Immunol.* **1997**, *12*, 91–97. [CrossRef]
49. Marquis, R.E. Antimicrobial actions of fluoride for oral bacteria. *Can. J. Microbiol.* **1995**, *41*, 955–964. [CrossRef]
50. Belli, W.A.; Buckley, D.H.; Marquis, R.E. Weak acid effects and fluoride inhibition of glycolysis by Streptococcus mutans GS-5. *Can. J. Microbiol.* **1995**, *41*, 785–791.
51. Lobritz, M.A.; Belenky, P.; Porter, C.B.M.; Gutierrez, A.; Yang, J.H.; Schwarz, E.G.; Dwyer, D.J.; Khalil, A.S.; Collins,

J.J. Antibiotic efficacy is linked to bacterial cellular respiration. *Proc. Natl. Acad. Sci. USA* **2015**, *112*, 8173–8180. [CrossRef]
52. Patti, G.J.; Yanes, O.; Siuzdak, G. Metabolomics: The apogee of the omics trilogy. *Nat. Rev. Mol. Cell Biol.* **2012**, *13*, 263–269. [CrossRef] [PubMed]
53. Zhu, S.; Zhao, W.; Sun, S.; Yang, X.; Mao, H.; Sheng, L.; Chen, Z. Community metagenomics reveals the processes of cadmium resistance regulated by microbial functions in soils with *Oryza sativa* root exudate input. *Sci. Total Environ.* **2024**, *949*, 175015. [CrossRef] [PubMed]
54. Bennett, B.D.; Kimball, E.H.; Gao, M.; Osterhout, R.; Van Dien, S.J.; Rabinowitz, J.D. Absolute metabolite concentrations and implied enzyme active site occupancy in *Escherichia coli*. *Nat. Chem. Biol.* **2009**, *5*, 593–599. [CrossRef] [PubMed]
55. Krupka, M.; Piotrowicz-Cieślak, A.I. Optimization of the method for isolating bacterial DNA from the aboveground part of lettuce. *Int. J. Mol. Sci.* **2024**, *25*, 8513. [CrossRef]
56. Bolyen, E.; Rideout, J.R.; Dillon, M.R.; Bokulich, N.A.; Abnet, C.C.; Al-Ghalith, G.A.; Alexander, H.; Alm, E.J.; Arumugam, M.; Asnicar, F.; et al. Reproducible, interactive, scalable and extensible microbiome data science using QIIME 2. *Nat. Biotechnol.* **2019**, *37*, 852–857. Correction in *Nat. Biotechnol*. **2019**, *37*, 1091. [CrossRef]
57. Martin, M. Cutadapt removes adapter sequences from high-throughput sequencing reads. *EMBnet J.* **2011**, *17*, 10–12. [CrossRef]
58. Callahan, B.J.; McMurdie, P.J.; Rosen, M.J.; Han, A.W.; Johnson, A.J.A.; Holmes, S.P. DADA2: High-resolution sample inference from Illumina amplicon data. *Nat. Methods* **2016**, *13*, 581–583. [CrossRef]
59. Quast, C.; Pruesse, E.; Yilmaz, P.; Gerken, J.; Schweer, T.; Yarza, P.; Peplies, J.; Glöckner, F.O. The SILVA ribosomal RNA gene database project: Improved data processing and web-based tools. *Nucleic Acids Res.* **2013**, *41*, D590–D596. [CrossRef]
60. Rognes, T.; Flouri, T.; Nichols, B.; Quince, C.; Mahé, F. VSEARCH: A versatile open source tool for metagenomics. *PeerJ* **2016**, *4*, e2584. [CrossRef]
61. Katoh, K.; Rozewicki, J.; Yamada, K.D. MAFFT online service: Multiple sequence alignment, interactive sequence choice and visualization. *Brief. Bioinform.* **2019**, *20*, 1160–1166. [CrossRef]
62. Price, M.N.; Dehal, P.S.; Arkin, A.P. FastTree: Computing large minimum evolution trees with profiles instead of a distance matrix. *Mol. Biol. Evol.* **2009**, *26*, 1641–1650. [CrossRef]

Disclaimer/Publisher's Note: The statements, opinions and data contained in all publications are solely those of the individual author(s) and contributor(s) and not of MDPI and/or the editor(s). MDPI and/or the editor(s) disclaim responsibility for any injury to people or property resulting from any ideas, methods, instructions or products referred to in the content.

Effects of Inorganic Fluoride and the Fluoroquinolone Antibiotic Pefloxacin on the Growth and Microbiome Structure of *Eruca sativa* L.

Supplementary material

Jan Kamiński and Agnieszka I. Piotrowicz-Cieślak

Department of Plant Physiology, Genetics and Biotechnology, University of Warmia and Mazury in Olsztyn, 10-720 Olsztyn, Poland

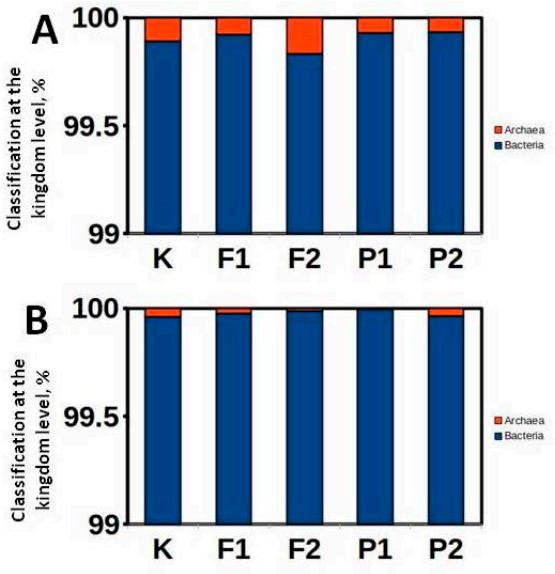


Figure S1. Isolated organisms (%) from the kingdoms Bacteria (■) and Archaea (■). Panel A: rhizosphere; Panel B: phyllosphere. Sample designations used in the figure: K – control without F^- ions; F1 – NaF at 10 μM/kg; F2 – NaF at 20 μM/kg; P1 – pefloxacin at 10 μM/kg; P2 – pefloxacin at 20 μM/kg.

Table S1. Functional categorization of predicted microbial metabolic pathways inferred from 16S rRNA gene data. Individual pathways (MetaCyc identifiers) were grouped into major metabolic categories (A–O) representing core cellular functions.

A.Central carbon metabolism		
GLYCOLYSIS	GLYCOLYSIS-E-D	GLUCONEO-PWY
TCA	REDCITCYC	GLYOXYLATE-BYPASS
TCA-GLYOX-BYPASS	GLYCOLYSIS-TCA-GLYOX-BYPASS	PENTOSE-P-PWY
ANAGLYCOLYSIS-PWY		
B.Carbohydrate metabolism		
FUCCAT-PWY	FUC-RHAMCAT-PWY	RHAMCAT-PWY
LACTOSECAT-PWY	GALACTUROCAT-PWY	GALACTARDEG-PWY
GALACT-GLUCUROCAT-PWY	GLUCARDEG-PWY	GLUCUROCAT-PWY
HEXITOLDEGSUPER-		

PWY		
C. Fermentation		
FERMENTATION-PWY	CENTFERM-PWY	ANAEROFRUCAT-PWY
D. Lipid and fatty acid metabolism		
FAO-PWY	FASYN-INITIAL-PWY	FASYN-ELONG-PWY
LIPASYN-PWY	PHOSLIPSYN-PWY	
E. Cell wall and envelope biosynthesis		
PEPTIDOGLYCANSYN-PWY	TEICHOICACID-PWY	LPSSYN-PWY
OANTIGEN-PWY	KDO-NAGLIPASYN-PWY	NAGLIPASYN-PWY
UDPNAGSYN-PWY		
F. Vitamin and cofactor biosynthesis		
BIOTIN-BIOSYNTHESIS-PWY	COBALSYN-PWY	FOLSYN-PWY
NAD-BIOSYNTHESIS-II	NADSYN-PWY	THISYN-PWY
PYRIDOXSYN-PWY	PANTO-PWY	PANTOSYN-PWY
G. Secondary metabolite biosynthesis		
ARO-PWY	COMPLETE-ARO-PWY	ALL-CHORISMATE-PWY
UBISYN-PWY	NONMEVIPP-PWY	POLYISOPRENSYN-PWY
H. Aromatic compound degradation		
CATECHOL-ORTHO-CLEAVAGE-PWY	PROTOCATECHUATE-ORTHO-CLEAVAGE-PWY	GALLATE-DEGRADATION-I-PWY
GALLATE-DEGRADATION-II-PWY	METHYLGALLATE-DEGRADATION-PWY	3-HYDROXYPHENYLACETATE-DEGRADATION-PWY
I. Polyamine metabolism		
POLYAMINSYN3-PWY	POLYAMSYN-PWY	ARG+POLYAMINE-SYN
J. Nucleotide metabolism		
DENOVOPURINE2-PWY	PRPP-PWY	SALVADEHYPOX-PWY
PYRIDNUCSYN-PWY	PYRIDNUCSAL-PWY	
K. Amino acid biosynthesis		
ARGSYN-PWY	ARGSYNBSUB-PWY	ASPASN-PWY
HISTSYN-PWY	TRPSYN-PWY	THRESYN-PWY
VALSYN-PWY	ILEUSYN-PWY	DAPLYSINESYN-PWY
BRANCHED-CHAIN-AA-SYN-PWY		
L. Amino acid degradation		
ARGDEG-PWY	ORNARGDEG-PWY	ORNDEG-PWY
HISDEG-PWY	LEU-DEG2-PWY	VALDEG-PWY
TYRFUMCAT-PWY		
M. Translation and protein biosynthesis		
TRNA-CHARGING-PWY	PPGPPMET-PWY	
N. Nitrogen metabolism		
DENITRIFICATION-PWY		
O. Sulfur metabolism		
SO4ASSIM-PWY	SULFATE-CYS-PWY	

Table S2. Quality specification of horticultural soil.

Parameter	Specification
Characteristic	Solid, loose form; fraction 0–25 mm; 100% high peat (degree of decomposition H3–H8); clay granulate; carbonate lime; organic NPK fertilizer with raw phosphate
pH (in H_2O)	5.5–6.5
Salt concentration	< 1.8 g NaCl/dm
Nitrogen (N)	200 mg/L
Phosphate (P_2O_5)	150 mg/L
Potassium oxide (K_2O)	200 mg/L
Magnesium (Mg)	120 mg/L
Sulfur (S)	120 mg/L

Table S3. Protocol of first stage of PCR reaction.

Cycle	Temperature	Duration	No. of cycles
Initial denaturation	98°C	30s	1
Denaturation	98°C	10s	25
Annealing	55°C	30s	
Elongation	72°C	20s	
Final elongation	72°C + 4°C	2min + hold	1

Table S4. Protocol of second stage of PCR reaction.

Cycle	Temperature	Duration	No. of cycles
Initial denaturation	98°C	30s	1
Denaturation	98°C	10s	7
Annealing	65°C	30s	
Elongation	72°C	20s	
Final elongation	72°C + 4°C	2min + hold	1

Olsztyn, 10 czerwca 2026
(miejscowość, data)

Jan Kamiński
(imię i nazwisko)

Nauki biologiczne
(dyscyplina naukowa)

Przewodniczący Rady Naukowej Dyscypliny Nauki Biologiczne
Uniwersytetu Warmińsko-Mazurskiego w Olsztynie
prof. dr hab. Nina Smolińska

OŚWIADCZENIE
autora rozprawy doktorskiej

Oświadczam, że w pracy pod tytułem **Kamiński, J.**, Piotrowicz-Cieślak, A. I. (2026) Effects of inorganic fluoride and the fluoroquinolone antibiotic pefloxacin on the growth and microbiome structure of *Eruca sativa* L. International Journal of Molecular Sciences, 27(7), 2931 mój wkład merytoryczny w jej przygotowanie polegał na współkoncepcji pracy, współautorstwie tekstu pracy, wykonaniu części eksperymentalnej, wizualizacji danych, analizie formalnej oraz opracowaniu i interpretacji wyników pracy.

Jan Kamiński
.....
(podpis kandydata)

Olsztyn, 8 czerwca 2026
(miejscowość, data)

prof. dr hab. Agnieszka I. Piotrowicz-Cieślak
(tytuł zawodowy/stopień/tytuł naukowy, imię i nazwisko)

Przewodniczący Rady Naukowej Dyscypliny Nauki Biologiczne
Uniwersytetu Warmińsko-Mazurskiego w Olsztynie
prof. dr hab. Nina Smolińska

OŚWIADCZENIE
współautora

Oświadczam, że w pracy pod tytułem:

Kamiński, J., Piotrowicz-Cieślak, A. I. (2026) Effects of inorganic fluoride and the fluoroquinolone antibiotic pefloxacin on the growth and microbiome structure of *Eruca sativa* L. International Journal of Molecular Sciences, 27(7), 2931

mój wkład merytoryczny w powstanie publikacji obejmował współkoncepcję pracy, redakcję naukową tekstu oraz wsparcie merytoryczne w procesie przygotowania publikacji.

Jednocześnie wyrażam zgodę na przedłożenie w/w pracy przez Jana Kamińskiego jako część rozprawy doktorskiej w formie spójnego tematycznie zbioru artykułów naukowych opublikowanych w czasopismach naukowych.

Oświadczam, iż samodzielna i możliwa do wyodrębnienia część ww. pracy wykazuje indywidualny wkład kandydata Jana Kamińskiego polegający na współkoncepcji pracy, współautorstwie tekstu pracy, wykonaniu części eksperymentalnej, wizualizacji danych, analizie formalnej oraz opracowaniu i interpretacji wyników pracy.

A. Piotrowicz-Cieślak
podpis